INFORMATION TO USERS

This manuscript has been reproduced from the microfilm master. UMI films the text directly from the original or copy submitted. Thus, some thesis and dissertation copies are in typewriter face, while others may be from any type of computer printer.

The quality of this reproduction is dependent upon the quality of the copy submitted. Broken or indistinct print, colored or poor quality illustrations and photographs, print bleedthrough, substandard margins, and improper alignment can adversely affect reproduction.

In the unlikely event that the author did not send UMI a complete manuscript and there are missing pages, these will be noted. Also, if unauthorized copyright material had to be removed, a note will indicate the deletion.

Oversize materials (e.g., maps, drawings, charts) are reproduced by sectioning the original, beginning at the upper left-hand corner and continuing from left to right in equal sections with small overlaps.

Photographs included in the original manuscript have been reproduced xerographically in this copy. Higher quality 6" x 9" black and white photographic prints are available for any photographs or illustrations appearing in this copy for an additional charge. Contact UMI directly to order.

ProQuest Information and Learning
300 North Zeeb Road, Ann Arbor, MI 48106-1346 USA
800-521-0600

UMI®

THERMO-MECHANICAL MODELING OF TOOL AND WORKPIECE INTERFACE IN METAL FORMING PROCESS

BY

OVAISULLAH KHAN

A Thesis Presented to the

DEANSHIP OF GRADUATE STUDIES

KING FAHD UNIVERSITY OF PETROLEUM & MINERALS

DHAHRAN, SAUDI ARABIA

In Partial Fulfillment of the
Requirements for the Degree of

MASTER OF SCIENCE

In

MECHANICAL ENGINEERING

Shawwal 1422H
January 2002

UMI Number: 1409911

ProQuest Information and Learning Company
300 North Zeeb Road
P.O. Box 1346
Ann Arbor, MI 48106-1346

KING FAHD UNIVERSITY OF PETROLEUM AND MINERALS
DHAHRAN 31261, SAUDI ARABIA

DEANSHIP OF GRADUATE STUDIES

This Thesis, written by **OVAISULLAH KHAN** under the direction of his Thesis Advisor and approved by his Thesis Committee, has been presented to and accepted by the Dean, College of Graduate Studies, in partial fulfillment of the requirements for the degree of **MASTER OF SCIENCE IN MECHANICAL ENGINEERING** .

Thesis Committee

Dr. Abul Fazal M. Arif (Thesis Advisor)

Anwar Khalil Sheikh

Prof. Anwar K. Sheikh (Member)

Dr. AbdulGhani Al-Farayedhi
Department Chairman

Prof. Syed M. Zubair (Member)

Prof. Osama A. Jannadi
Dean, College of Graduate Studies

9/6/2002

Date

dedicated to
my Grand Father and his Family

ACKNOWLEDGEMENTS

Words cannot at all express my thankfulness to Almighty **Allah**, *subhanahu-wa-ta ala*, the most Merciful; the most Benevolent Who blessed me with the opportunity and courage to complete this task.

First and foremost gratitude is due to the esteemed institution, the **King Fahd University of Petroleum and Minerals** for my admittance, and to its learned faculty members for imparting quality learning and knowledge with their valuable support and able guidance that has led my way through this point of undertaking my research work.

My heartfelt gratitude and special thanks to my thesis advisor learned **Professor Abul Fazal M. Arif.** I am grateful to him for his consistent help, untiring guidance, constant encouragement and precious time that he has spent with me in completing this course of work. I do admire his exhorting style that has given me tremendous confidence and ability to do independent research. Working with him in a friendly and motivating environment was really a joyful and learning experience.

I must appreciate and thank **Professor S. M. Zubair** for his constructive and positive criticism, extraordinary attention and thought-provoking contribution in my

research. It was surely an honor and an exceptional learning experience to work with him.

I am grateful to Professor **A. K. Sheikh** for his help, advice, cooperation and comments.

I would like to acknowledge the Chairman of Mechanical Engineering Department **Dr. Abdul Ghani Al-Farayedhi** for his cooperation in providing the computer lab facility.

Sincere friendship is the spice of life. I owe thanks to my graduate fellow students from Pakistan, India and Saudi Arabia; most particularly, Iftekhar, Arshad, Zamin, Ahmad, Zahid Qamar, Mofazzal, Mujtaba, Salman, Fahim, Sohail, Naser and Fahad.

Family support plays a vital role in the success of an individual. I am thankful to my entire family for its love, support and prayers throughout my life especially my grandfather Habibullah Khan, my uncles: Nabiullah Khan, AbdulSattar Khan and Zakaullah Khan. Not to forget the affection and encouragement of my siblings Khalid, Obaid, Junaid, Shoaib, Zafar, Shahnaz, Asma, Saima and Samina; my sisters-in-law Rafat and Fahmida; and bundles of joy - my nieces Namrah, Tooba, Ashnah, Abeera and Umna; and my nephew Saad; whatever little time I spent with them was really enjoyable.

Above all, I am grateful to my parents for all the hardships in supporting their family and making bright future for their children - undoubtedly credit of my success goes to them.

Thank you all for making this dream come true.

May Allah help us in following Islam according to Quran and Sunna ! *(Aameen)*

Contents

List of Figures

List of Tables

Abstract

Name: Ovaisullah Khan

Title: Thermo-Mechanical Modeling of Tool and Workpiece Interface in Metal Forming Process.

Major Field: Mechanical Engineering

Date of Degree: January 2002

In a metal forming process plastic deformation of workpiece is acquired at tool and workpiece interface region. Tool has been identified as one of the key parameters in controlling the productivity of any manufacturing industry. The deformation of metals, and friction at the tool and workpiece contact region produce large amount of heat, a part of that heat is conducted towards the tool where it is removed by forced convection. For rolling process, these cooling and heating cycles finally result in a substantial change in the temperature distribution in the roll.

In first part of this work, an attempt is made to study the temperature and heat flux distribution in the roll by considering a non-uniform heat flux at the roll-workpiece interface. Adopting an elemental approach, a methodology has been proposed to model non- uniform heat flux at the interface. It is demonstrated that the present approach of modeling is more general than that available in the literature. For example, a constant value of heat flux at the interface that is considered by several investigators is shown to be a special case of the present investigation, particularly when the deformation and relative velocity is very small. In addition, the variation of heat flux due to friction at the interface and deformation energy in the workpiece is also shown.

The temperature distribution along with the mechanical load results in roll deformation with large localized stresses. Roll deformation is an important phenomenon that is critical not only for controlling the shape and size of final product but also for minimizing its cost. Under the assumption of an elastic roller and including the heat transfer effects; in the second part of this study the distribution of elastic deformation of the roller has been modeled by using thermo-elastic finite element method. Thermal and deformation models have been coupled and an iterative procedure has been developed to calculate roll diameter. Finally, the deformed roll radius is utilized for calculating the exit strip thickness. It is found that the calculated gauge under thermo-mechanical load agrees very well with the experimental value reported in the published literature.

Master of Science Degree
King Fahd University of Petroleum and Minerals
January 2002

خلاصة الرسالة

الاسم : أويس الله خـان

عنوان الرسالة : النموذج الميكانيكي الحراري للسطح المشترك بين أداة التصنيع في عملية تشكيل المعادن

التخصص : هندسة ميكانيكية

تاريخ الشهادة : يناير ٢٠٠٢ م

في عملية تشكيل المعادن، يحصل التغير اللدائني (البلاستيكي) لشكل القطعة، المراد تصنيعها، في السطح المشترك (البيني) بين أداة التصنيع والقطعة المصنعة وتعتبر أداة التصنيع أحد أهم المتغيرات المؤثرة في التحكم للمصانع. وينتج عن التغير في شكل المعادن، الخاضعة للتصنيع، والاحتكاك في منطقة التلامس بين أداة التصنيع والقطعة المصنعة كمية كبيرة من الحرارة، جزء من تلك الحرارة ينتقل عن طريق التوصيل الحراري إلى أداة التصنيع ويتم إزالة هذه الحرارة عن طريق الحمل الحراري بواسطة غاز أو سائل مسلط. وفي إحدى عمليات التصنيع المسماة بالدرج أو الركل، ينتج في النهاية عن العمليات المتكررة للتبريد والتسخين تغير ضخم في توزيع درجة الحرارة في أداة الدرج.

في الجزء الأول من هذا العمل، عملت محاولة لدراسة توزيع الحرارة والتدفق الحراري في أداة الدرج باعتبار تدفق حراري غير منتظم في السطح المشترك بين أداة الدرج والقطعة المدرجة. وباختيار طريقة أولية، تم اقتراح طريقة لعمل نموذج يحاكي التدفق الحراري الغير منتظم في السطح البيني. لقد وضح بجلاء أن الطريقة المستخدمة حاليا لعمل هذا النموذج تعتبر أعم وأشمل من تلك الموجودة في الأبحاث المطبوعة سابقاً. فعلى سبيل المثال، فإن الدراسة الحالية قد أوضحت أن التدفق الحراري المنتظم في المنطقة البينية الذي أعتبره عدد من الباحثين في دراساتهم إنما هو حالة خاصة من البحث المدروس حاليا، وخاصة عندما يكون التغير في الشكل والسرعة النسبية صغيرة جداً. بالإضافة إلى ذلك، فقد عرضت هذه الدراسة التغير في التدفق الحراري الناتج عن الاحتكاك في السطح البيني وكذلك الطاقة الناتجة عن تغير شكل القطعة المصنعة.

إن توزيع درجة الحرارة مع الحمل الميكانيكي ينتج عنه تغير في شكل أداة الدرج مع إجهاد واسع متمركز في أماكن معينة منها. وقد أصبح تغير شكل آلة الدرج ظاهرة مهمة ليس فقط في التحكم في الشكل والمقاسات النهائية للقطعة المصنعة ولكن أيضا للتقليل من تكلفة استبدالها. وبافتراض أداة درج مصنوعة من معدن مرن قابل للتمدد واعتبار تأثيرات الانتقال الحراري، فإنه في الجزء الثاني من هذه الدراسة قد عمل نموذج يمثل توزيع التغير في الشكل للمعدن المرن لأداة الدرج باستخدام طريقة العناصر المحدودة لحرارة المعدن المرن. وقد قرن النموذج الحراري ونموذج التغير في الشكل وأنشئت طريقة حسابية تعتمد على التكرار التخميني من أجل حساب قطر أداة الدرج. وأخيراً فإن نصف قطر أداة الدرج المتغيرة الشكل استخدم لحساب سماكة صفيحة معدنية خارجة من التصنيع. وبعمل مقارنة بين قياس سماكة الصفيحة المعدنية المصنعة والخاضعة للحمل الميكانيكي الحراري وبين نتائج التجارب في الأبحاث السابقة للنشر، وجد أن هناك توافقا في القيم بدرجة كبيرة جداً.

درجة الماجستير في العلوم

جامعة الملك فهد للبترول والمعادن

الظهران، المملكة العربية السعودية

يناير ٢٠٠٢م، الموافق شوال ١٤٢٢هـ

Nomenclature

a	thermal diffusivity, (m^2/sec)
B	pre-strain coefficient
e	rate of deformation heat generation per unit volume, (W/m^3)
f	friction factor
h	heat transfer coefficient, $(W/m^2\ ^oC)$
k	thermal conductivity, $(W/m\ ^oC)$
K	strength coefficient, (MPa)
L	bite length, (m)
n	strain hardening exponent
P	pressure between tool and workpiece, (MPa)
q	heat flux, (W/m^2)
q_f	friction heat flux, (W/m^2)
R	roll radius, (cm)
S_o	yield stress in plane strain, (MPa)
T	temperature difference $(T = T_r - T_\infty)$, (^oC)
T_∞	surrounding or coolant temperature, (^oC)
y	strip thickness, (cm)
V_{rel}	relative slipping velocity, (m/sec)
V	velocity, (m/sec)
Pe	Peclet number $\left(\frac{V_r R}{a_r}\right)$
Bi	Biot number $\left(\frac{hR}{k_r}\right)$
E	modulus of elasticity (GPa)
G	modulus of rigidity (GPa)

Greek symbol

θ_T	total bite angle
σ_f	front tension (MPa)
σ_b	back tension (MPa)
$\bar{\epsilon}$	mean effective strain or von Mises effective strain
$\bar{\sigma}$	mean true stress or von Mises effective stress, (MPa)
$\dot{\bar{\epsilon}}$	mean strain rate
ϵ_o	pre-strain
τ	friction stress, (MPa)
μ	coefficient of friction
α	angle between heating and cooling regions
ψ	angle of cooling spray region
r, θ	polar coordinates
x, y	cartesian coordinates
ν	Poission's ratio
α_{th}	coefficient of thermal expansion $\left(C^{o^{-1}}\right)$

Subscripts

o	initial value
f	final value
r	related to roll
s	related to strip
a	average value
j	elemental region

Chapter 1

Introduction

One of the ways of creating wealth is to convert raw materials into finished products through materials processing or manufacturing. Manufacturing is an honorable endeavor, which is essential to a people's standard of living and way of life [1].

1.1 Definition

Metalworking or metal forming is defined as an operation that induces shape changes on the workpiece by plastic deformation under forces applied by various tools and dies. In these processes change in shape of workpiece is not accompanied by an extensive amount of metal removal as the principal method of altering shape.

1.2 Classification of metal forming processes

A number of criteria or mechanisms have been proposed and are being used for the classification of metalworking processes. Boulger [2] has classified metal forming operations or processes as follows:

1. According to the *type of workpiece*:

   (a) *Massive or bulk forming processes* – the starting material is in the form of semifinished shapes, bars, etc.; the workpiece has a small surface to volume

ratio; forming causes large changes in shapes and cross section; the elastic recovery is usually negligible.

(b) *Sheetmetal processes*– the starting material is rolled sheet; the workpiece has a large surface to volume ratio; forming causes changes in shape but small changes in thickness; the elastic recovery is usually significant.

2. According to the *effect of deformation and temperature* on mechanical properties:

   (a) *Hot working* – dynamic recovery occurs, no strain hardening,deformation temperature range is $0.7 < T_M < 0.8$ where T_M = incipient melting temperature.

   (b) *Warm working* – some strain hardening and/or precipitation hardening may occur, deformation temperature range is $0.3 < T_M < 0.5$.

   (c) Cold working – strain hardening occurs, deformation temperature range is $< 0.3T_M$.

3. According to the *mode of deformation*:

   (a) *Steady state*– continuous wire drawing,

   (b) *Non – steady state*– die forging, and

   (c) *Mixed or transitory*– extrusion.

4. According to the *system of stresses* imposed on the workpiece:

   (a) Compression

(b) Tension

(c) Tension and compression

(d) Bending

(e) Torsion

(f) Shear

For the purpose of discussing the basic theory of metalworking processes, these methods may conveniently be classified as bulk deformation and sheet metal working processes, because they represent two different classes of work being done. Bulk deformation processes encompass method of metal working like forging, rolling, extrusion, drawing etc. In our study we will model tool and workpiece interaction for large deformation process. Initially, we have chosen rolling process to implement our analysis. Following rolling process has been discussed.

1.3 Rolling process

In its earliest beginning, the rolling of flat materials was limited to those metals of sufficient ductility. It is assumed that rolling technique was first, used by goldsmiths or those manufacturing jewelry or work of art. Metal rolling as with many other important processes, cannot be traced to a single inventor. Rolling is very important metal working process used for both cold and hot rolling of material. It is amongst the most popular metal forming process, all of the steels, aluminum, copper produced annually, about 90% of them are produced by rolling. In this process bulk deformation of material is achieved by passing it between the rolls. Rolls used as tool to deform

strip, are moving with a high constant speed resulting in the plastic deformation of the workpiece.

There are basically two types of rolling – hot rolling and cold rolling. It is to be noted that the basic difference between the two processes is strictly the same as the difference between other metal working processes.

Mainly, hot rolling differs from cold rolling in a way that hot rolling involves pre-heating of workpiece preferably above room temperature and in some cases up to a temperature of incipient melting (solidus temperature). Metals have much lower flow stress at high temperatures and generally immune to cracking so hot rolling is used for obtaining relatively high changes in processed materials, that is why, a much higher coefficient of friction exists in hot rolling which finally causes a large angle of bite during hot rolling [3]. Briefly, a major goal of hot rolling is to reduce the size of passing strip at as high a temperature as possible, thereby reducing mill load and increasing tonnage.

Cold rolling is done with thin sheets of thickness ≤ 0.2 inches and width to thickness ratio ≥ 10. The strip is passed between the rolls having radius of the order of one hundred times the thickness of the strip [4]. The aim of cold rolling includes the production of sheets possessing high quality surfaces, accurate and consistent dimensions in addition to high speeds as an increase demand of industry for high rate of production [5].

Rolling used to manufacture massive, semi-finished and finished products of ferrous or non-ferrous materials. Tonnage stuff like structural shapes, rails, bars, pipes, plates, hot-rolled sheets and strips, semi-finished products like plates, bars, and fin-

ished shapes such as cold rolled sheets employed in automobile bodies and cans are greatly produced by rolling process.

1.3.1 Mechanics of deformation

It is relatively a complex process as compared to the other metal forming processes like forging, extrusion or drawing. The basic principal of rolling is to achieve the deformation of workpiece in large scale. Rolling is performed, by passing the workpiece between the rolls that rotate in opposite direction. The rolls are hardened steel cylinders, during passing between the rolls the thickness of the workpiece is reduced. Width of the workpiece is large as compared to its thickness, while passing between the rolls the thickness is reduced, which results in lateral changes in the workpiece that is increase in the width but this increase is nominal up to 1 or 2 percent, therefore one can easily neglect this and assume plane strain deformation of the workpiece. Although, at narrow zones near the edges this assumption is not valid, consideration of these zones in analysis makes process more difficult to model that's why this consideration has hardly progressed beyond the empirical stage [4].

In rolling, workpiece and roll interaction form the contact surfaces, and as a result friction is always present there. In fact, in rolling process friction is necessary as it helps work rolls push the workpiece forward by inducing frictional stresses at the roll-workpiece interface (these frictional stresses draw workpiece into the roll gap). Friction is also necessary to transfer force and heat at the interface. The frictional stresses are actually shear stresses which result from normal pressure exerted on the workpiece by rolls and ratio of their average value is defined as coefficient of friction.

At the entry zone, the speed of the workpiece is quiet less then the roll speed, but when it comes in contact with the rolls and starts deforming its speed begins increasing as shown in Figure 1.1.

Therefore, there must be a point at the arc of contact where the (local) velocity of the local elements of passing workpiece and roll must be same. This point is called no slip point or neutral point where coefficient of friction has its maximum value. At neutral point the speeds of workpiece and roll are same, after this point the workpiece velocity surpasses the roll speed value and keeps on increasing until the exit zone where the deformed workpiece leaves the roll, at the exit zone the workpiece has speed higher than that of rolls. There is an interesting phenomenon that occurs at the interface which needs to be considered; that is, at the left side of the neutral plane the frictional stresses draw the workpiece into the roll gap and workpiece experience a pushing effect, whereas on the right side of the neutral plane where workpiece speed is higher, the frictional stresses try to hinder its motion thereby introducing a pulling affect on it (workpiece). In steady state condition as usually encountered in rolling the workpiece adjusts its speed relatively to the speed of work roll, in such away that the external stresses acting on the workpiece are in equilibrium. This determines the location of neutral point.

Since rolls are usually made up of steels (of high quality) huge amount of power would be required to move them, the amount of energy necessary to drive them at an efficient speed remains in the neighborhood of millions Btu's per minute [6]. This input power should be enough that rolls could be able to squeeze the workpiece as well as overcome the friction at the interface. Almost all this energy is converted into

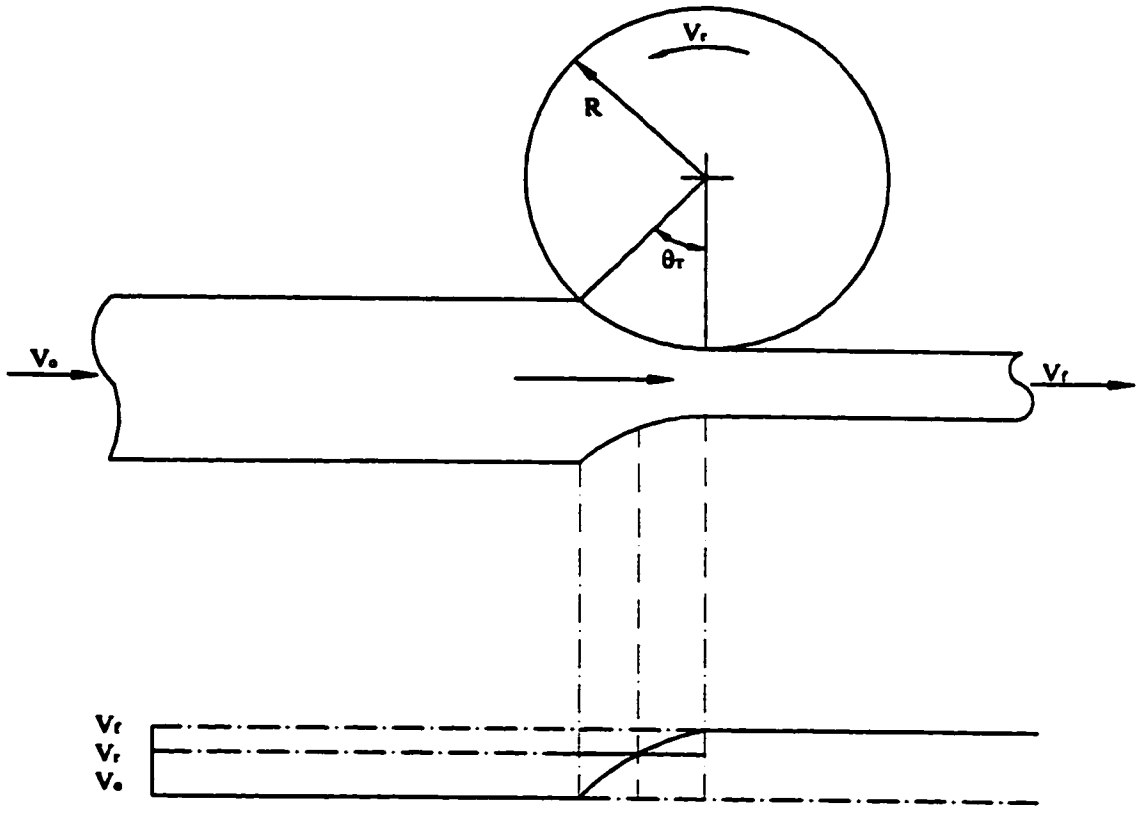

Figure 1.1: Relative velocity distribution between roll and strip surfaces.

heat. Deformation energy contributes in the plastic deformation of the workpiece. And frictional stresses at the arc of contact of the roll and workpiece generate friction energy [4].

1.4 Thermal aspects of metal working

In metal forming plastic deformation of metals is achieved that results in high temperature distribution at the contact region in the neighborhood of several hundred degree Celsius. Thus region of tool and workpiece interaction has always remained an important issue for researchers in this area from past several decades. The high temperature gradient at tool -workpiece interaction has profound effects on both components; that is, tool and workpiece materials' properties are severely influenced by this high temperature rise. Therefore a heat transfer phenomenon is of critical importance in metal forming processes. Thermal modeling, however, requires a careful attention in almost all metal forming processes but it needs some special care when we talked about rolling of metals. In metal rolling process the motion of tool (work roll) along with workpiece makes this process quiet difficult to model. As it is mentioned earlier large amount of energy is required in rolling process such that rolls could be able to squeeze the workpiece as well as overcome the friction at the interface. A large fraction of this energy is converted into heat, where a part of it is conducted in the roll and a part is transferred in the strip.

1.4.1 Heat generation in metal forming

Large amount of energy is released during bulk deformation of metals in the form of heat, this heat energy has been generated mainly at two points –between tool and workpiece interface and other within the deforming material.

Frictional energy dissipation at the tool-workpiece contact takes place because of frictional (shearing) forces, which occur due to friction at the interface. The fraction of total energy that is converted into frictional energy is dependent on the reduction given to workpiece and the coefficient of friction along the contact surface. All this friction energy is converted into heat and it is a valid assumption that this energy is equally partioned between workpiece and tool [6].

Plastic deformation energy is generated when metals are plastically deformed. Since large stresses required causing a permanent deformation in metals even at small strain rate, therefore expenditure of energy involved in cold reduction of metals is high. Almost all plastic deformation is converted into heat [7].

Chapter 2

Literature review

Thermal modeling in metal forming processes has been remained an interesting issue from the past few decades. Lots of work has been devoted in this field. Heat transfer phenomena at the interface become extremely intricate due to high pressure, high relative velocity and high heat flux. Although a lot of work has been done for thermal problem, but limited attention has been focused on heat transfer phenomena across the interface [8]. There are different analysis methods that have been developed by researchers to model the heat transfer phenomena at the interface. Some of them are not capable of handling the complexity of the process. Recently, Tseng [8] discussed three most frequently available techniques used to model the heat transfer process at the interface. These are:

1. Prescribed heat flux along the interface

2. Prescribed convective heat transfer coefficient on contact boundary

3. Prescribed thermal contact conductance on contact boundary

2.1 Prescribed heat flux along the interface

This approach requires either strip or roll to be modeled. Generally, in studying temperature distribution during rolling process, often, the roll or the strip temperature has to be analyzed. Since in this method, boundary condition has to be specified on the contact boundary or at the interface, therefore, strip or roll can be singly modeled. Mathematically, the boundary condition for this approach is of Neumann type and can be represented as

$$-k_r(\frac{\partial T_r}{\partial n})_b = q_{b_r}$$

for roll and

$$-k_s(\frac{\partial T_s}{\partial n})_b = q_{b_s}$$

for strip, where T is the temperature, k is the thermal conductivity, $(\frac{\partial}{\partial n})$ is the gradient normal to the boundary or interface, subscripts r and s represent the quantities associated with roll and strip respectively and subscript b represents the contact region. This approach is relatively easy, as only roll or strip needs to be studied. Also, the boundary condition is of Neumann type, so it is easy to handle it analytically as compared with mixed or Robin type, thus, the mathematics of this approach is relatively easy.

The disadvantage of this method is its sensitivity related to the prescribed heat flux data which may ultimately results in wrong temperature values. A careful check

is necessary in imposing heat flux value at the interface because any error or flaw in the input data can directly affect the accuracy of temperature distribution.

2.2 Prescribed convective heat transfer coefficient on contact boundary

This approach more efficiently models the heat transfer phenomena at the interface again we can only model either the strip or roll separately. Mathematically, the boundary condition can be written with the help of Newton's cooling law as

$$-k_s(\frac{\partial T_s}{\partial n})_b = h_{es}(T_s\mid_b - T_{core\ r})$$

for strip and

$$-k_r(\frac{\partial T_r}{\partial n})_b = h_{er}(T_r\mid_b - T_{core\ s})$$

for roll, where h_e is the equivalent, or effective, convective heat transfer coefficient also known as film or convective conductance. T_{core} is the core temperature which is generally assumed constant. Usually, $T_r\mid_b$ is lower than $T_{core\ s}$ while $T_s\mid_b$ is higher than $T_{core\ r}$. By increasing the roll or strip surface temperature, the heat transfer rate across the interface can be increased, therefore, this approach closely represents the reality of heat transfer phenomena at the interface [8]. The heat transfer coefficient h_e is usually obtained from temperature or heat flux measurements. When temperature measurements are used some additional computational efforts are also required.

2.3 Prescribed thermal contact conductance on contact boundary

This method of analysis considers both roll and workpiece in modeling interface problems. Thus, analysis is of coupled type in which interface heat flux becomes a part of the solution. Thermal coupling between workpiece and roll interface implies that the compatibility conditions; that is, 1−the continuity of temperature and 2−the continuity of heat flux at the interface must be properly specified.

Compatibility of temperature at the interface implies that at the bite region, both workpiece and roll should have equal temperatures. This could be true, because tremendous pressure occurred during rolling process at the interface which results in intimate contact of the two components. However, the interface resistance can be included in the analysis because of some scale or coolant film might be present at the contact and thermal resistance of this film or scale should be considered. Most of the previous studies have discarded this resistance because the thickness of lubrication film or scale is very small in the order of micron [9] and assumed a perfect contact of tool and workpiece. Mathematically, temperature compatibility for perfect contact given by Tseng [8]

$$T_s \mid_b = T_r \mid_b \tag{2.1}$$

where $T_s \mid_b$ is workpiece temperature $T_r \mid_b$ is roll temperature at the roll gap.

Compatibility of heat flux is also termed as energy conservation condition. Math-

ematically, continuity of heat flux discussed by Tseng [10], [11] and can be written as

$$k_r(\frac{\partial T_r}{\partial n})_b + k_s(\frac{\partial T_s}{\partial n})_b - q_f = 0 \tag{2.2}$$

where q_f is the friction heat flux generated within the interface.

Many studies have been performed by using above equations (2.1) and (2.2). Recently, more general formulations developed by Tseng [12] for non-perfect contact can be expressed for roll as

$$-k_r(\frac{\partial T_r}{\partial n})_b = h_c(T_r \mid_b - T_s \mid_b) - \frac{q_f}{2} \tag{2.3}$$

and for strip

$$-k_s(\frac{\partial T_s}{\partial n})_b = h_c(T_s \mid_b - T_r \mid_b) - \frac{q_f}{2} \tag{2.4}$$

where h_c is the thermal contact conductance or interface heat transfer coefficient. When h_c tends to infinity, the contact becomes perfect where as for h_c equal to zero, a fully insulated interface has been obtained. Half of the q_f value has been incorporated which indicates that friction flux is evenly distributed at the interface. The thermal contact conductance is the reciprocal of the thermal contact resistance and is a function of different parameters, for example

$$h_c = f(pressure,\ roughness,\ temperature)$$

The boundary conditions given by equations (2.3) and (2.4) also satisfies law of conservation of energy. By simple manipulation between equations (2.3) and (2.4), conservation of energy (the continuity of heat flux of equation (2.2)) can be acquired. If h_c tends to infinity, that is, for a perfect contact either the equation (2.3) or (2.4) can be reduced to equation (2.1) i.e., $T_s \mid_b = T_r \mid_b$.

In present work, the above mentioned three approaches have been categorized mainly in two classes:

1. Un-Coupled Analysis

2. Coupled Analysis

2.4 Un-Coupled Analysis

This method of analysis encompasses 1−prescribed heat flux at the interface and 2−prescribed convective heat transfer coefficient on contact boundary. Decoupling of workpiece and tool interface has to be performed as shown in Figure 2.1. Boundary condition has to be specified at the contact region separately for each component, thus, allows a flexibility of modeling either the roll or workpiece individually. For example, in predicting temperature distribution over the roll it requires only knowledge about interface heat flux q_r, in case of prescribed heat flux approach . And in case of convective heat transfer on contact boundary method, it requires effective convective heat transfer coefficient h_c. Once the main ingredients q_r or h_c of the two approaches become known, roll temperature distribution can be evaluated easily. No need of strip model arises in there for calculating roll temperature distribution. Similarly, for

modeling strip temperature distribution, there is no need of modeling roll portion of the process.Following literature review has been conducted for un-coupled analysis of rolling process.

2.4.1 Prescribed Heat Flux

In the beginning period of analytical study of rolling process, prescribed heat flux was utilized as the boundary condition along the interface. Johnson and Kudo [13], Avitzur and Nowakowski [14] used analytical and Dawson [15] used numerical techniques to study the strip temperature by assuming no heat flux across the interface, i.e. $q_{bs} = 0$. Haubitzer [16] developed an analytical model for calculating two dimensional steady state temperature distribution in a rotating roll with prescribed surface temperature boundary condition. Patula [17] modified Haubitzer's model by utilizing constant heat flux and convection cooling boundary conditions over a portion of the cylindrical roll. He got an exact solution in an infinite series form for two dimensional steady state temperature distribution for a rotating roll. The results indicated that for normal cold rolling situations under steady state conditions, the penetration of the surface heating and cooling effects, that occur during every roll revolution is very low usually remain less than 4 % of the radius. His temperature plots showed that as position of cooling spray moved farther from the point of heat input a cusp started to form at the point where cooling was initiated. He also suggested that the approximate roll bulk temperature can be determined which would help in predicting roll thermal crown.

Troeder et al. [18] and Guo [19] performed analytical study to determine roll

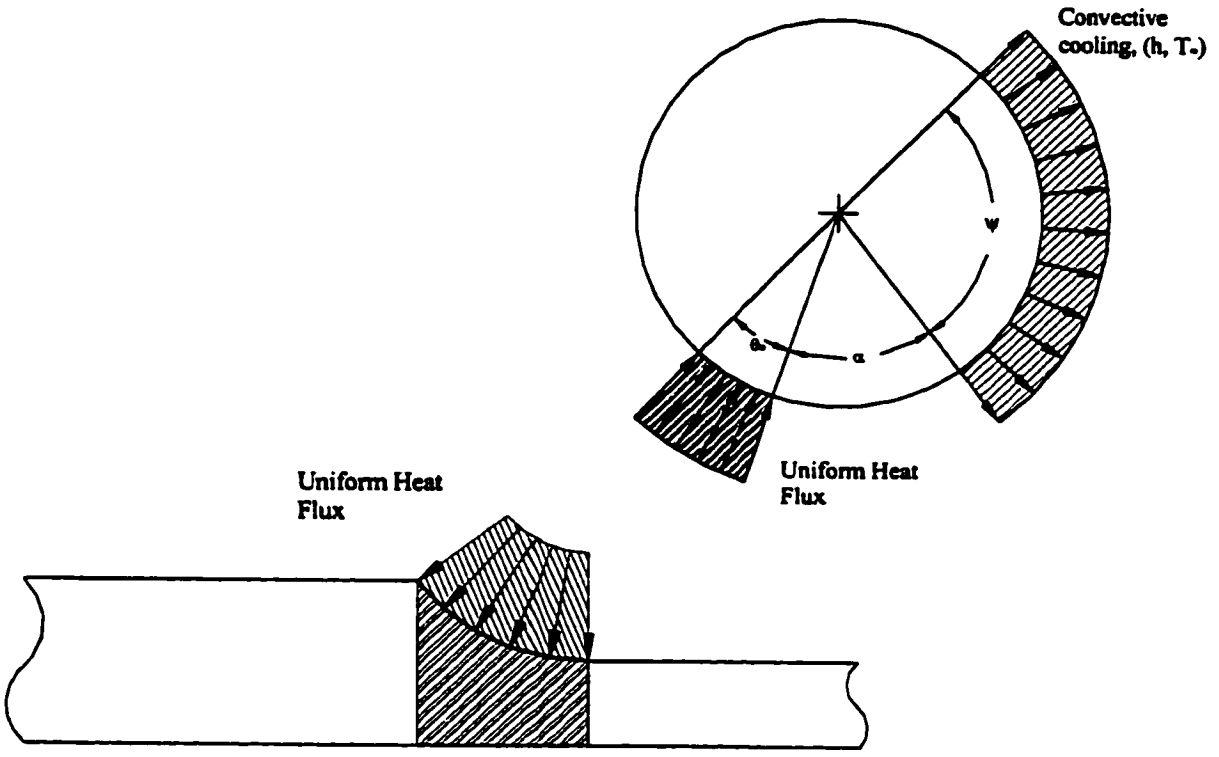

Figure 2.1: Un-Coupled approach considers only one compoment.

temperature by employing uniform heat flux distribution at the interface.

The heat input to the roll can not be uniform over the whole bite angle, because roll and strip always remain in motion during the deformation process. Yuen [20] and [21] extended Haubitzer's formulation by taking linear heat flux distribution and variable convection heat transfer coefficient over a portion of roll. The modified model had heat input flux and convection heat transfer coefficient as a function of bite angle. He also took into account the presence of scale layer between roll and strip, which is always present in hot rolling. He found that in case of hot rolling scaled oxide layer has a dominant effect on the heat transfer process and acts as an insulating layer which can reduce the heat transfer rate significantly (he neglected the curvature effects i.e. roll diameter >> strip thickness).

Gecim and Winer [22] used an integral transform technique (Finite Fourier transform) to solve heat conduction equation in cylindrical coordinates for a rotating cylinder exposed to uniform heat flux and convection cooling. They neglected the heat conduction in circumferential direction as compare to heat conduction in the radial direction or heat convection in the circumferential direction because of high rotating speed of the roll. Their predicted characteristic curves for temperature distribution over roll showed peak temperature occurred at the bite region over the roll surface. The temperature variations remain small in region below the roll surface and the depth of this thermal skin would be decreased by increasing the roll speed.

By neglecting the circumferential heat conduction term from two dimensional heat equation as did by [22], Tseng et al. [23] studied the thermal behavior of roll. An analytical model was obtained by using integral transform technique. The roll

was subjected to uniform heat flux and convective cooling over a portion of its circumference. High temperature gradients occurred within a thin surface layer of the roll, resulted in the generation of high thermal stresses and also affected the thermal properties of tool and workpiece.

Understanding of cyclic thermal stresses is necessary in order to get information about roll wear and also in designing suitable roll cooling criteria, thus, resulted in increasing roll life and better product surface quality. In an accompanying paper, [24] Tseng discussed the cyclic stresses generated in the roll during rolling process. By considering the steady state behavior of thermal stresses an exact solution has been obtained. It is found that the thermal stresses vary rapidly (oscillate rapidly) within a very thin layer near the roll surface, outside the bite region variations were moderate. Maximum absolute shear stress took place at the location of one third of the bite angle and maximum radial stress occurred at the entry point of the bite region.

2.4.2 Numerical models

Tseng [25] solved roll heating problem with respect to Eulerian coordinate system by using upwind finite difference technique with reasonably fine mesh. Upwind differencing is used to stabilize the numerical oscillations often induced in convection-dominated heat transfer problems. He mentioned that, since roll rapidly moves and temperature varies only in thin layer near the roll surface, so the problem could be analyzed only for thin layer of the roll. A parametric study had been performed at different Pe and Bi numbers where Pe is Peclet number given as $\left(\frac{VR}{\alpha}\right)$ and Bi is Biot number equal to $\left(\frac{hR}{k}\right)$, v is roll velocity, R is roll radius, α is thermal diffusivity, h is

convective heat transfer coefficient and k is thermal conductivity. He then compared his results with analytical model given by Patula [17] and concluded that disagreement between the numerical and analytical results near the bite region is decreased as Pe number is increased.

2.5 Coupled Analysis

This approach uses thermal contact conductance (h_c) at the interface and considers both roll and workpiece in modeling heat transfer phenomenon at the interface. For modeling non-perfect contact h_c has to evaluated experimentally or from correlations whereas for perfect contact its (h_c) value becomes infinity and equations 2.1 and 2.2 have been used. Additional information is required for workpiece deformation and friction heat generated at the contact of roll and strip. Knowledge about friction heat has been obtained from pressure information of mechanical model and for deformation heat generated in the workpiece, strip deformation behavior has to be studied.

2.5.1 Analytical models

Cerni [26] and Cerni et al. [27] studied the thermal stress problem of hot rolling. They developed an analytical model based on Lagrangian formulation to predict the two dimensional transient temperature distribution in a roll. They assumed that the whole roll was subjected to 360 degrees uniform convection cooling and heat transferred in the roll gap from strip to the roll may be approximated by a line source. The heat transfer solution was found by integrating the line heat source into

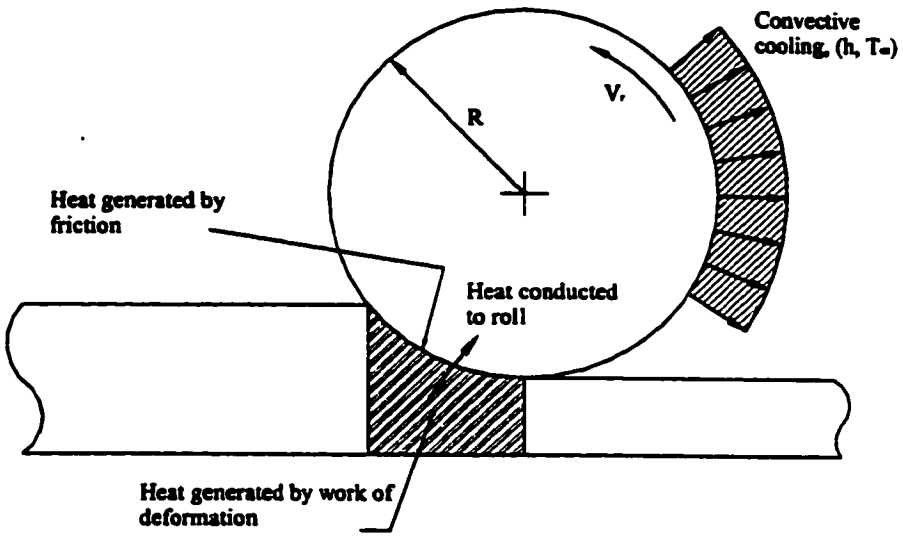

Figure 2.2: Coupled approach considers both components.

a band source and convection was also allowed at the region where the band source applied. They did not consider the condition where cooling present over a portion of the roll only. Hogshead [28] simplified Cerni's analysis and gave a convenient analytical expression.

Pawelski [29] obtained mathematical expressions for the transient roll temperature distribution near the roll surface by assuming only radial heat conduction in the roll and exponential time dependent variation in roll surface temperature.

Polukhin et al. [30] and [31] obtained one dimensional analytical solution to study the transient temperature distribution, both in strip and roll. They mentioned that their analytical solution remain valid only when strip had been regarded as semi-infinite slab, that is cooling effect of roll did not penetrate during contact up to the center of the strip. They developed a condition of applicability for their analytical model; for the cases that did not fulfill the condition of applicability, they solved one dimensional heat equation by finite difference method. It was reported that the temperature of the roll rises in the beginning of the contact with the strip, and then starts to decrease behind it. A uniform distribution of friction heat generated at the interface had also been assumed. They did not provide detailed analysis, also information were hazy.

Yuen [32] developed an analytical solution by considering a scaled layer between roll and strip. He assumed a uniform distribution of friction heat flux and deformation heat generated in the workpiece and expected that this is a valid assumption for hot rolling. It has been found that scaled layer has dominant effect on heat transfer process between strip and roll.

In rolling process, work roll always remain in continuous motion and it has been proved that a thermal equilibrium is reached after some period of time. Through passing the roll between heating and cooling cycles a steady state temperature distribution can be achieved [33]. By considering steady state process, Tseng et al. [34] studied the thermal behavior of both roll and strip and developed an analytical model for aluminum cold and hot rolling. The roll subjected to uniform heat flux and convective cooling over a portion of its circumference. Roll temperature distribution is obtained by using Fourier integral technique and for strip temperature; separation of variable principal was adopted. Compatibility condition was adopted in order to link both roll and strip solutions. High temperature gradients occurred within a thin surface layer of the roll, resulted in the generation of high thermal stresses and also affected the thermal properties of tool and workpiece.

2.5.2 Numerical models

Without giving details and using finite difference approach, Parke and Baker [35] developed a two dimensional model to study transient roll behavior. The work roll was subjected to cooling over a portion of its circumference, and heat loss to backup roll was taken into account. Their work was conducted for specific roll dimensions and speeds.

The model given by Parke and Baker was based on Lagrangian formulation resulted in parabolic-type governing equation that includes conduction terms only. This type of formulation utilizes fixed coordinates in the roll, and boundary conditions rotate with respect to the roll. Lagrangian system requires a very fine mesh or number

of steps to simulate the rolling process. If an implicit scheme is employed the number of nodes should be higher than the explicit scheme, in order to get numerical convergence. The model given by Parke and Baker [35] (based on Lagrangian formulation) uses 240 steps to simulate one revolution for a typical rotating speed, therefore, steady-state temperature may be reached after several hundred thousands of steps, which obviously neither efficient nor economical. Another drawback of Lagrangian formulation is its failure to study the interface behavior, that is, when roll contact another body. This is because; Lagrangian approach only allows the use of uniform circumferential mesh for modeling the rotating boundary condition.

Lahoti et al. [36] developed two dimensional finite difference model for strip and for a small region of roll. They did not consider the region of the roll exposed to convection cooling. They arranged a non-orthogonal finite difference mesh in the deformed strip portion so their model was inefficient or had some distinct limitations. They predicted a very uniform temperature along the interface and quiet large thermal layer in the roll, the results showed deviations which may be due to the selection of non-orthogonal grid.

Poplawski and Seccombe [33] modified numerical model of Parke and Baker [35] based on finite difference scheme to incorporate the third dimension. They used finite difference technique to obtain transient temperature distribution in the strip, in the skin of work roll and at the backup roll/work roll interface zone. Their reported characteristic curve for temperature variation was same as that of Patula's [17]. They also calculated the work roll core temperature at various distances below the roll surface versus time, and told that after a period of time most of the roll gets an equal

temperature gradient. Lahoti et al. [36] and Poplawski et al. [33] s' studies were based on Lagrangian formulation.

On the other hand, Eulerian approach uses fixed boundary conditions, but gives temperature distribution in a moving roll. This approach uses fewer steps, thus results in eliminating the efforts required to model the moving boundary condition as well as decreases the computing time. One drawback of Eulerian formulation is that elliptic-type governing equation comes out, which includes both conduction and convection terms. This type of equation is difficult to handle numerically when Peclet number is high, as usually happens in rolling process.

Based on Eulerian formulation, Tseng [10] and [11] introduced generalized finite difference scheme with upwind differencing. Generalized finite difference discretization is used for heat transfer problem involving high convective heat flow, irregular geometry and high local thermal gradients. While upwind differencing is employed to overcome numerical instability resulting from high velocity. He analyzed the thermal behavior of hot and cold rolling processes by considering both strip and roll and obtained steady state temperature distribution in both roll and strip. The non-orthogonality of mesh taken place at the bite region has been handled by generalized finite difference scheme. Lahoti et al. [36] did not consider orthogonality of mesh in their study. They concluded that the accuracy of results was affected at high Peclet number but could remain in the limits with the help of a reasonably fine mesh size. Also, his calculated peak roll temperature was in good agreement with the value given by Poplawski and Seccombe [33].

Tseng and Wang [37] discussed thermal contact resistance for cold rolling case.

They concluded that interface resistance which depends on surface roughness, contact pressure, coolant, lubricant or oxide layer between roll and workpiece, hampered heat transfer from strip to the roll and temperature difference between roll and workpiece increases significantly as the thermal resistance increases.

Tseng [38] implemented thermal resistance concept on hot and cold rolling problems. First time, he estimated the specific values of the parameters used to correlate the corresponding thermal contact conductance for the typical cold and hot rolling of steels.

Tseng and Wang [37] and Tseng [38] have obtained the values for friction heat flux and deformation heat generation from rigid-viscoplastic finite element code developed by [39] and [40].

Chang [41] modeled two dimensional heat transfer phenomenon between roll and strip by one dimensional heat conduction equation following Lagrangian coordinate system on the contacting surfaces. He mentioned that at high Peclet number the depth of thermal boundary layer remains very small in both roll and strip (usually in few percent of respective lengths); therefore, roll and strip may be treated as semi infinite solids. Finite difference and analytical solutions have been combined in his work for predicting temperature distribution in roll and strip.

Some people performed finite element analysis for strip rolling process. Yamada et al. [42] performed two dimensional thermo-mechanical analysis of flat rolling process using finite element analysis. They developed finite element code for two dimensional steady state thermal analysis and combined it with rigid-plastic finite element code for deformation analysis. After comparing the results acquired from purely mechanical

analysis with thermo-mechanical analysis, they recommended that for precise estimation of stress and strain distribution in the roll bite thermo-mechanical analysis is indispensable.

Woodbury and Beaudoin [43] discussed thermal aspects of modeling strip rolling. They emphasized on paying special attention on thermal interaction between tool and deforming material. They also mentioned that proper description of the temperature field is a must for correct evolution of strain rates and hardnesses.

Dawson [44] developed a finite element model to solve the coupled thermal and mechanical problems in hot rolling of strips. Later, material hardening behavior has been incorporated by means of an internal variable constitutive equation [45].

Hwang et al. [46] used Petrov-Galerkin finite element scheme for heat transfer analysis of both strip and roll in hot rolling process, they found that roll speed, reduction and interface heat transfer coefficient have significant effects on roll-strip temperatures, metal flow and roll pressure distribution.

2.6 Experimental studies

Along with analytical and numerical studies the thermal behavior of rolling process has also been studied by some keen researchers. Stevens et al. [47] provided some interesting and significant experimental results related to the transient temperature build up in rolls. Their work was conducted for specific roll dimensions and speeds.

Denisov et al. [48] performed experiments which precisely measured the temperature distribution for hot rolling. They used thermocouples to measure the temperature values over the roll surface and on the zones near the roll surface, that is at the

interface and backup roll.

Raudensky et al. [49], based on on-line temperature measurements obtained specific values of temperature and heat flux for hot rolling of shaped steels. They employed inverse heat conduction technique to convert measured data into surface heat flux and heat transfer coefficient.

Jeswiet and Rice [50] measured temperature distribution in strip at the bite region for cold rolling process. Yoshida et al. [51] developed an integrated mathematical simulator for hot strip mills and measured temperature for rolled material and roll, along with this they also measured rolling loads.

Based on the above literature review it has been found that almost all studies performed in modeling temperature distribution over roll or strip consider uniform heat flux distribution at the interface. A very little attention has been paid in evaluating deformation energy generated in the workpiece, some studies reported about this and some did not. Those who reported considered uniform distribution of energy generated in the deforming workpiece. Tseng [8] gave a review on heat flux distribution. His given information has been categorized and updated here with respect to coupled and un-coupled approaches in Tables 2.1 and 2.2. These tables indicate the heat flux distributions used in different analyses. By considering this data one can say that none has performed analysis by employing non-linear heat flux distribution.

Table 2.1: Boundary heat flux for un-coupled approach.

Un-Coupled Approach			
Investigator	Process	Boundary heat flux	Comment
Avitzur and Nowakowski [14]	steel rolling	0	modeling strip
Dawson [15]	aluminum rolling	0	modeling strip
Guo [19]	steel rolling	uniform heat flux	modeling roll
Johnson and Kudo [13]	metal rolling	0	modeling strip
Patula [17]	steel rolling	uniform heat flux	modeling roll
Raudensky et al. [49]	steel hot rolling	38 MW/m^2	roll measurment
Troeder et al. [18]	steel rolling	uniform heat flux	modeling roll
Tseng [25]	steel rolling	uniform heat flux	modeling roll
Tseng et al. [23]	aluminum rolling	uniform heat flux	modeling roll
Tseng et al. [24]	steel rolling	uniform heat flux	modeling roll
Yuen [20]	steel hot rolling	linear heat flux	modeling roll
Yuen [21]	steel rolling	uniform heat flux	modeling roll
Gecim et al. [22]	steel rolling	uniform heat flux	modeling roll

Table 2.2: Boundary heat flux for coupled approach.

Coupled Approach			
Investigator	Process	Boundary heat flux	Comment
Cerni [26]	steel rolling	uniform heat flux	modeling roll/strip
Hogshead [28]	steel rolling	uniform heat flux	modeling roll/strip
Tseng [11]	steel rolling	uniform heat flux	modeling roll/strip
Tseng et al. [10]	steel rolling	uniform heat flux	modeling roll/strip
Tseng et al. [34]	aluminum rolling	uniform heat flux	modeling roll/strip
Yuen [32]	steel rolling	uniform heat flux	modeling roll/strip

2.7 Deformation and friction heat flux scenario

It has been discussed earlier that there are mainly two sources of heat deformation and friction present at tool and workpiece interface for a metal forming process. For rolling process modeling little attention has been paid to this aspect. Lahoti et. al. [36] in their analysis used Orowan's theory of rolling [52] for calculating heat generation due to plastic deformation of workpiece and friction at the interface. Yuen [32] assumed uniform distribution of deformation heat in the workpiece and friction heat at the interface, he did not discuss the procedure for calculating these values and suggested that these can be obtained from [52] and [53]. Tseng and Wang [37], andTseng [38] in their study for temperature prediction over roll, utilized rigid-viscoplastic finite element model of [39] and [40] for calculating deformation and friction heats.

Tseng et al. [34] analyzed thermal behavior of roll and strip, the information on heat generation by friction and deformation were obtained from a computer program ROLLING developed by Maslen and Tseng [54], the computer code was based on modified version of Alexander's theory of rolling [55]. Tseng [10] in his study of temperature distribution obtained deformation and friction energies from direct measurements of power. There is uncertainty in dividing the measured power into the above mentioned two sources of heat.

Woodbury and Beaudoin [43] evaluated deformation energy by integrating flow stress-deformation rate product over the deformation zone. Friction energy was also determined by integral of the product of shear stress and relative slip velocity.

Hwang, Joun and Kang [46] employed penalty rigid-viscoplastic finite element

method for modeling deforming material.

It has been cleared that for predicting temperature distribution over tool, information about previously mentioned two major sources is necessary. Based on literature review table 2.3 has been developed which describes the type of values for friction and deformation heats used by different authors.

Table 2.3: Deformation heat and friction flux behavior considered by different authors

Author	Friction heat generation	Deformation heat generation
Yuen [32]	uniform distribution	uniform distribution
Lahoti et al. [36]	constant value	constant value
Tseng [38]	non-uniform distribution	constant value
Tseng and Wang [37]	non-uniform distribution	constant value
Tseng et al. [34]	constant value	constant value
Woodbury and Beaudoin [43]	constant value	constant value
Hwang et al. [46]	not reported	not reported

Chapter 3

Present Study

3.1 Objective

Tools with highly finished surface are always being in great demand by the metal processing industry. Tool surface finish is an important parameter in controlling the quality of product. Manufacturers take great care in designing proper tool for a particular metal deformation process. For rolling process, roll (tool) surface finish is a key parameter in controlling the rolled product quality, especially in cold rolling that is normally a final operation in the process performed on the strip. Mechanical properties of the rolled strips are also subjected to great variations due to the thermal gradient. In metal rolling, plastic deformation of workpiece is achieved at the region where roll becomes in contact with the workpiece. As a consequence, large amount of heat is generated at the interface resulted in high heat flux at the interface. Also high relative speed between workpiece and roll (up to the order of 10 m/s) that is always demanded by mill operators makes heat transfer phenomenon at the interface very complicated. In addition to this, mechanical load is also acted at the bite region in the form of pressure and friction stress distributions. This thorny behavior of pressure and friction stress at the interface and thermal gradient in the roll markedly distorts the roll and induces large stress variations, as a consequence wear of roll is

also started: These stresses cause fatigue and roll spalling. Finally, complex thermal and mechanical loadings produce severe distortion of the rolls with undesirable surface and shape, and with short life. Such type of roll always affects the product quality and size which ultimately result in decreasing mill efficiency thereby

a) decreasing roll speed,

b) increase number of roll changes, and

c) decrease yield due to irregular shape and wrong gauge

By considering all these aspects, one can say that an efficient heat transfer arrangement is a must to control roll temperature profiles. Knowledge of temperature and stress distributions in the roll is necessary in order to protect its deterioration and increase life, and a complete history of roll deformation behavior is essential for controlling final strip thickness with satisfactory quality. Therefore, it is of paramount importance that thermal aspects associated with the process be efficiently modeled and their effects on stresses and deformation behavior be carefully considered.

3.2 Problem Description

Present work involves the study of heat transfer phenomenon at the tool and workpiece interface and the effects of thermal gradient and mechanical load over tool deformation for a cold strip rolling process. Roll (tool) remains in continuous motion at a constant surface speed and is subjected to heating and spray cooling cycles. Figure 3.1 shows a typical model for a rotating roll subjected to different boundary conditions proposed by many authors following un-coupled approach. θ_T represents uniform heating region, ψ shows the arc exposed to uniform forced convective cool-

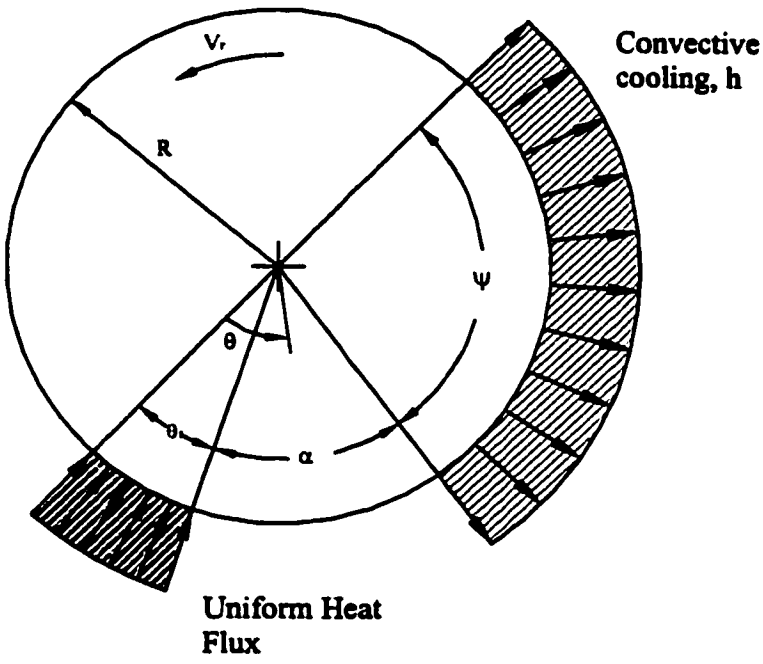

Figure 3.1: Classical roll model used by different authors composed of rotating cylinder exposed to surface heating and forced convective cooling.

ing and α represents a gap between heating and cooling regions. On the basis of assumptions given below:

1. Long cylinder that is, temperature variation along axial direction is neglected
2. Uniform mechanical and thermal properties of roll material
3. Temperature becomes steady state after a certain period of time
4. Rotational speed is constant
5. Uniform heat flux distribution

and with respect to Eulerian Reference frame, the governing differential equation for temperature distribution can be written as [56]

$$\frac{1}{r}\frac{\partial}{\partial r}\left(r\frac{\partial T}{\partial r}\right)+\frac{1}{r^2}\frac{\partial^2 T}{\partial \theta^2}=\frac{V_r}{a_r R}\frac{\partial T}{\partial \theta} \tag{3.1}$$

with boundary conditions

$$-k_r\frac{\partial T(R,\theta)}{\partial r}=\left\{\begin{array}{cc} -q_r & 0<\theta<\theta_T \\ 0 & \theta_T<\theta<\alpha+\theta_T \\ h(T(R,\theta)-T_\infty) & \alpha+\theta_T<\theta<\alpha+\theta_T+\psi \\ 0 & \alpha+\theta_T+\psi<\theta<2\pi \end{array}\right\} \tag{3.2}$$

k_r is thermal conductivity for roll material, h is convective heat transfer coefficient, $a_r$is thermal diffusivity and R is the roll radius, V_r is the roll velocity and T_∞ is

surrounding temperature.

Our interest is to calculate a temperature distribution, which can satisfy above system of equations. We know surrounding temperature T_∞, thermal properties, roll speed and geometry, the only unknown remains is heat flux (q_r) entered towards the roll. This unknown heat flux (q_r), makes analysis extremely difficult. Figure 3.1 shows a uniform distribution of roll heat flux at the bite region. In actual rolling process this heat flux may not remain constant over the whole bite angle. Also pressure distribution is not remained uniform at the interface, which results in a non-uniform friction flux at that area. In addition to this, heat flux (q_s) coming out from the strip is varying greatly due to strip deformation. Therefore, assumption of uniform heat flux is not correct. In present analysis variation of heat flux at the bite region has been considered, this issue will be discussed in Chapter 6 named Temperature Distribution Module.

Roll stresses and deformation behavior have also been predicted by considering both mechanical and thermal loads. Also roll deformation effects in controlling the size of rolled strip have been simulated. Mechanical load constitutes both contact pressure and friction stress distributions at the interface whereas temperature distribution is evaluated by employing non-linear variation of heat flux at the roll and strip interface. Finally, strip exit gauge has been calculated by considering deformed roll and compared with the experimental data available in the literature. Since, in actual rolling process both thermal and mechanical loads are present; therefore, proposed work is realistic in a way that it closely simulates the actual process.

3.3 Proposed Approach

The problem has been defined as first– to evaluate roll temperature distribution, which requires roll heat flux. Heat flux entered into the roll is the summation of heat flux comes out from deforming strip and heat flux generated at the interface due to friction called friction heat flux [34]. Following un-coupled approach earlier studies used either prescribed heat flux along the roll interface or prescribed convective heat transfer coefficient at the contact region. This un-coupled analysis does not properly simulate the heat transfer phenomenon. It has been cleared after literature review that coupled approach closely models the actual heat transfer process because in this technique roll heat flux (q_r) has to be evaluated instead of prescribing from outside; therefore, in present study roll temperature distribution has been predicted by using coupled modeling approach. A coupled approach model with non-uniform heat flux distribution at the interface is shown in Figure 3.2. With the assumption of perfect contact between roll and strip the compatibility of temperature and heat flux at the interface can be expressed as

$$\overline{T}_s \mid_c = \overline{T}_r \mid_c \tag{3.3}$$

$$\overline{q}_r = \overline{q}_s + \overline{q}_f \tag{3.4}$$

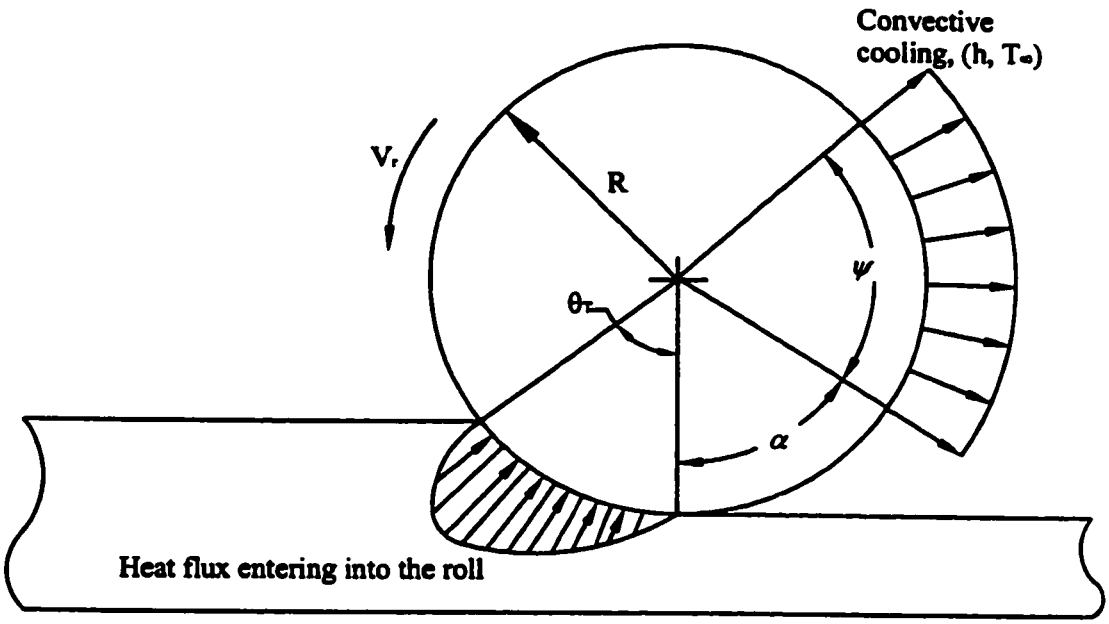

Figure 3.2: Coupled approach model showing variation of heat flux at the interface.

where $\overline{T}_r$ is average roll temperature, $\overline{T}_s$ is average strip temperature, $\overline{q}_s$ is the average heat flux from deforming strip and $\overline{q}_f$ is the average heat flux generated at the interface, subscript c represents the contact region.

Second part of current study consists of evaluating roll stresses, introducing roll deformation effects in the analysis and calculating optimum roll diameter so that exit strip gauge can be controlled. The stress and deformation analysis has been conducted with finite element method by considering both mechanical and thermal loads.

Different models have been developed, which consist of relevant information necessary for performing this study. Details of each model is given below.

3.3.1 Pressure module

In metal forming processes high pressure occurs at tool and workpiece interface, which is related to the friction stress at the contact region. This module is capable of evaluating pressure and friction stress distributions at the interface for cold strip rolling operation. It is semi-analytical model based on slab method of analysis. The details will be discussed in Chapter four.

3.3.2 Heat flux module

This module utilizes data obtained from pressure module. Friction heat flux at the interface and deformation energy generated in the workpiece has been calculated here. Friction heat flux 'q_f' at the interface is obtained as a function of various

parameters,

$$q_f = f(\mu, P, V_{rel}, \tau, y_f, R, \theta_T) \tag{3.5}$$

where μ is the friction coefficient, P is the pressure, V_{rel} is the relative slip velocity, τ is the shear stress, y_f is the final strip thickness, R is the roll radius, θ_T is the bite angle. An expression for evaluating distribution of deformation energy density rate 'e' in the deforming strip has been obtained as function of following parameters

$$e = f(K, V_s, y_o, y_f, L, R, \theta_T) \tag{3.6}$$

where y_o and y_f are initial and final strip thicknesses. K is strength coefficient, V_s is the strip velocity, L is the arc length. This module will be discussed in Chapter five.

3.3.3 Roll temperature module

It consists of semi-analytical model for predicting roll temperature distribution. A non-uniform heat flux behavior at the interface and uniform convective cooling over the roll periphery has been considered. This aspect will be discussed in Chapter six.

3.3.4 Roll deformation module

Based on finite element code, this module is developed to calculate roll stresses and to simulate roll deformation phenomenon occurred in strip rolling process. Both mechanical and thermal loads have been utilized here.

3.4 Description of developed master module

Previously mentioned analytical and numerical models have been interfaced together so that a coupled master module has been formed in order to perform different parametric studies. The developed master module can be understood by the flow chart shown in Figure 3.3. The process parameters, like material properties, thermal properties and geometry of the roll and strip will be set with respect to a typical rolling process for conducting numerical experiments. The developed master module will start working from pressure module that will give the location of neutral point and the distributions of pressure and friction at the interface. The outputs from pressure module will be used in heat flux module for calculating friction heat flux at the interface. Rate of deformation energy generated in the workpiece will also be calculated in this module. Distributions of friction heat flux and deformation energy will be used as inputs in roll temperature module for predicting roll temperature distribution. Finally, roll deformation module will be utilized for calculating roll stresses and deformed roll radius. Pressure and friction stress from pressure module; and temperature distribution from roll temperature module will be imposed over the roll. The deformed roll radius calculated in deformation module is utilized for next step calculation. An iterative procedure will be used over the entire developed coupled module and a convergence criteria is made until error in calculated deformed roll radius becomes very small. Above mentioned procedure can be grasped by Figure 3.3.

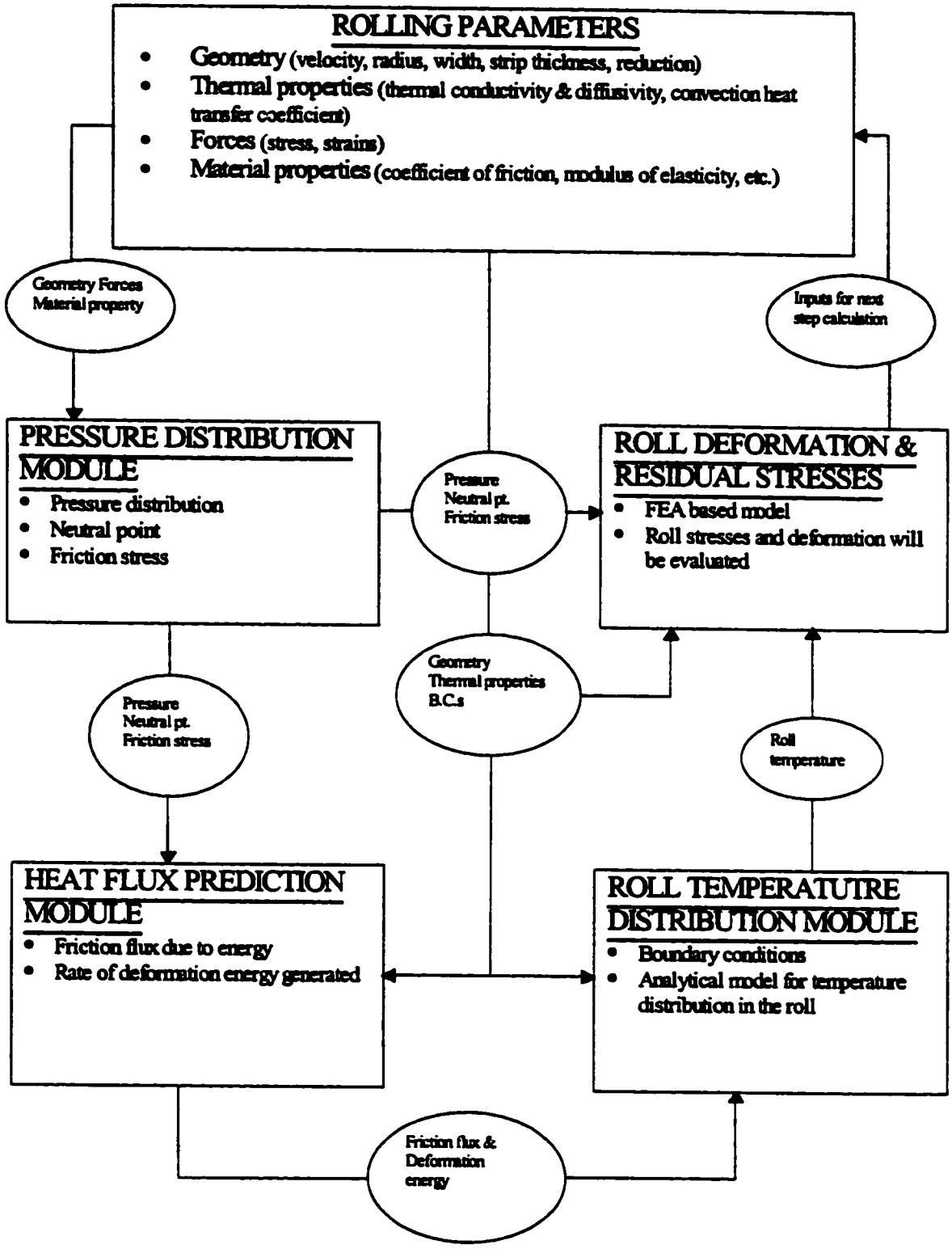

Figure 3.3: Developed master module showing coupling of different sub modules

Chapter 4

Pressure Distribution Module

4.1 Introduction

High pressure occurs at the roll and workpiece interface during rolling process. For evaluating this pressure distribution Pressure distribution module has been developed. This module consists of a semi-analytical model for predicting pressure and friction stress distributions based on slab method in plate rolling given by Christensen et al. [57]. Following assumptions have been made

1. homogeneous deformation
2. plane strain deformation
3. rigid roll surface
4. constant friction factor
5. rigid plastic material for workpiece
6. von Mises' yield criterium

Christensen et al. [57] in their study use both initial and final strip thicknesses of the workpiece (strip). Initial thickness (y_o) refers to the thickness of workpiece before deformation whereas final thickness (y_f) refers to the thickness of workpiece

after passing through the roll gap. Since in present study the exit strip gauge will also be controlled; therefore, only initial strip thickness should be present in the analysis so that after calculating the deformed roll diameter, final strip thickness could be evaluated. The model given by [57] has been modified by using the initial workpiece thickness (y_o), following relation has been developed from the geometry of Figure 4.1

$$y = y_o + 2R(\cos\theta_T - \cos\theta) \tag{4.1}$$

where y is any arbitrary strip thickness at the bite region, θ_T is the total bite angle and θ is any arbitrary angle. Finally, the friction stress obtained from this module will be used in getting friction heat flux generated at the interface. Formulation of basic governing equation is given below.

4.1.1 Governing differential equations:

Referring to the element shown in Figure 4.2, the static equilibrium equations can be written as for equilibrium in x direction [57]

$$d(\sigma_x y) + 2P\tan\theta dx \pm 2\tau dx = 0 \tag{4.2}$$

and for equilibrium in y direction [57]

$$\sigma_y dx + Pdx \mp \tau\tan\theta dx = 0 \tag{4.3}$$

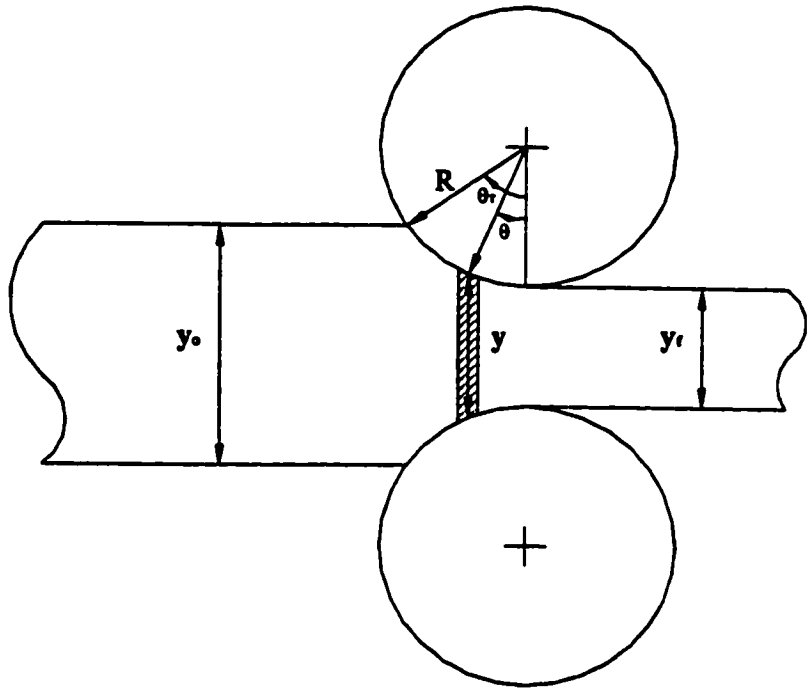

Figure 4.1: Free body diagram for strip geometry.

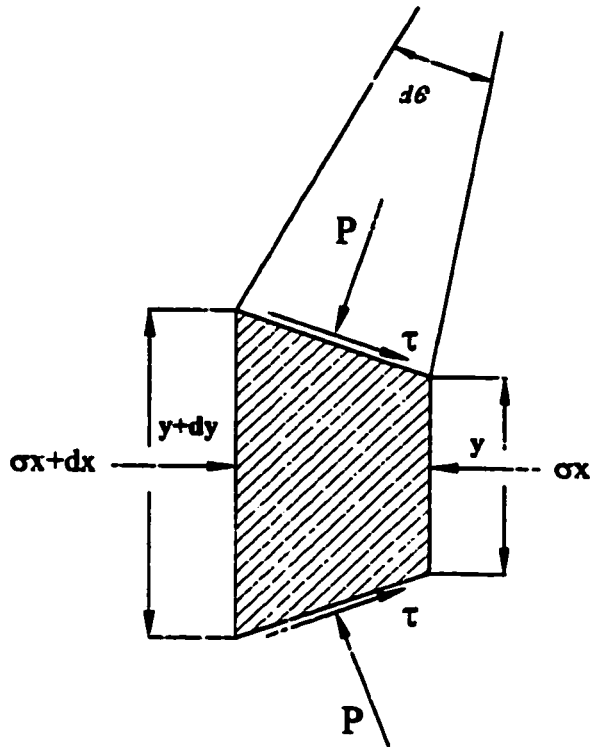

Figure 4.2: Free body digram of strip slab taken from the entry side of the roll gap.

where the upper sign corresponds to the exit zone and the lower sign corresponds to the entry zone of the roll gap.

Since deformation is homogeneous therefore internal shearing will not occur, thus one can assume σ_x and σ_y to be principal stresses and inserting in von Mises' yield criterion gives the following physical condition

$$\sigma_x - \sigma_y = \frac{2}{\sqrt{3}}\sigma_o = S_o \tag{4.4}$$

where S_o is yield stress in plane strain, inserting equation (4.4) in equation (4.3) gives

$$\sigma_x = S_o - P \pm \tau \tan\theta \tag{4.5}$$

by substituting equation (4.5) in equation (4.2) we get

$$d\left[(S_o - P \pm \tau \tan\theta)\, y\right] + 2P \tan\theta dx \pm 2\tau dx = 0 \tag{4.6}$$

from the geometry of Figure 4.1 we have

$$y = y_o + 2R(\cos\theta_T - \cos\theta) \tag{4.7}$$

differentiating above equation (4.7) with respect to θ will give

$$dy = 2R \sin\theta d\theta \tag{4.8}$$

also we have

$$dx = R\cos\theta d\theta \tag{4.9}$$

by using equations (4.7), (4.8), and (4.9) in equation (4.6), we get

$$\pm\frac{d\tau}{d\theta}\tan\theta y + \frac{dS_o}{d\theta}y - \frac{dP}{d\theta}y + 2RS_o\sin\theta \pm \tau\sec^2\theta(y_o + 2R\cos\theta_T) = 0 \tag{4.10}$$

The above equation has been used for evaluating pressure distribution at the interface. In this equation the expressions for friction stress (τ) are subtituted.

4.2 Friction stress

Friction occurred at the tool (roll) and workpiece interface which results in friction stress. For modeling friction effects, traditionally Amonton's law $\tau = \mu p$, full stiction $\tau = S_o$ or a combination of these two has been widely used. Wanheim and Bay $[58-60]$, have shown that neither of these two laws are usually valid. Figure 4.3 shows their general model for friction. Gerved [61] developed an approximated analytical expression for the friction curves that are given by [57]

$$\tau = \mu p \tag{4.11}$$

for pressure less than limit of proportionality that is $p \leq p'$ and

$$\tau = \tau' + (0.5S_o f - \tau')(1 - exp((p' - p)C_3)) \tag{4.12}$$

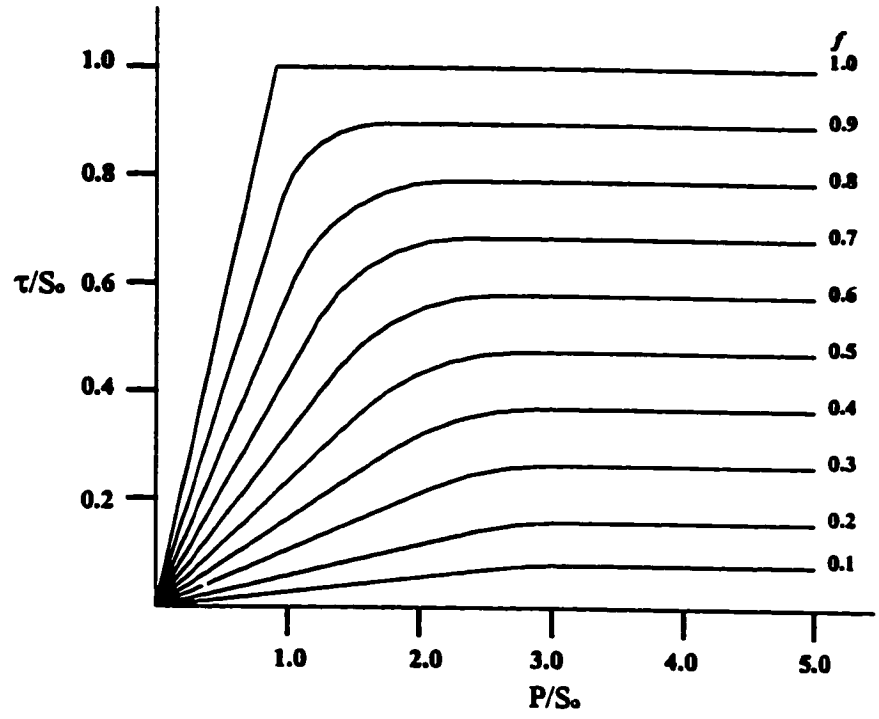

Figure 4.3: Friction stress as a function of normal stress and friction factor [57].

for pressure less than limit of proportionality that is $p \leq p'$ and

$$\tau = \tau' + (0.5S_o f - \tau')(1 - exp((p' - p)C_3)) \tag{4.12}$$

holds for pressure greater than limit of proportionality that is $p \geq p'$, where p' and τ' represent the limit of proportionality, given by

$$\begin{aligned} p' &= \sqrt{3}S_o \\ \tau' &= 0.5S_o(1 - \sqrt{1 - f}) \text{ and} \\ C_3 &= \frac{\tau'}{p'(0.5S_o f - \tau')} \end{aligned} \tag{4.13}$$

f is friction factor related to the coefficient of friction μ with the following relation [57]

$$\mu = \frac{f}{1 + \frac{\pi}{2} + \cos^{-1} f + \sqrt{1 - f^2}} \tag{4.14}$$

by using expressions for friction stress equation (4.11) and (4.12) in equation (4.10), the equations for low ($p \leq p'$) and high ($p \geq p'$) normal pressures can be obtained [57].

4.3 Ordinary differential equations for low and high pressures

Following two equations have been obtained by incorporating friction stress equations in equation (4.10).

4.3.1 For Low Pressure:

When pressure remains up to the limit of proportionality that is $p \leq p'$, the following relation is derived for calculating pressure distribution.

$$\frac{dP}{d\theta} = M_1(\theta)P(\theta) - M_2(\theta) \tag{4.15}$$

where

$$M_1(\theta) = \frac{\pm\mu(y_o + 2Rcos\theta_T)(1 + tan^2\theta)}{(\mp\mu tan\theta - 1)(C_4 - 2Rcos\theta)} \tag{4.16a}$$

$$M_2(\theta) = \frac{2S_oRsin\theta + \frac{dS_o}{d\theta}(C_4 - 2Rcos\theta)}{(\pm\mu tan\theta - 1)(C_4 - 2Rcos\theta)} \tag{4.16b}$$

$$C_4 = y_o + 2Rcos\theta_T \tag{4.16c}$$

4.3.2 For High Pressure:

When pressure crosses the limit of proportionality that is $p \geq p'$, the following relation is derived.

$$\frac{dP}{d\theta} = N_1(\theta) - N_2(\theta) \tag{4.17}$$

where

$$N_1(\theta) = \frac{\mp(C_1 - C_2 exp((p' - p)C_3))C_4(1 + tan^2\theta)}{C_2C_3 tan\theta exp((p' - p)C_3)(C_4 - 2Rcos\theta) - (C_4 - 2Rcos\theta)} \quad (4.18a)$$

$$N_2(\theta) = \frac{2S_oRsin\theta\frac{dS_o}{d\theta}(C_4 - 2Rcos\theta)}{C_2C_3 tan\theta exp((p' - p)C_3)(C_4 - 2Rcos\theta) - (C_4 - 2Rcos\theta)} \quad (4.18b)$$

$$C_1 = \tau' + (0.5S_of - \tau') \quad (4.18c)$$

$$C_2 = 0.5S_of - \tau' \quad (4.18d)$$

$$C_3 = \frac{\tau'}{p'(0.5S_of - \tau')} \quad (4.18e)$$

$$C_4 = y_o + 2Rcos\theta_T \quad (4.18f)$$

By introducing friction stress equations, the governing equations are developed for low and high pressure ranges. Friction stress equation (4.11) gives differential equation (4.15) for low pressure range which is linear, whereas friction stress equation (4.12) results in non-linear differential equation (4.17) for high pressure range. The pressure and friction stress evaluated from pressure module will be used as mechanical loads in deformation analysis of the roll.

4.3.3 Boundary conditions

The boundary conditions for evaluating the integration constants have been obtained by utilizing Mohr's circle [57]. If front tension σ_f is applied at the out coming strip from the roll bite then for exit section we get

$$\left(\frac{S_o}{2}\right)^2 = (\mu P)^2 + \left(P - \left(\frac{S_o}{2} - \sigma_f\right)\right)^2 \quad (4.19)$$

where σ_f is the front tension, upon simplification the following relation is obtained for exit section

$$P(\theta = \theta_T) = \frac{S_o - 2\sigma_f + \sqrt{(S_o - 2\sigma_f)^2 - 4(1+\mu^2)(\sigma_f^2 - S_o\sigma_f)}}{2(1+\mu^2)} \tag{4.20}$$

a similar boundary condition has been obtained for entry zone but only front tension has to be replaced by the back tension σ_b, mathematically

$$P(\theta = 0) = \frac{S_o - 2\sigma_b + \sqrt{(S_o - 2\sigma_b)^2 - 4(1+\mu^2)(\sigma_b^2 - S_o\sigma_b)}}{2(1+\mu^2)} \tag{4.21}$$

4.3.4 Strain hardening

Authors [57] assumed strain hardening of the deforming material according to the Swift equation [3]

$$\overline{\sigma} = K(\epsilon_o + \bar{\epsilon})^n \tag{4.22}$$

where $\overline{\sigma}$ is von Mises effective stress, K is strength coefficient, ϵ_o is pre-strain, n is strain hardening exponent and $\bar{\epsilon}$ is von Mises effective strain. Yield stress in plane strain S_o can be written as

$$S_o = \frac{2}{\sqrt{3}} K(\epsilon_o + \bar{\epsilon})^n \tag{4.23}$$

Von Mises (*average*) effective strain for plane strain deformation is given by

$$\bar{\epsilon} = \frac{2}{\sqrt{3}} ln \left(\frac{y_o}{y_o + 2R\,(cos\theta_T - cos\theta)} \right) \tag{4.24}$$

where S_o is yield stress in plane strain, f is friction factor, y_o is initial strip thickness. Figure 4.4 describes the way of obtaining pressure distribution.

4.4 Description of Pressure Module

Main governing differential equation (4.10) will be used for calculating pressure distribution at the interface. By introducing friction stress equations the governing equations have been developed for low and high pressure ranges. Substitution of friction stress equation (4.11) gives differential equation (4.15) for low pressure range which is linear. While subtitution of friction stress equation (4.12) results in non-linear differential equation (4.17) for high pressure range. Finally, these two equations have been solved numerically to get pressure distribution by fourth order Runge-Kutta method. The point at which pressure becomes maximum at the interface, indicates the location of neutral point.

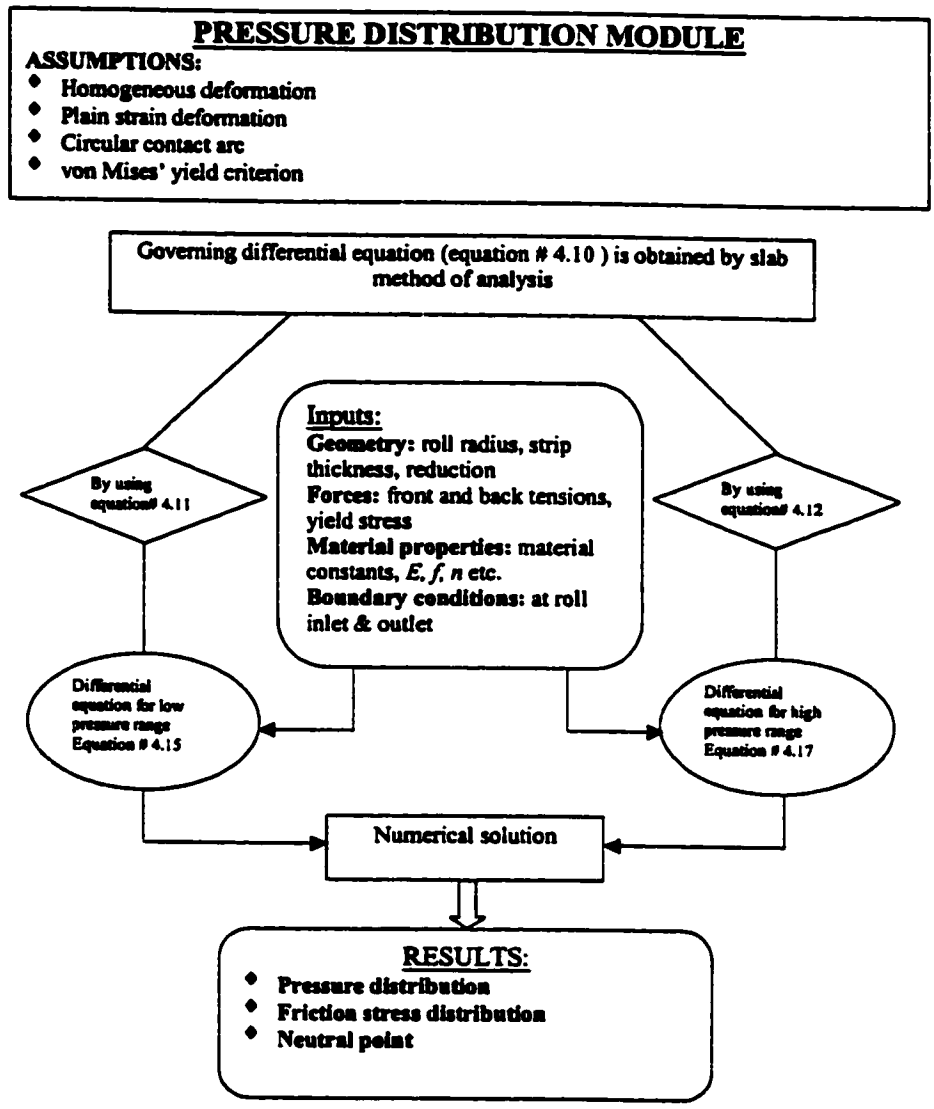

Figure 4.4: Pressure distribution module.

Chapter 5

Heat Flux Module

5.1 Introduction

As it has been mentioned earlier that large amount of heat is generated in metal deformation processes. This heat results in a temperature rise of tool and workpiece. Heat transferred to the roll is not remained constant over the whole bite region and based on previous discussion the assumption of uniform heat flux into the roll is not valid. Present analysis is pragmatic in this aspect that it considers non-linear heat flux distribution at the interface. In current work, distributions of friction and deformation energies at the bite region have also been evaluated. Semi-analytical model for evaluating friction heat flux at the interface and deformation heat generation rate in the workpiece have been developed and presented in this chapter.

5.2 Friction heat flux model

This model is developed on the basic approach given by Roberts [6] and Koot [62], which is based on the following relation for friction heat flux

$$q_f = \tau . V_{rel} \tag{5.1}$$

where τ is friction stress, V_{rel} is relative slipping velocity and q_f is friction heat flux. Friction stress obtained from pressure module will be utilized in evaluating friction heat flux at the interface. The model given by [6] and [62] have been modified by using friction stress expressions of Gerved [61] given as

$$\tau = \mu p \tag{5.2}$$

for friction stress less than limit of proportionality i.e. $\tau \leq \tau'$ and

$$\tau = \tau' + (0.5 S_o f - \tau')(1 - exp((p' - p)C_3)) \tag{5.3}$$

for pressure greater than limit of proportionality i.e. $\tau \geq \tau'$. Where p' and τ' represent the limit of proportionality as

$$\begin{aligned} p' &= \sqrt{3} S_o \\ \tau' &= 0.5 S_o \left(1 - \sqrt{1 - f}\right) \end{aligned} \tag{5.4}$$

the magnitude of relative slipping velocity V_{rel} can be obtained as

$$V_{rel} = V_s - V_r \tag{5.5}$$

where strip velocity V_s has been calculated by the continuity of mass. From entry zone up to neutral point it can be expressed as

$$V_s.y = V_r.y_n \tag{5.6}$$

and from neutral point up to exit zone

$$V_r.y_n = V_s.y \tag{5.7}$$

where y is any arbitrary strip height and y_n is the strip height at neutral point, given by

$$y = y_o + 2R(\cos\theta_T - \cos\theta) \tag{5.8a}$$

$$y_n = y_o + 2R(\cos\theta_T - \cos\theta_n) \tag{5.8b}$$

where y_o is strip height at the entry section, θ_T is the total bite angle, θ_n is the angle of neutral point obtained from pressure module. Using above mentioned relations from equations (5.6) to (5.8*b*) into equation (5.5) will give

$$V_{rel} = \frac{2V_r R(\cos\theta_n - \cos\theta)}{y_o + 2R(\cos\theta_T - \cos\theta)} \tag{5.9}$$

Figure 5.1 represents the dimensionless plot of relative slip velocity distribution between roll and strip at the interface region. A zero value occurred at the neutral point that shows both roller and strip have same velocity values at that point

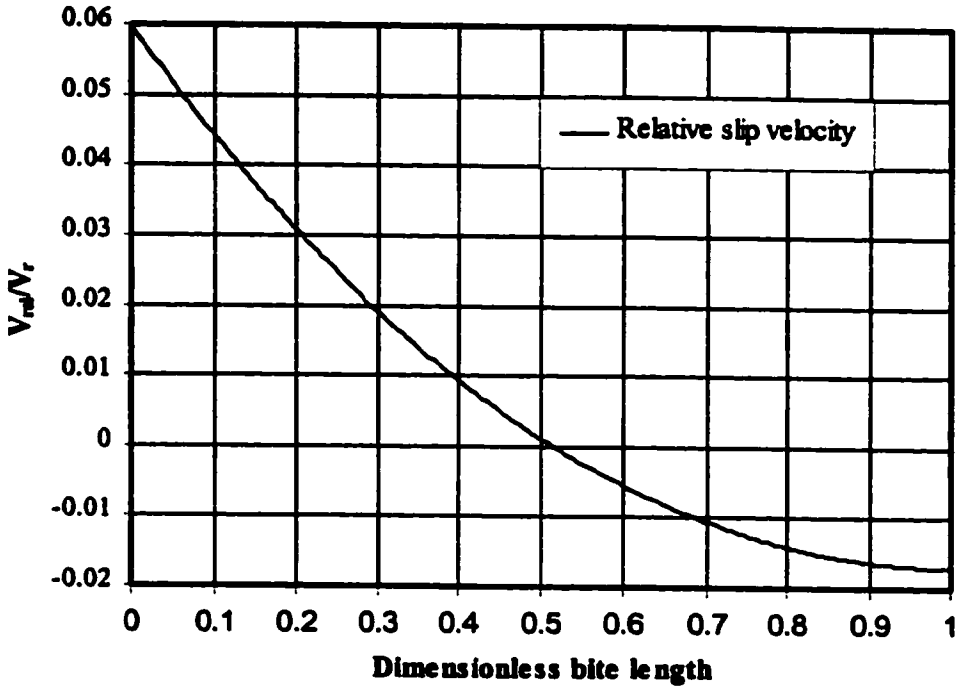

Figure 5.1: Relative slip velocity between roll and strip interface.

5.3 Deformation energy generation rate

Heat is generated in the workpiece because of plastic deformation. Research indicates that almost all of this deformation energy is converted into heat. After conducting a detailed literature review, it has been found that little attention has been given in deformation energy issue. Previous studies [10], [34], [37], [38], [43],and [46] either used integral value of deformation energy or employed direct measured values obtained from a rolling mill. The information available regarding this issue are hazy in the literature.

In this work an analytical expression has been developed in order to obtain distribution of deformation heat generated in workpiece. Considering the following assumptions

1. Rigid plastic material behavior

2. Plane strain deformation

3. All deformation work is converted into heat

An analytical expression has been obtained for evaluating deformation heat generation rate per unit volume in the workpiece for rolling process. Consider a small strip element of volume dV between the roll gap that has initial height y_1 and after deforming its height becomes y_2. If $\overline{\sigma}$ is the mean true stress, $\dot{\overline{\epsilon}}$ is the mean strain rate then for this element, rate of deformation work (or energy generation rate) can

be expressed as

$$\dot{E}_D = \int_v \bar{\sigma}\, \dot{\bar{\epsilon}}\, dV \tag{5.10}$$

where $\dot{E}_D$ is the deformation energy generation rate. Since element is small; therefore, stress and strain variations can be assumed independent of volume change. Thus, rate of deformation work per unit volume can be expressed as

$$e = \bar{\sigma}\, \dot{\bar{\epsilon}} \tag{5.11}$$

As discussed in Chapter 4, strain hardening of the material is assumed to be in accordance with the Swift equation so that prior cold working effects can be incorporated. The Swift equation is given by [3]

$$\bar{\sigma} = K(\epsilon_o + \bar{\epsilon})^n \tag{5.12}$$

by using Swift equation (5.12) into equation (5.11), the resulting deformation energy rate per unit volume is given by

$$e = K(\epsilon_o + \bar{\epsilon})^n\, \dot{\bar{\epsilon}} \tag{5.13}$$

The von Mises effective strain ($\bar{\epsilon}$) and effective strain rate $\left(\dot{\bar{\epsilon}}\right)$can be written as

$$\bar{\epsilon} = \frac{2}{\sqrt{3}}\epsilon_1 \tag{5.14}$$

$$\dot{\bar{\epsilon}} = \frac{2}{\sqrt{3}}\dot{\epsilon}_1 \tag{5.15}$$

substitution of equations (5.14) and (5.15) into equation (5.13) gives

$$e = \frac{2}{\sqrt{3}}K\left(\epsilon_o + \frac{2}{\sqrt{3}}\epsilon_1\right)^n \dot{\epsilon}_1 \tag{5.16}$$

where stain ϵ_1, and strain rate $\dot{\epsilon}_1$ for small strip element in the rolling process can be expressed as

$$\epsilon_1 = ln\left(\frac{y_1}{y_2}\right) \tag{5.17}$$

$$\dot{\epsilon}_1 = \frac{\epsilon_1}{time} = \frac{V_s}{\Delta l} ln\left(\frac{y_1}{y_2}\right) \tag{5.18}$$

where y_1 is elemental initial height, y_2 is elemental final height, Δl is the width of elemental region and V_s is the velocity of that element. By using equations (5.17) and (5.18) in equation (5.16), the deformation energy rate (e) for small strip element

can be expressed as

$$e = \frac{2KV_s}{\sqrt{3}\triangle l}\left(\epsilon_o + \frac{2}{\sqrt{3}} ln\left(\frac{y_1}{y_2}\right)\right)^n ln\left(\frac{y_1}{y_2}\right) \tag{5.19}$$

strip velocity V_s in the bite region is given by equation (5.6)

$$V_s = \frac{V_r y_n}{y} \tag{5.20}$$

finally substituting equation (5.20) into equation (5.19) results in

$$e = \frac{2KV_r y_n}{\sqrt{3}y\triangle l}\left(\epsilon_o + \frac{2}{\sqrt{3}} ln\left(\frac{y_1}{y_2}\right)\right)^n ln\left(\frac{y_1}{y_2}\right) \tag{5.21}$$

Pre-strain coefficient ϵ_o which occurs due to prior cold working remains small. It has been found that neglecting its value does not affect the magnitude of deformation energy significantly ($\pm 0.1\%$). Therefore, for $\epsilon_o \approxeq 0$

$$e = \frac{KV_r y_n}{y\triangle l}\left(\frac{2}{\sqrt{3}} ln\left(\frac{y_1}{y_2}\right)\right)^{n+1} \tag{5.22}$$

where V_r is roll velocity and y_n is strip height at the neutral point. The above derived equation is used for calculating deformation energy rate in the strip at the bite region.

5.4 Description of heat flux module

Figure 5.2 describes the developed module that consists of friction heat flux model and a model for deformation heat generated in the workpiece. Friction heat flux 'q_f'

at the interface has been obtained as a function of various parameters

$$q_f = f(\mu, P, V_{rel}, \tau, y_f, R, \theta_T) \tag{5.23}$$

where μ is the friction coefficient, P is the pressure, V_{rel} is the relative slip velocity, τ is the shear stress, y_f is the final strip thickness, R is the roll radius, θ_T is the bite angle. The deformation energy density rate 'e' has also been calculated as function of different parameters

$$e = f(K, V_s, y_o, y_f, L, R, \theta_T) \tag{5.24}$$

where y_o and y_f are initial and final strip thicknesses. K is strength coefficient, V_s is the strip velocity, L is the arc length. The outputs from heat flux module has been incorporated in the Roll temperature module for predicting roll temperature distribution as shown in Figure 5.2

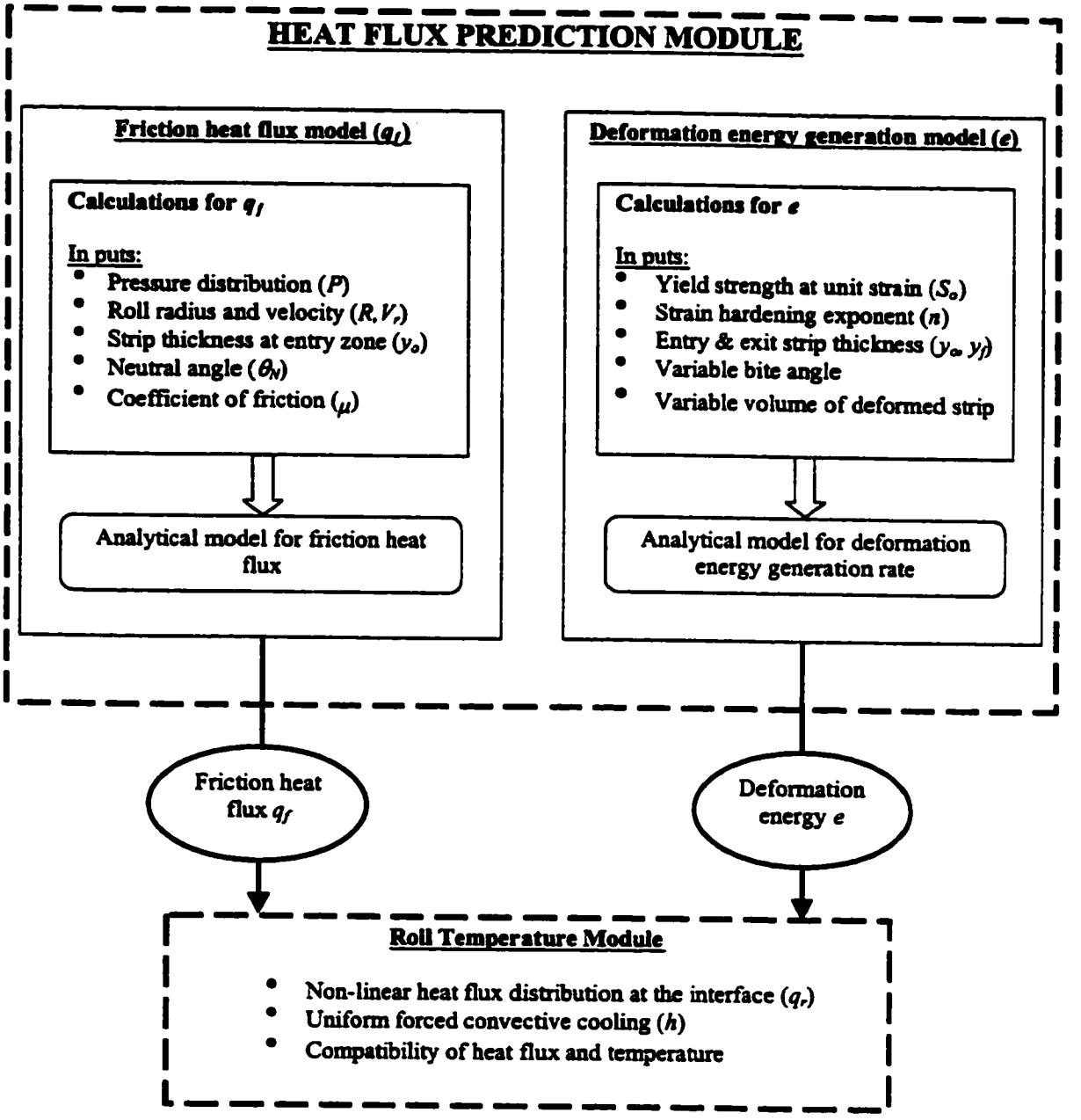

Figure 5.2: Heat flux prediction module

Chapter 6

Temperature Distribution Module

6.1 Introduction

Heat is generated in the rolling process at the roll and workpiece interface due to friction at the contacting surfaces and deformation in the workpiece. This heat flux through the bite region entered towards the roll resulting in roll temperature rise. Understanding of roll temperature is necessary for protecting its life as well as designing proper cooling system. In this chapter temperature distribution over the rotating roll has been predicted. The Temperature module is based on semi-analytical model for calculating temperature distribution over the constant speed rotating cylinder that is subjected to uniform heating and cooling cycles over its surface.

6.2 Importance of non-linear heat flux

As it has been discussed in Chapter 3 that heat flux entered into the roll is not remained uniform over the bite region, Figure 6.1 shows the non-uniform heat flux behavior at the interface. Research indicates that this flux is not remained constant over the whole bite length [6]. Yuen [20] in his investigation recommended that non-uniform heat input should be taken into consideration. It is explicitly crucial because

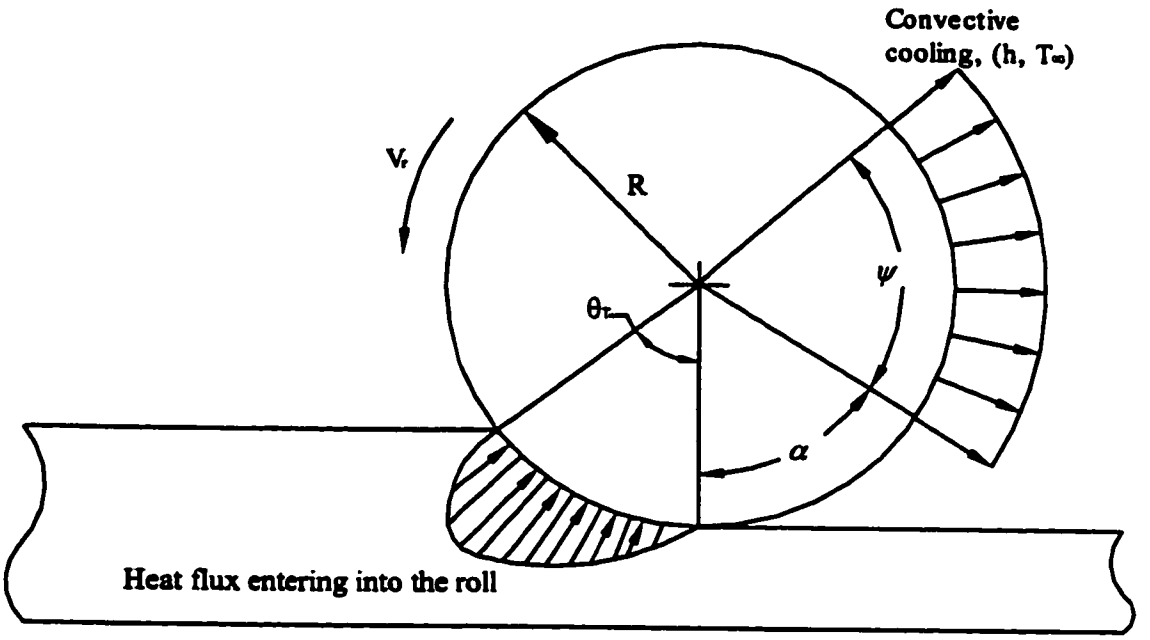

Figure 6.1: Actual heat flux distribution at the bite region.

non-linear heat flux distribution may not only affect the maximum temperature and temperature gradients in the neighborhood of the roll gap but it may also influence the distribution of overall temperature especially in cases when large reduction is required. Roll stress values may also be affected when variable heat flux is introduced in the modeling. In present analysis this non-linear heat flux behavior has been considered.

6.3 Modified Temperature Model

This model is based on the classical work of Patula [17]. The temperature model of [17] was developed by assuming uniform heat flux entered towards the roll. The governing differential equation for steady state two-dimensional heat transfer problem of a cylinder rotating at constant speed with respect to fixed Eulerian coordinates is given by [56]

$$\frac{1}{r}\frac{\partial}{\partial r}\left(r\frac{\partial T}{\partial r}\right)+\frac{1}{r^2}\frac{\partial^2 T}{\partial \theta^2}=\frac{V_r}{a_r R}\frac{\partial T}{\partial \theta} \tag{6.1}$$

where V_r is roll surface speed, h is convective heat transfer coefficient, a_r is thermal diffusivity and R is the roll radius. Here, the interest is to obtain the unknown temperature distribution T, which is temperature difference between the roll and coolant (that is $T = T_r - T_\infty$ where T_r is actual roll temperature and T_∞ is surrounding or coolant temperature). For simulating actual heat flux distribution at the interface, the bite region (where flux enters to the roll) has been divided into 'M' number of small regions and then an assumption of linear variation of heat flux in each small region is made. This approach is appeared to be more realistic and practical, because

it properly models the variation of heat flux at the interface that is not considered by the previous investigators. The modified model is described in Figure 6.2.

6.3.1 Boundary conditions

For the modified roll model, heat flux boundary condition for a single elemental region can be written as

$$-k_r \frac{\partial T_j(R,\theta_j)}{\partial r} = -q^e_{r_j} \qquad \theta_i < \theta < \theta_{i+1} \tag{6.2}$$

where $q^e_{r_j}$ is heat flux entering towards the roll for any arbitrary element j, j is the number of elemental region that varies from $1, 2, ...M$ (*Figure* 6.2), superscript e shows quantity related to the element, subscript i indicates values at nodes of element and varies from $1, 2, ...M+1$ (*Figure* 6.2), k_r is thermal conductivity for roll material. For the whole domain, boundary conditions for the present model will take following form

$$-k_r \frac{\partial T(R,\theta)}{\partial r} = \left\{ \begin{array}{ll} -\sum_{j=1}^{M} q^e_{r_j} & \theta_i < \theta < \theta_{i+1} \\ 0 & \theta_T < \theta < \alpha + \theta_T \\ hT(R,\theta) & \alpha + \theta_T < \theta < \alpha + \theta_T + \psi \\ 0 & \alpha + \theta_T + \psi < \theta < 2\pi \end{array} \right\} \tag{6.3}$$

where M indicates total number of elemental divisions. Following the same assump-

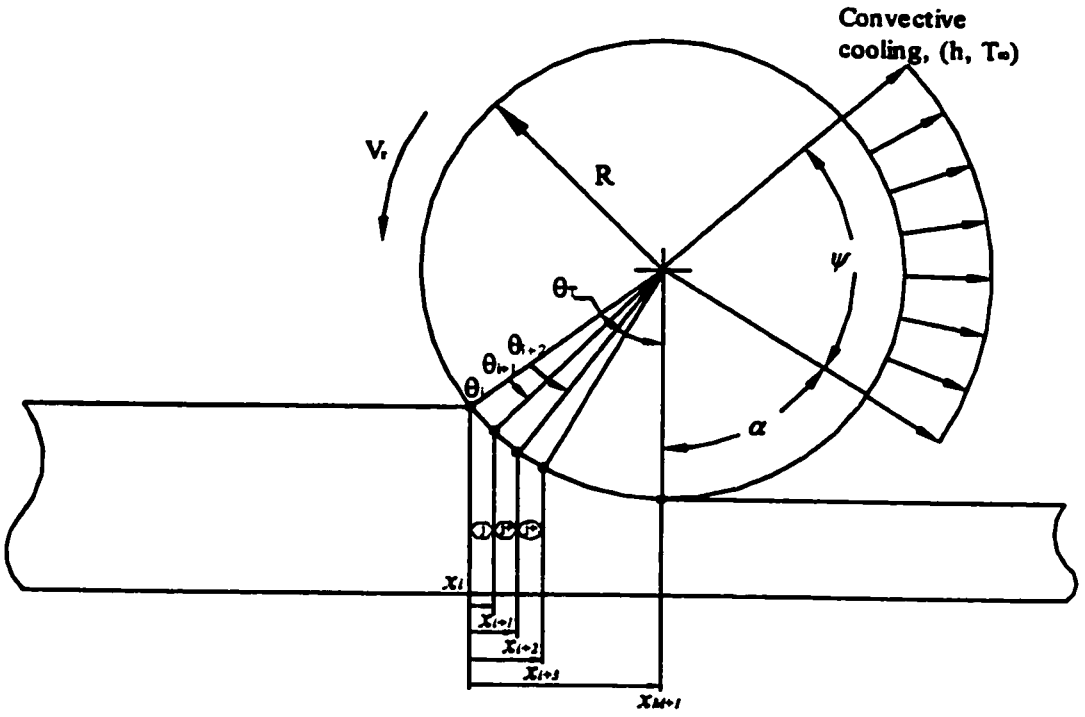

Figure 6.2: Modified roll model showing division of elements.

tion adopted by [17], the solution of differential equation (6.1) can be written as

$$T = \Re(r)e^{in\theta} \tag{6.4}$$

where $\Re(r)$ is a complex function. Using equation (6.4) in equation (6.1) will give

$$r^2\frac{d^2\Re}{dr^2} + r\frac{d\Re}{dr} - \left(i\frac{nV_r}{Ra_r}r^2 + n^2\right)\Re = 0 \tag{6.5}$$

By introducing the following change of independent variable similar to [17]

$$x = \sqrt{\frac{nV_r}{Ra_r}} \tag{6.6}$$

in equation (6.5) will give

$$x^2\frac{d^2\Re}{dx^2} + x\frac{d\Re}{dx} - \left(ix^2 + n^2\right)\Re = 0 \tag{6.7}$$

The general solutions of above equation (6.7) are called Kelvin function and can be found in [63]. The existing solution for the present problem can be written as

$$\Re = ber_n(x) + ibei_n(x) \tag{6.8}$$

where $ber_n(x)$ and $bei_n(x)$ are called real and imaginary parts of Kelvin functions respectively. Kelvin functions are related to the Bessel functions $J_n(x)$, with a complex

argument; that is $J_n\left(xe^{\frac{3ix}{4}}\right) = ber_n(x) + ibei_n(x)$, where $i^2 = -1$.

By using same superposition principle as used by [17], a generic form of solution to the original differential equation (6.1) can be written in the form of equation (6.4)

$$T(r,\theta) = \sum_{n=-\infty}^{\infty} A_n[ber_n(\sqrt{\frac{nV_r}{Ra_r}}r) + ibei_n(\sqrt{\frac{nV_r}{Ra_r}}r)]e^{in\theta} \tag{6.9}$$

where $A_n$is a complex constant. Upon simplification the following form is obtained

$$\begin{aligned} T_r(R,\theta) &= T_\infty + B_o + \sum_{n=1}^{\infty} B_n[ber_n(\lambda_n)cos(n\theta) - bei_n(\lambda_n)sin(n\theta)] \\ &\quad + C_n[ber_n(\lambda_n)sin(n\theta) + bei_n(\lambda_n)cos(n\theta)] \end{aligned} \tag{6.10}$$

where

$$\lambda_n = \sqrt{\frac{nV_rR}{a_r}} = \sqrt{nPe} \tag{6.11}$$

and B_o, B_n and C_n are real constants. Pe is the Peclet number that is proportional to the ratio of bulk heat transfer to the conductive heat transfer$\left(\frac{\textit{bulk heat transfer}}{\textit{conductive heat transfer}}\right)$ and is used in heat transfer in general and forced convection calculations in particular.

The following modified relations have been utilized for transforming the Kelvin functions of negative order and imaginary arguments

$$ber_{-n}(ix) = i^n\left[\cos\left(\frac{3n\pi}{2}\right)ber_n(x) - \sin\left(\frac{3n\pi}{2}\right)bei_n(x)\right] \tag{6.12}$$

$$bei_{-n}(ix) = -i^n\left[\cos\left(\frac{3n\pi}{2}\right)bei_n(x) + \sin\left(\frac{3n\pi}{2}\right)ber_n(x)\right] \tag{6.13}$$

Since solution is in the form of Fourier series with respect to θ, the temperature gradient $\frac{\partial T}{\partial r}\,|_{r=R}$ also represents a Fourier series as a function of θ. Thus, the real constants in equation (6.10) can be evaluated by expanding the boundary condition given by equation (6.3) in Fourier series. According to [17], the right hand side of the boundary condition (6.3), can be written with Fourier series expansion in the following form

$$f(\theta) = \left\{ \begin{array}{ll} -\sum_{j=1}^{M} q_{r_j}^{e} & \theta_i < \theta < \theta_{i+1} \\ 0 & \theta_T < \theta < \alpha + \theta_T \\ hT\,(R,\theta) & \alpha + \theta_T < \theta < \alpha + \theta_T + \psi \\ 0 & \alpha + \theta_T + \psi < \theta < 2\pi \end{array} \right\} \tag{6.14}$$

and

$$f(\theta) = \frac{e_o}{2} + \sum_{m=1}^{\infty} e_m \cos(m\theta) + g_m \sin(m\theta) \tag{6.15}$$

where

$$e_m = \frac{1}{\pi} \int_0^{2\pi} f(\theta) \cos(m\theta)\, d\theta \tag{6.16}$$

$$g_m = \frac{1}{\pi} \int_0^{2\pi} f(\theta) \sin(m\theta)\, d\theta \tag{6.17}$$

The Fourier series expansion of the right hand side of boundary condition is equated with the first order derivative of temperature field T, presented by equation (6.10) and then coefficients of similar trigonometric functions are compared. In this way following system of linear equations has been generated for calculating set of unknown constants.

$$\begin{bmatrix} [F_1]_{1\times 1} & [G_1(n)]_{1\times n} & [H_1(n)]_{1\times n} & [Q_1]_{1\times j} \\ [F_2(m)]_{m\times 1} & [G_2(m,n)]_{m\times n} & [H_2(m,n)]_{m\times n} & [Q_2(m)]_{m\times j} \\ [F_3(m)]_{m\times 1} & [G_3(m,n)]_{m\times n} & [H_3(m,n)]_{m\times n} & [Q_3(m)]_{m\times j} \end{bmatrix} \begin{Bmatrix} [B_o]_{1\times 1} \\ [B_N]_{n\times 1} \\ [C_N]_{n\times 1} \\ [\overline{q}_{r_j}]_{j\times 1} \end{Bmatrix} = 0 \tag{6.18}$$

where B_o, B_N, C_N and $\overline{q}_{r_j}$ are sets of unknown constants. The average roll heat flux over an elemental region is $\overline{q}_{r_j} = \int_{\theta_i}^{\theta_{i+1}} q_{r_j}^e d\theta$. The above system of equations (6.18) has four sets of unknown constants along with three sets of linear equations. In order to solve this system of equations another set of linear equation is needed, which comes out from compatibility condition.

6.3.2 Compatibility condition

In a perfect contact temperature at any material point of roll surface in the bite region is equal to the corresponding material point on the strip surface. Tseng et al. [34] discussed compatibility of temperatures at the interface during rolling of metals. They mentioned that, though, pressure is very high; some coolant film or

scale could be accumulated in the interface that generates a non-perfect contact and thermal resistance for this case needs to be considered. It was discussed that the compatibility of temperature at the interface can be expressed as

$$T_s\,|_{y=y_e} = T_r\,|_{r=R}\,.C \tag{6.19}$$

where $T_r\,|_{r=R}$ is temperature for the outer roll surface at the bite region, $T_s\,|_{y=y_e}$ is strip surface temperature at the bite region and C is thermal resistance parameter which should be calculated experimentally. By assuming a perfect contact between the roll and strip, a value of $C = 1$ has been set in the present analysis.

Compatibility of heat flux should have to be satisfied at the interface. From the physics of problem, it is obvious that heat flux out of strip plus friction heat flux must be equal to the roll heat flux, i.e.,

$$q_r = q_s + q_f \tag{6.20}$$

where q_s is heat flux for strip, q_f is heat flux generated due friction at the interface, q_r is heat flux entering to the roll. For using compatibility of temperature,we need strip temperature distribution at the bite region along with roll temperature distribution.

A contribution in compatibility condition is that it has been developed for each single element; that is, first the bite region has been divided into 'M' number of elemental regions then roll and strip temperature equations have been evaluated for each element. For a single element the modified forms of above two compatibility

equations are given as

$$T_{s_j} \mid_{y=y_{a_j}} = T_{r_j} \mid_{r=R} .C_j \tag{6.21}$$

$$\bar{q}_{r_j} = \bar{q}_{s_j} + \bar{q}_{f_j} \tag{6.22}$$

where subscript j is the number of elemental region that varies from $1, 2, ...M$ (*Figure* 6.2), y_{a_j}.is the height of elemental region j and bar represents elemental average.

6.3.3 Strip Temperature Model

As the requirement of compatibility of temperature at the interface, workpiece (strip) temperature distribution needs to be evaluated. For this purpose, the analytical model given by Tseng et al. [34] is utilized, again this model has also been modified for 'M' number of regions as shown in Figure 6.2. Mathematically the governing partial differential equation for strip temperature is given by [56]

$$\frac{\partial^2 T_s}{\partial y^2} - \frac{V_s}{a_s}\frac{\partial T_s}{\partial x} + \frac{e}{k_s} = 0 \tag{6.23}$$

with the division of strip into 'M' number of small elements at the bite region the boundary conditions for a single element will become

$$T_{s_j}(x_i, y) = T_{s_{j-1}}(x_i, y) \qquad 0 \le y \le y_{a_j} \qquad (6.24a)$$

$$\frac{\partial T_{s_j}(x,0)}{\partial y} = 0 \qquad x_i \le x \le x_{i+1} \qquad (6.24b)$$

$$-k_s \frac{\partial T_{s_j}(x, y_{a_j})}{\partial y} = \sum_{j=1}^{M} \overline{q}^e_{s_j} \qquad x_i \le x \le x_{i+1} \qquad (6.24c)$$

where $\overline{q}^e_{s_j}$ is the uniform heat flux out of single strip element. It is linearly varying in the small elemental region, mathematically $\overline{q}^e_{s_j} = \int_{x_i}^{x_{i+1}} q^e_{s_j} dx$. y_{a_j} is elemental strip height and T_{s_j} elemental strip temperature. By solving above system of equations, the following expression for evaluating strip temperature distribution is obtained

$$T_{s_j} = T_{s_{j-1}} + \left(e_j - \frac{\overline{q}_{s_j}}{y_{a_j}}\right) \frac{a_s (x - x_{i-1})}{k_s V_{s_j}} + \frac{\overline{q}_{s_j} \overline{y}_{a_j}}{2k_s} \left[\frac{1}{3} - \left(\frac{y}{y_{a_j}}\right)^2\right] + \frac{4}{\pi^2} \left(\frac{\overline{q}_{s_j} y_{a_j}}{2k_s}\right) \sum_{n=1}^{\infty} \frac{(-1)^2}{n^2} exp\left[-\left(\frac{n\pi}{y_{a_j}}\right)^2 \frac{a_s (x - x_{i-1})}{V_{s_j}}\right] cos\left(\frac{n\pi y}{y_{a_j}}\right) \qquad (6.25)$$

By using compatibility of temperature and heat flux given by equations (6.21) and (6.22), following equation is obtained

$$\left[[F_j]_{j\times 1} \quad [G_j(n)]_{j\times n} \quad [H_j(n)]_{j\times n} \quad [Q_j]_{j\times j} \right] \left\{ \begin{array}{c} [B_o]_{1\times 1} \\ [B_N]_{n\times 1} \\ [C_N]_{n\times 1} \\ [\overline{q}_{r_j}]_{j\times 1} \end{array} \right\} = \{[P_j]_{j\times 1}\} \qquad (6.26)$$

Combining equations (6.25) and (6.17) will result in

$$\begin{bmatrix} [F_1]_{1\times1} & [G_1(n)]_{1\times n} & [H_1(n)]_{1\times n} & [Q_1]_{1\times j} \\ [F_2(m)]_{m\times1} & [G_2(m,n)]_{m\times n} & [H_2(m,n)]_{m\times n} & [Q_2(m)]_{m\times j} \\ [F_3(m)]_{m\times1} & [G_3(m,n)]_{m\times n} & [H_3(m,n)]_{m\times n} & [Q_3(m)]_{m\times j} \\ [F_j]_{j\times1} & G_j(n)]_{j\times n} & [H_j(n)]_{j\times n} & [Q_j]_{j\times j} \end{bmatrix} \begin{Bmatrix} [B_o]_{1\times1} \\ [B_N]_{n\times1} \\ [C_N]_{n\times1} \\ [\overline{q}_{r_j}]_{j\times1} \end{Bmatrix} = \{[P_j]_{j\times1}\} \tag{6.27}$$

Once constants are known, equation (6.10) will be used to obtain the temperature distribution over the roll. It should be noted that there are two unknown parameters that exist in strip temperature (T_{s_j}) expression, equation (6.25); one is friction heat (q_f) and other is deformation heat (e) energy. In current study distributions of friction and deformation energies at the bite region have been evaluated. Semi-analytical model for evaluating friction heat flux at the interface and deformation heat generation rate in the workpiece have been developed as discussed in Chapter five. A FORTRAN computer code is developed for determining the sets of unknown constants in the above system, which will be discussed in Chapter eight of Results and Discussions.

Chapter 7

Roll Deformation Module

7.1 Introduction

In its beginning epoch, rolling theories assumed that roll remained rigid when comes in contact with the workpiece. This assumption can be justified while analyzing rolling of soft material with large reduction, but for rolling of tough material or thin sheets, this assumption is not valid because roll flattening occurs. In roll flattening phenomenon, when roll comes in contact with the workpiece it becomes flatten and the arc of contact is increased considerably. This type of behavior occurs only in temper rolling. For normal rolling condition, the work roll appears to deform in such a way that the arc of contact is generally regarded as possessing a curvature corresponding to a deformed work roll radius R' which is larger than the actual roll radius [6]. Thus, it is said that roll and strip deformation is highly coupled. Contact stresses and thermal load occurred due to strip contact, result in roll deformation. Finally, any change in the roll profile or shape directly affects the product. Product's shape could be distorted, its final size would be changed and surface finish would also be ruined. In order to control the required output specifications, careful analysis of roll deformation is the key. Once deformed roll diameter is known, one can predict the required strip thickness. Also roll flattening has significant effects on rolling force

estimation in rolling of thin gauge strip. In addition to this, information about strains and stresses in the roll is necessary for evaluating whether yielding of the roll material is occurred. Therefore, by considering these aspects roll deformation analysis has been performed in this module.

7.1.1 Modeling Roll Deformation Effects

Roll Deformation occurred in rolling process changes the roll bite geometry that finally influence the strip deformation. Many investigators have proposed different techniques for modeling roll/strip deformation coupling effects, a good bibliographic review can be found in [64] and [65]. Hitchcock [66] was the first who calculate the deformed roll radius R' by assuming circular arc of contact at the bite during roll deformation phenomenon. His proposed model is commonly known as Hitchcock formula and is given by [3]

$$R = R'\left(1 + \frac{16\,(1-\nu^2)}{\pi E}\frac{F}{\Delta y}\right) \tag{7.1}$$

where

R = initial roll radius

ν = Poission's ratio

E = Young's modulus of elasticity

Δy = $y_o - y_f$

F = Rolling for per unit width of workpiece

Hitchcock formula has a significant importance in rolling theory. This formula is always used in combining with slab method [64], and an iterative procedure is necessary because of coupling. Ford et al. [67] and Bland et al. [68] modified this relation by introducing the effects of entry and exit elastic zones in the strip and for strip tensions. Alexander [55] provided a classical form of this analysis. From the past until now, this relation is very much utilized in many studies for evaluating deformed roll radius. Good precision and fast computing speed are the marked advantages of using this formula. Off course some limitations are present there, for rolling processes with low reduction and in thin hard strip rolling, the iterative procedure does not converge and the analysis is affected. Jortner et al. [69] used elastic influence functions for modeling roll deformation; they were the first who account non-circular contact arc of the deformed roll surface. Finite element method is also utilized for roll deformation analysis and a review is given in [65]. In current study thermo-elastic finite element analysis has been performed in order to model roll deformation phenomenon and a comparison is made with Hitchcock formula.

7.1.2 Modeling Roll Stresses

Many studies have been done for investigating rolling process, and results have been reported in the literature for predicting temperature distribution in both roll and strip. But for predicting stresses and deformation behavior in rolling process most of the studies limited to the analysis of strip and little attention has been given to the evaluation of roll stresses and deformation behavior. Cerni et al. [27] discussed transient thermal stress problem of hot rolling. By assuming 360 degree

uniform convective cooling and heat input as a line heat source, they developed an infinite series solution for stress distribution of a two dimensional roll model. Troeder et al. [18] studied the same problem of hot rolling given by Cerni et al. [27] with the inclusion of third dimension. They did not provide calculation details; and heat generated due to plastic deformation of strip was not included in the analysis. By employing uniform heat flux distribution at the bite region and convective cooling over the remaining roll portion, Tseng et al. [24] predicted roll thermal stresses. They analyzed thermal stress behavior as steady state and by utilizing general stress function, a traction free roll surface has been modeled which is not considered by Cerni et al. [27]. By considering strip and roll as semi infinite solids, Chang [70] obtained one dimensional steady state solution for thermal stress in the integral form for a rotating roll at high Peclect number. He considered non-uniform heating at the interface occurred due to friction at the interface and plastic deformation in the strip. All above mentioned studies involved roll stress determination by considering thermal only. In current work, roll stresses have been evaluated by considering both thermal and mechanical loads.

7.2 Developed Model

It has been discussed earlier that pressure and friction stress are present at the contact surfaces of roll and workpiece, along with this heat is also generated during metal rolling process, a significant portion of this heat is conducted towards the roll. Consequently, temperature changes occurred in roll and strip and it is necessary that both temperature and mechanical load be considered in analyzing roll deformation phenomenon and evaluating roll stresses. The proposed roll deformation model is more practical and reliable, because it is capable of modeling mechanical as well as thermal load applied over the roll. The proposed algorithm is based on following assumptions:

(1) Roll depth is very long as compare to it diameter thus variations of strains in axial direction are negligible, that is plain strain case

(2) Temperature and stress variations at the roll center are negligible

(3) Roll material behavior remains in elastic range

(4) Properties for roll material are isotropic

A thermoelastic finite element model has been developed by using commercial software ANSYS [71]; the mesh is shown in Figure 7.1. Pressure and friction stress generated at the contact have been used in the analysis with the help of pressure module, so that strip reaction at the roll can be modeled. Along with this, temperature distribution obtained from roll temperature module has also been incorporated in the calculations. Thus, problem has been analyzed thermo-mechanically in order to obtain stresses and deformed roll radius. Following basic stress-strain relations

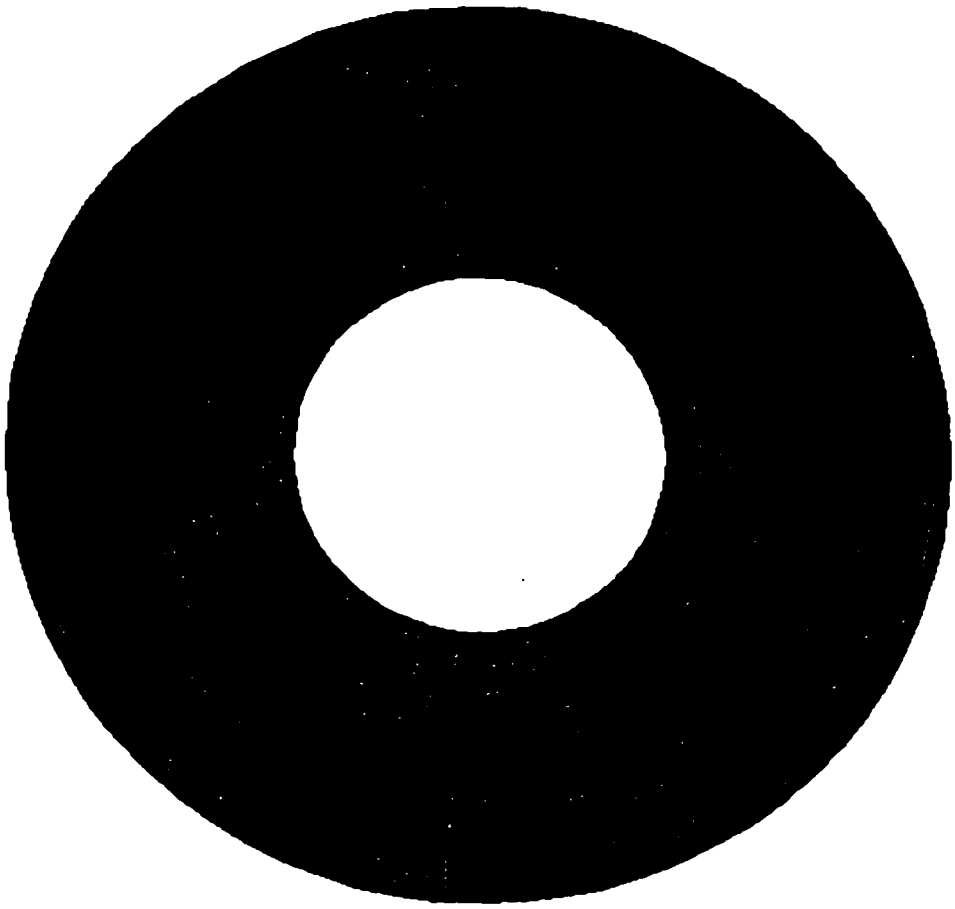

Figure 7.1: Finite element mesh for roll.

used and detailed description of finite element model have been discussed.

7.2.1 Stress modeling

The stress is related to strain by

$$\{\sigma\} = [D]\{\epsilon^e\} \tag{7.2}$$

where σ is the stress vector, D is the elasticity matrix and

$$\{\epsilon^e\} = \{\epsilon\} - \{\epsilon^{th}\} \tag{7.3}$$

where $\{\epsilon\}$ is the total strain vector and $\{\epsilon^{th}\}$ is the thermal strain vector.

Equation (7.2) may also be written as

$$\{\epsilon\} = [D]^{-1}\{\sigma\} + \{\epsilon^{th}\} \tag{7.4}$$

Since the present case is plane strain, and the material is assumed to be isotropic with no initial stress, the above stress-strain relations can be written as

$$\begin{aligned} \epsilon_{rr} &= \frac{1}{E}[\sigma_{rr} - \nu(\sigma_{\theta\theta} - \sigma_{zz})] + \alpha_{th}T \\ \epsilon_{\theta\theta} &= \frac{1}{E}[\sigma_{\theta\theta} - \nu(\sigma_{rr} - \sigma_{zz})] + \alpha_{th}T \\ \epsilon_{r\theta} &= \frac{1}{G}\sigma_{r\theta} \end{aligned} \tag{7.5}$$

where E is the modulus of elasticity, G is the modulus of rigidity, ν is Poisson's ratio,

α_{th} is the coefficient of thermal expansion and T is the temperature rise at a point (x, y) at time t with respect to that at $t = 0$.

A typical component of thermal strain from equation (7.5) is

$$\epsilon^{th} = \alpha_{th} \triangle T = \alpha_{th} (T - T_{ref}) \tag{7.6}$$

where T_{ref} is the reference temperature at $t = 0$.

If α_{th} is a function of temperature, equation (7.6) becomes

$$\epsilon^{th} = \int_{T_{ref}}^{T} \alpha_{th} (T)\, dT \tag{7.7}$$

The present study uses a mean or weighted-average value of α_{th}, so that

$$\epsilon^{th} = \overline{\alpha}_{th} (T) (T - T_{ref}) \tag{7.8}$$

where

$$\overline{\alpha}_{th} (T) = \frac{\int_{T_{ref}}^{T} \alpha_{th} (T)\, dT}{T - T_{ref}} \tag{7.9}$$

Thus, $\overline{\alpha}_{th} (T)$ is the mean value of the coefficient of thermal expansion. The principal

stresses $(\sigma_1, \sigma_2, \sigma_3)$ are calculated from the stress components by the cubic equation

$$\begin{vmatrix} \sigma_{rr} - \sigma_p & \sigma_{r\theta} \\ \sigma_{\theta r} & \sigma_{\theta\theta} - \sigma_p \end{vmatrix} = 0 \tag{7.10}$$

where σ_p is the principal stress.

The von Mises or equivalent stress σ' is computed as

$$\sigma' = \sqrt{\frac{1}{2} \times \frac{1}{2} \left[(\sigma_1 - \sigma_2)^2 + (\sigma_2 - \sigma_3)^2 + (\sigma_3 - \sigma_1)^2 \right]} \tag{7.11}$$

The equivalent stress is related to the equivalent strain through

$$\sigma' = E\epsilon' \tag{7.12}$$

where ϵ' is the equivalent strain.

7.2.2 Calculation procedure for stresses

The standard displacement-based finite element method is used for computing stresses in the roll. The basis of this approach is the principle of virtual work, which states that the equilibrium of any body under loading requires that, for any compatible small virtual displacements (which are zero at the boundary points and surfaces and correspond to the components of displacement that are prescribed at those points and surfaces) imposed on the body in its state of equilibrium, the total internal virtual work or strain energy, δU, is equal to the total external work due to the applied

thermally induced loads, δV, i.e. $\delta U = \delta V$. For the static analysis of problems with linear geometry and thermoelastic material behavior, the following equation can be derived using the standard procedure [72]:

$$\int_v \left(\{\delta\epsilon\}^T [D] \{\epsilon\} - \{\delta\epsilon\}^T [D] \{\epsilon^{th}\} \right) dV = \int_v \{\delta U\}^T \{f^B\} dV + \int_f \{\delta U_s\}^T \{P\} d\mathcal{S} + \sum \{\delta \overline{U}\}^T \{\overline{F}\} \tag{7.13}$$

where $\{f^B\}$ is the applied body force, $\{P\}$ is the applied pressure vector, $\{\overline{F}\}$ is the concentrated nodal force to the element, $\{\delta U_s\}$ is the virtual displacement on the boundary where pressure is prescribed and $\{\delta \overline{U}\}$ is the virtual displacement of boundary nodes where a concentrated load is prescribed.

The strains may be related to the nodal displacement by

$$\{\epsilon\} = [B] \{\overline{U}\} \tag{7.14}$$

where $[B]$ is the strain displacement gradient matrix and $\{\overline{U}\}$ is the vector of displacements within the elements. These are related to the nodal displacement by

$$\{U\} = [N] \{\overline{U}\} \tag{7.15}$$

where $[N]$ is the matrix of shape (or interpolation) functions.

Equation (7.13) can be reduced to the following matrix form:

$$[K_e]\{\overline{U}\} - \{F^{th}\} = \{F^b\} + \{F^s\} + \{\overline{F}\} \tag{7.16}$$

where $[K_e] = \int_v [B]^T [D] [B] \, dV$ is the element stiffness matrix, $[F^{th}] = \int_v [B]^T [D] [\epsilon^{th}] \, dV$ is the element thermal load vector, $[F^b] = \int_v [N]^T \{f^B\} \, dV$ is the body force vector, $[F^s] = \int_f [N_n]^T \{P\} \, d\mho$ is the element pressure vector and $[N_n]$ is the matrix of shape functions for normal displacement at the boundary surface. The assembly of element matrices and vector of equation (7.16) yields

$$[K]\{\overline{d}\} = \{\overline{R}\} \tag{7.17}$$

where $[K]$, $\{\overline{d}\}$ and $\{\overline{R}\}$ are the global stiffness matrix, global nodal displacement vector and global nodal load vector respectively. Solution of the above set of simultaneous algebraic equations gives unknown nodal displacements and reaction forces. Once the displacement field due to temperature rise and mechanical load is known the corresponding strains and stresses can be easily evaluated.

Chapter 8

Results and Discussion

8.1 Introduction

This chapter consists of the implementation of previously discussed modules. Results obtained by performing different parametric studies have been presented. First an algorithm developed for the evaluation of real and imaginary parts of Kelvin function has been discussed and results are compared with the available literature. Than a practical rolling case chosen from the literature is used in order to check the applicability of developed modules and algorithm, and comparisons have been made with the available data.

8.1.1 Temperature algorithm

As discussed earlier, the general solution of equation (6.1) for calculating temperature distribution over the roll is given by equation (8.1)

$$\begin{aligned} T_r(R,\theta) &= T_\infty + b_o + \sum_{n=1}^{\infty} b_n[ber_n(\lambda_n)cos(n\theta) - bei_n(\lambda_n)sin(n\theta)] \\ &\quad + c_n[ber_n(\lambda_n)sin(n\theta) + bei_n(\lambda_n)cos(n\theta)] \end{aligned} \tag{8.1}$$

where

$$\lambda_n = \sqrt{\frac{nV_r R}{a_r}} \tag{8.2}$$

B_o, B_n and C_n are real constants and $ber_n(\lambda_n)$ and $bei_n(\lambda_n)$ are the real and imaginary parts of Kelvin functions, respectively. The real constants can be evaluated by equating first order derivative with respect to radius (r) of above equation (8.1) with expansion of boundary condition in Fourier series and then comparing the coefficients of similar trigonometric functions. Mathematically, infinite number of real constants B_n and C_n can be generated which means that infinite number of linear equations could be formed for calculating these constants. Implementation of this theory is not possible so a finite number of terms (n) must be held on to the series solution. Some authors Patula [17], Yuen [20] and Tseng [25] discussed this issue and reported their results by using different number of terms (n). Tseng [25] investigated in details that how the temperature distribution over roll is affected by varying the number of terms (n) of series expansion. But nobody reported about the expansion of coefficients of Kelvin function that is $ber_n(\lambda_n)$ and $bei_n(\lambda_n)$.

In the analytical solution of roll temperature distribution equation (8.1) , $ber_n(\lambda_n)$ and $bei_n(\lambda_n)$ are ascending series, for a real argument x that can be written as [63]

$$ber_n(x) = \left(\frac{1}{2}x\right) \sum_{k=0}^{\infty} \frac{\cos\left\{\left(\frac{3}{4}n + \frac{1}{2}k\right)\pi\right\}}{k!\Gamma(n+k+1)} \left(\frac{1}{2}x\right)^{2k} \tag{8.3}$$

$$bei_n(x) = \left(\frac{1}{2}x\right) \sum_{k=0}^{\infty} \frac{\sin\left\{\left(\frac{3}{4}n + \frac{1}{2}k\right)\pi\right\}}{k!\Gamma\left(n+k+1\right)} \left(\frac{1}{2}x\right)^{2k} \tag{8.4}$$

where n is real, x is real and non-negative and k is index of infinite series. Unfortunately, the available literature did not clearly mentioned the limitation of above series expansions. In the above equations, computational errors will arise when x becomes large and in some cases the calculated number becomes so big that it crosses the computer memory and computational scheme crashes. Basically, the above mentioned series expansions for Kelvin function will only work for small values of x. For large values of x asymptotic expansion of Kelvin function has to be considered, which is expressed in terms of modulus and phase forms, given by [63]

$$ber_n(x) = M_n \cos\theta_n \tag{8.5}$$

$$bei_n(x) = M_n \sin\theta_n \tag{8.6}$$

where modulus (M_n) is

$$M_n = \frac{e^{\frac{x}{\sqrt{2}}}}{\sqrt{2\pi x}} \left\{1 - \frac{\mu-1}{8\sqrt{2}}\frac{1}{x} + \frac{(\mu-1)^2}{256}\frac{1}{x^2} - \frac{(\mu-1)\left(\mu^2+14\mu-399\right)}{6144\sqrt{2}}\frac{1}{x^3} + O\left(\frac{1}{x^4}\right)\right\} \tag{8.7}$$

and phase (θ_n) is given as

$$\theta_n = \frac{x}{\sqrt{2}} + \left(\frac{1}{2}n - \frac{1}{8}\right)\pi + \frac{\mu-1}{8\sqrt{2}}\frac{1}{x} + \frac{\mu-1}{16}\frac{1}{x^2} - \frac{(\mu-1)(\mu-25)}{384\sqrt{2}}\frac{1}{x^3} + O\left(\frac{1}{x^5}\right) \tag{8.8}$$

In the present study the above two expansions (one for small and other for large argument) have been categorized as method−1 and method−2. Method−1 consists of series expansion given by equations (8.3) and (8.4), whereas method−2 involves calculations for large arguments given by equations (8.5) to (8.8). In all foregoing discussions these two classifications will be used for the series expansions.

In current study a combined ascending-modulus algorithm based on numerical expansion of Kelvin function has been developed, in order to check the validity and limitations of method−1 and method−2. An Un-Coupled case of rolling studied by Tseng [25] has been chosen for implementing the current (algorithm) analysis. The heat input q_r at the bite region of $\theta_T = 10^o$ is assumed to be uniformly distributed and uniform convective cooling h_o over the remaining portion of 350^o is also considered. Forty (40) terms (n) of infinite series solution has been retained for the present analysis whereas Tseng [25] used 200 terms (n) of series solution. Since the argument of Kelvin function is $\sqrt{\frac{nV_rR}{a_r}}$, or more precisely the square root of Peclet number $\sqrt{nPe}$, different studies have been performed by varying Peclet number (Pe) from 10^3 to 10^5 and with Biot number (Bi) equal to 10. Biot number (Bi) did not vary because changing Biot number only produces a shift in overall temperature level.

For Pe numbers 10^3, 10^4 and 10^5 the respective plots of normalized temperature

over the roll surface are shown in Figures 8.1 to 8.6. At Pe $= 10^3$, the temperature curve obtained by method-1 is closed to the one given by Tseng [25] see Figure 8.1 (full view). It is interesting to note that method-1 is also sensitive to k which is the index for $ber_n(\lambda_n)$ and $bei_n(\lambda_n)$ expansions. When we set $k = 40$ the peak of method-1 was below the peak of Tseng [25] but as k increased, the peak also increased and for $k = 77$ the peaks of two curves were almost equal as shown in Figure 8.2 (zoom view). For $k > 77$ the numerical algorithm did not work and crash. Since, in the present analysis only 40 terms has been incorporated, it is expected that a close approximation could be achieved by increasing number of terms (n).

For Pe $= 10^4$, the temperature plots are shown in Figure 8.3 and 8.4. The disagreement between actual curve and the curves of method-1 indicates that for large arguments of Kelvin function method-2 should be used. Although the curve obtained from method-1 indicates a tendency towards the actual curve when k is increased but after a certain limit on k ($k > 63$ for this case)the algorithm crashed. Again, a closed match between present analysis and the curve of Tseng [25] can be obtained when the number of terms (n) for infinite series solution are increased.

At Pe $= 10^5$, the curve of method-2 exactly matches with the curve of [25] (refer to Figure 8.5 and 8.6). This indicates that for relatively large arguments increasing the number of terms (n) in the infinite series solution does not have a significant effect.

On the basis of above discussions it can be concluded that for analyzing a typical rolling process

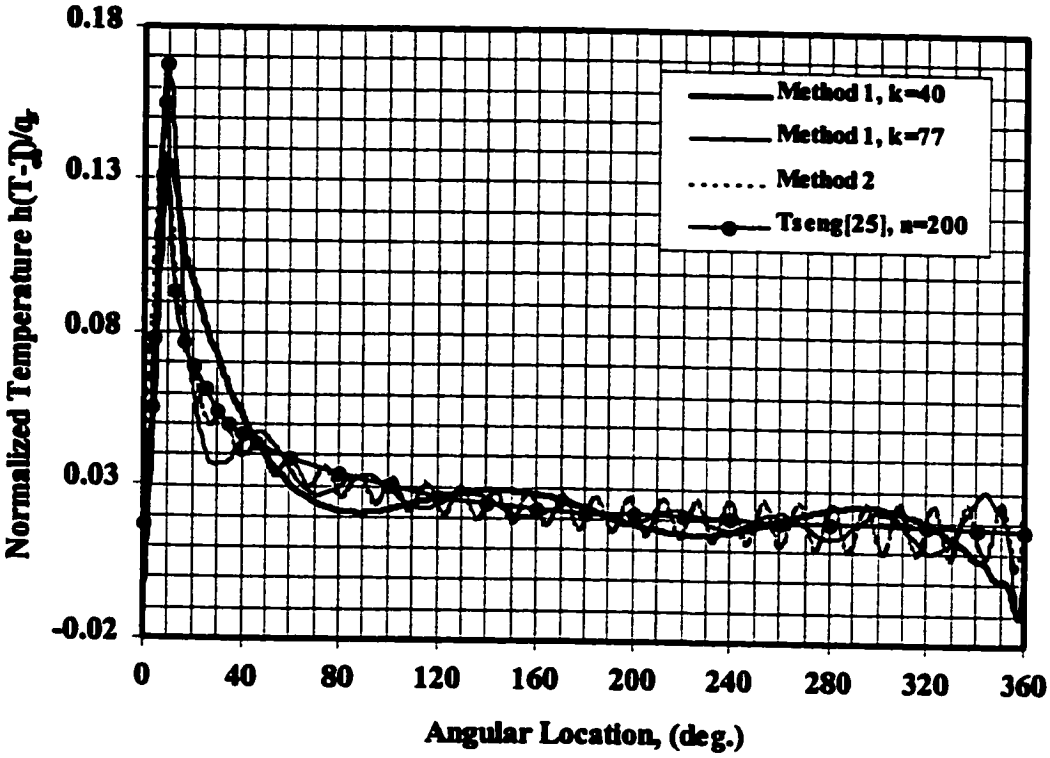

Figure 8.1: Normalized temperature distribution over the roll for Pe = 1000.

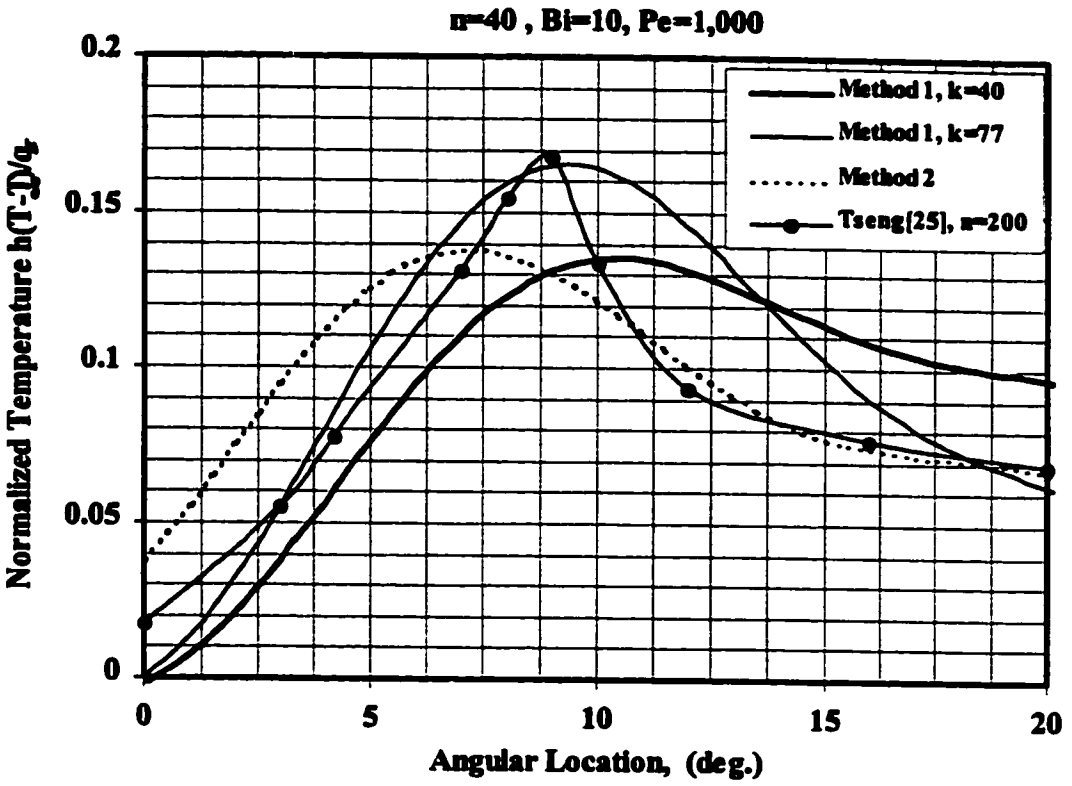

Figure 8.2: Normalized temperature over the roll; zoom view for 20 degrees from the entry side.

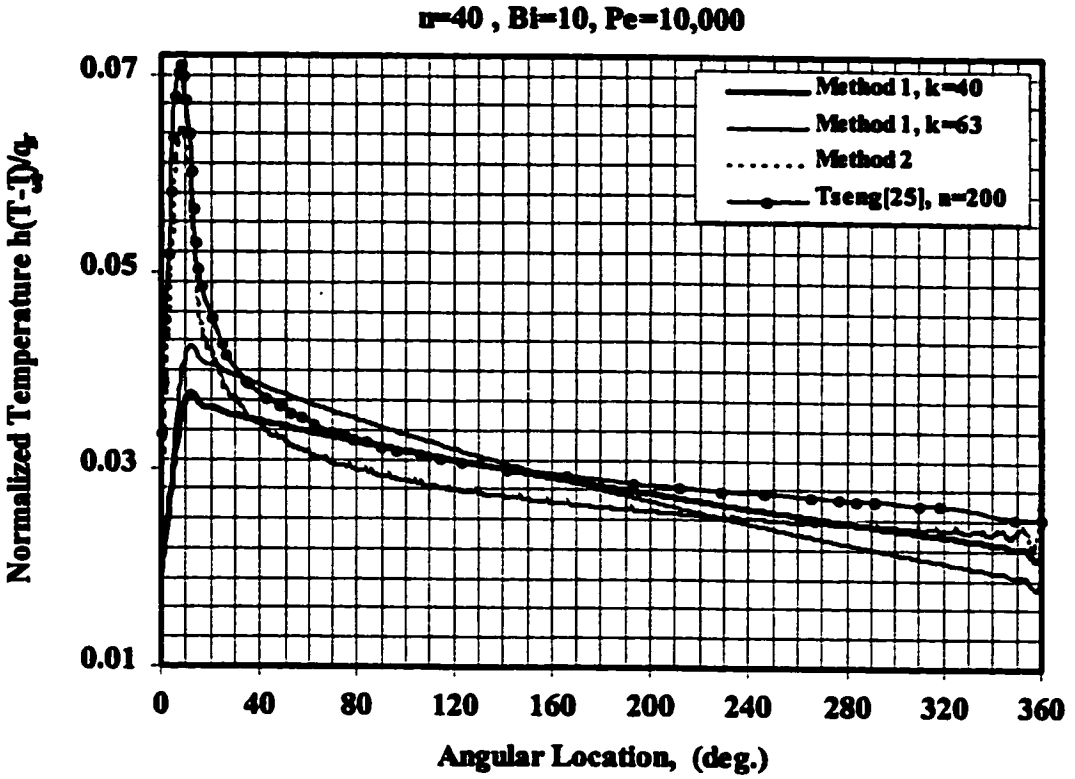

Figure 8.3: Normalized temperature distribution over the roll for Pe = 10,000.

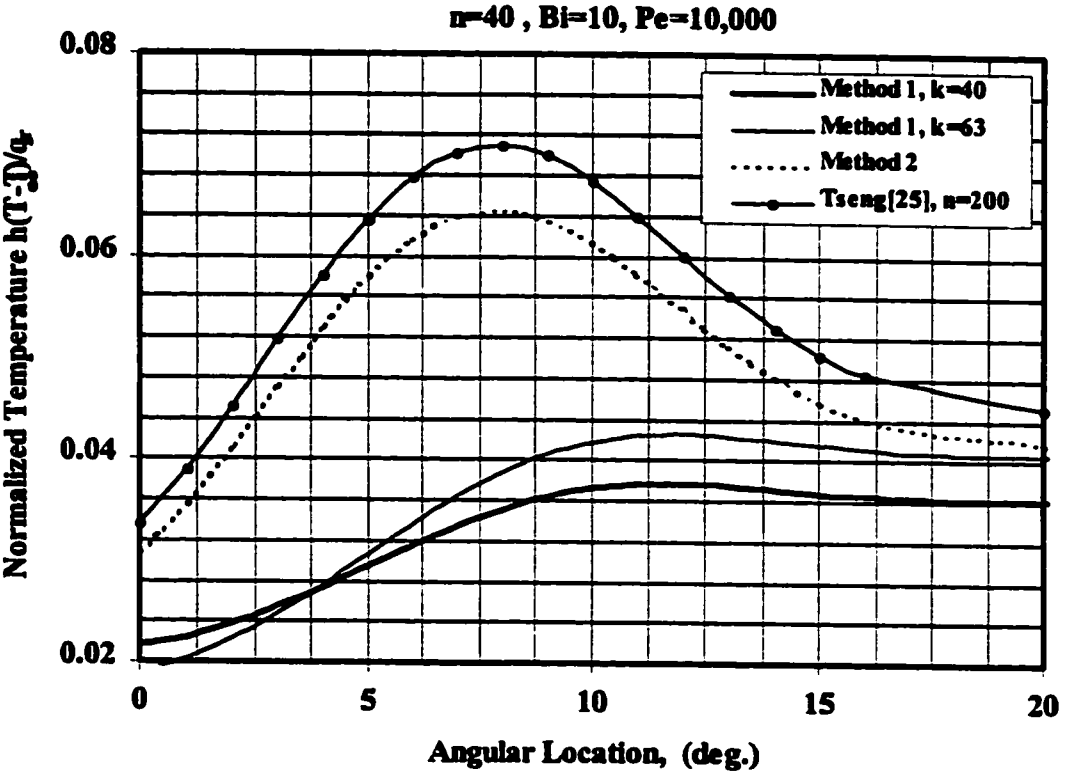

Figure 8.4: Normalized temperature over the roll; zoom view for 20 degrees from the entry side.

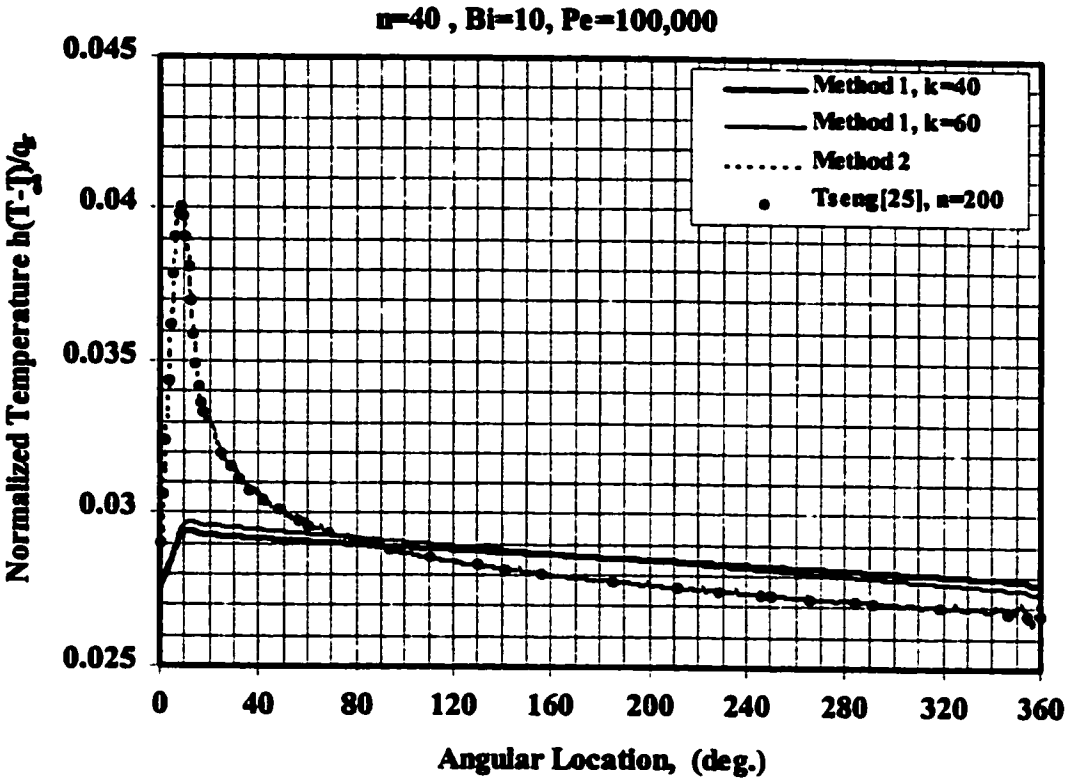

Figure 8.5: Normalized temperature distribution over the roll for Pe = 100,000.

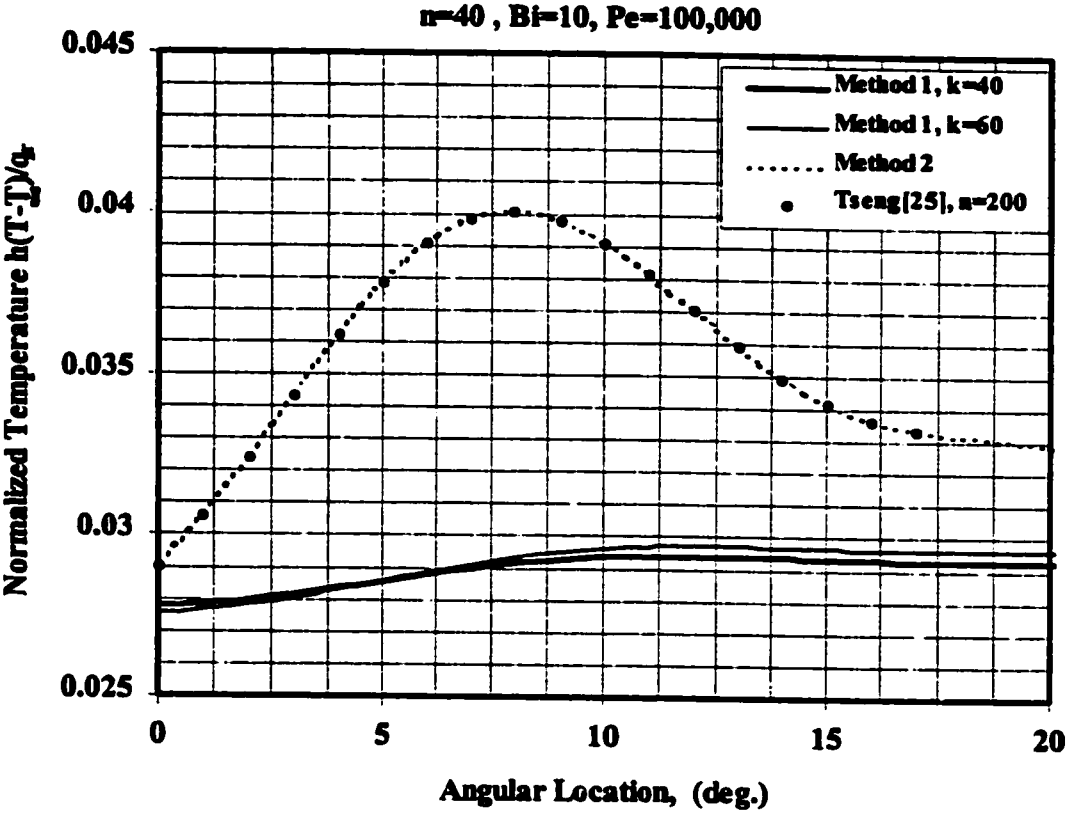

Figure 8.6: Normalized temperature over the roll; zoom view for 20 degrees from the entry side.

- At high Peclet number method−2 will give better results and
- For low Peclet number method−1 will give better results.
- Method−1 is sensitive to k which is the index for kelvin series expansions. This sensitivity is insignificant for very large arguments of $ber_n(x)$ and $bei_n(x)$.
- The sensitivity of algorithm with respect to number of terms for infinite series solution is decreased for very large argument.

It is important to note that very large argument lies in the range of $\geq 3 \times 10^2$ for the present analysis. This number has been found after performing several numerical tests. Oscillatory behavior of the curves shown in Figures 8.1 to 8.6 is discussed by Tseng [25], he mentioned that these oscillations represent inherent behavior of the Fourier series solution associated with large change within a small bite angle. This phenomenon is known as Gibbs phenomenon. Kovach [73] explained that this phenomenon persist even though a large number of terms are summed.

8.2 Results for Actual Rolling Data

8.2.1 Introduction

The data for implementing the developed modules has been obtained from Tseng et al. [34], for cold rolling of Aluminum alloy 1100 and is given in Table 8.1. The values obtained from the actual operating conditions of an aluminum rolling mill, a Devy-Loewy four-high cold strip mill located in Martin Marietta's plant. The data also includes measured value of the final strip thickness (y_f).

Table 8.1: Mechanical properties and data used in the analysis [34].

Strip material		1100 *Al Alloy*
Roll material		*Steel Alloy*
Strip entry Gauge	(y_o)	0.259 cm
Strip exit Gauge	(y_f)	0.159 cm
Strength Coefficient for *Al Alloy*	(K)	160 MPa
Strain Hardening Exponent *Al Alloy*	(n)	0.26
Yield Strength for *Al Alloy*	(σ_y)	34.5 MPa
Friction coefficient	(μ)	0.05
Entry tension	(σ_b)	12.065 MPa
Exit tension	(σ_f)	1.9677 MPa
Roll radius	(R)	25.4 cm
Roll surface speed	(V_r)	10.91 m/s
Bite angle	(θ_T)	3.51°
Yield Strength for *Steel Alloy*	(σ_y)	220 MPa
Cooling angle	(ψ)	356.49°
Modulus of elasticity	(E)	69 Gpa
Poission's ratio	(ν)	0.33

8.2.2 Flow Chart

In order to check the validity and applicability of the developed modules, two computer codes named ROLLTHERM and ROLLDEFORM have been developed and successfully coupled. The coupled ROLLRTHERM-ROLLDEFORM algorithm is shown in Figure 8.7. Computer code ROLLTHERM is composed of three different modules; that is, pressure, heat flux and temperature modules. It works in such a way that first by setting process parameters (structural, thermal, mechanical) for a cold rolling process it predicts pressure and friction stress at the interface by using the pressure module, then it calls the heat flux module for calculating deformation and friction heat energies, finally, it utilizes temperature module for calculating temperature distribution over the roll surface. The developed temperature algorithm is also incorporated in the temperature module of program ROLLTHERM. For performing roll deformation and predicting stress distribution ROLLDEFORM code has been written. It consists of roll deformation and residual stress module. The computer code ROLLDEFORM utilizes the mechanical and thermal loads evaluated in the ROLLTHERM code for performing roll deformation analysis, deformed roll radius and resulting stresses have been obtained here. The deformed roll radius is utilized for next step calculation. An iterative procedure is implied over the entire developed coupled module and a convergence criteria is made until error in calculated deformed roll radius becomes very small. At the end stresses are calculated for the converged value of roll radius. Following some results have been discussed.

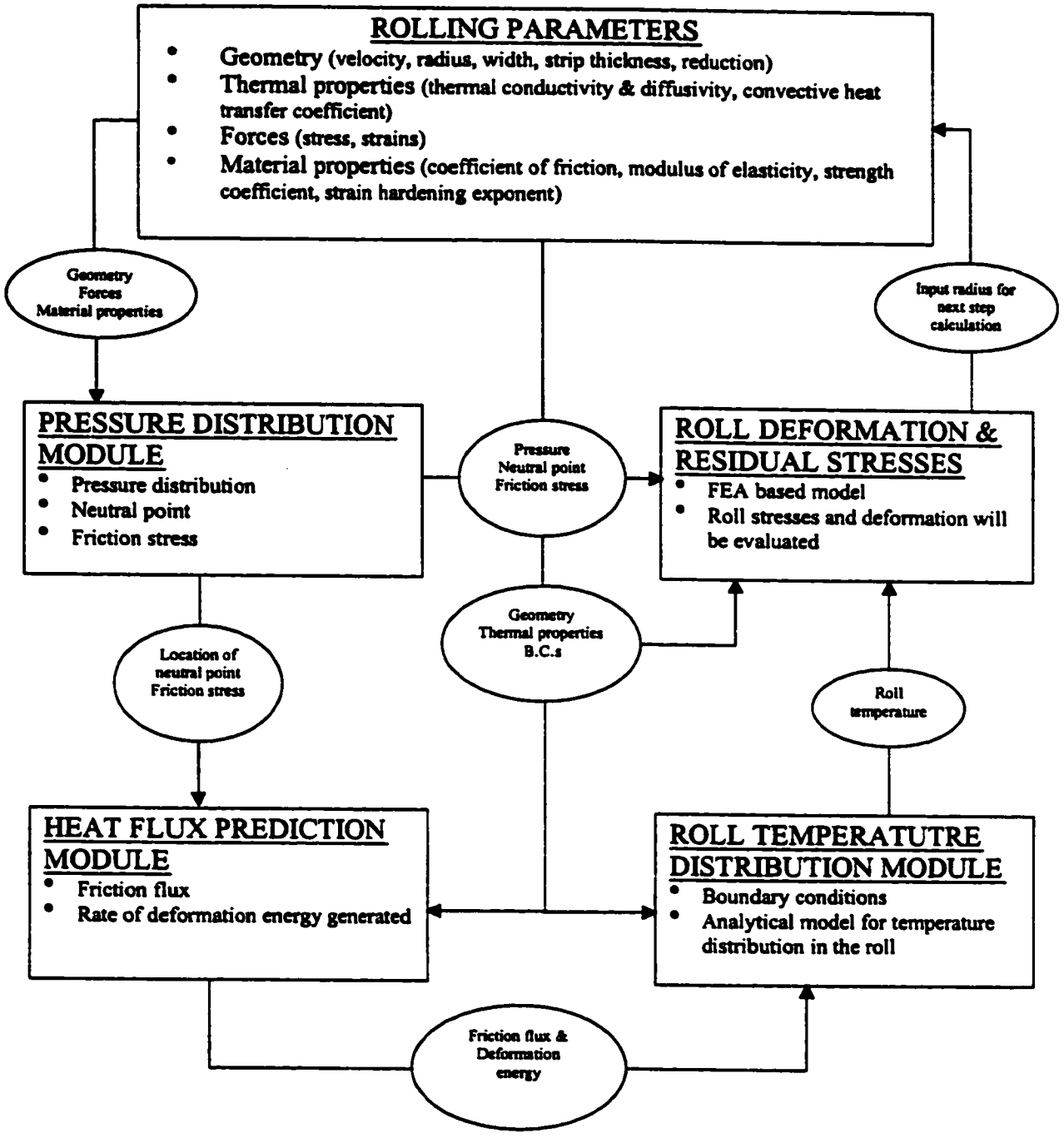

Figure 8.7: Developed combined algorithm for temperature prediction and roll deformation analysis.

8.2.3 Pressure distribution

The pressure module of computer code ROLLTHERM has been utilized to evaluate pressure distribution at the interface. This module consists of a fourth order Runge-Kutta scheme for solving low and high pressure equations discussed in the pressure model. Calculation for pressure distribution can be started either from the entry or exit side of the process. The algorithm works in such a way that initially it calculates the pressure by the low pressure equation (4.15) indicated in Chapter 4, when the value of pressure crosses the proportionality limit, then calculation transfers on the high pressure equation (4.17). The point of maximum pressure (pressure hill) determines the location of neutral point. Pressure distribution is shown in Figure 8.8 for different numbers of elemental division of strip at the bite region. It can be seen that for a course number of divisions pressure distribution was not correct and location of neutral point was varying, but as the number of divisions increased from 5 up to 200 the location of neutral point converged. For 400 number of elemental divisions, neutral point was same as that of 200 so in present study of rolling process maximum number of elemental division is 200. The highest peak point of pressure hill determines the location of no-slip or neutral point. Once pressure is known, shear stress can be calculated. Shear stress τ is positive at the roll surface before the neutral point, when the neutral point is reached it becomes zero and then changes its sign. This behavior is obvious from friction stress distribution curves shown in Figure 8.9. Again friction stress distribution is also converged towards a neutral point by increasing the number of divisions of strip at the roll gap.

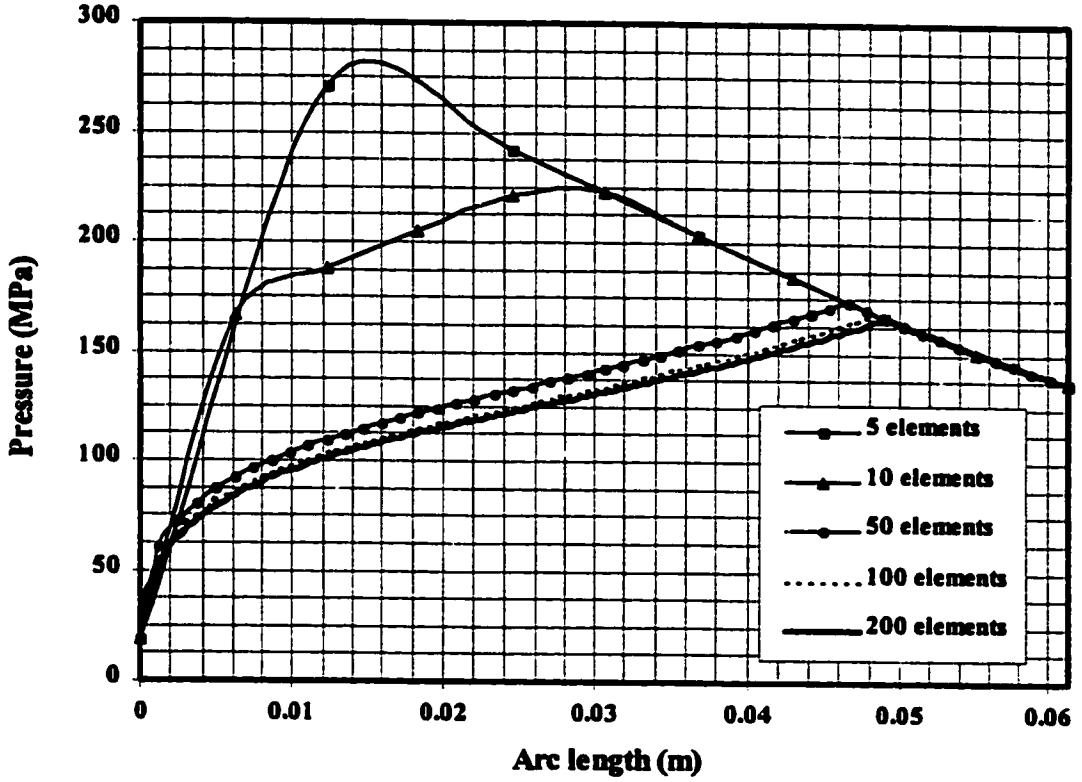

Figure 8.8: Pressure distribution at different number of division for the bite angle.

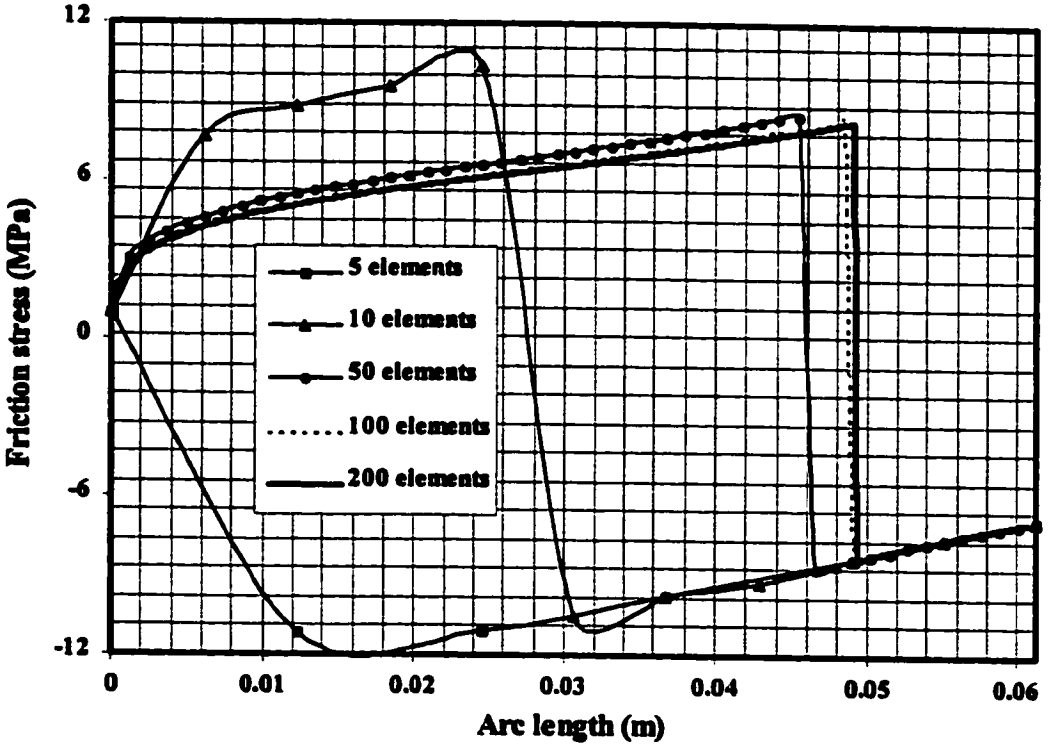

Figure 8.9: Friction stress distribution at different number of division for the bite angle.

8.2.4 Heat Flux distribution

Table 8.2 indicates the data used for heat transfer analysis by [34]. Friction stress distribution calculated from pressure model is used in calculating friction heat flux distribution at tool and workpiece interface. Figure 8.10 shows friction heat flux distribution at the interface, as it can be seen that friction heat flux is not remained uniform at the whole bite region. By increasing elemental division a convergence in the plot indicates the accuracy of current work, also the uniform (constant) value used by [34] is shown in the same figure. Although some recent studies for example [37] and [38], consider distribution of friction heat flux at the interface, but they did not provide enough information about how to calculate the distribution of deformation energy in workpiece. In present work, the following expression

$$e = \frac{KV_r y_n}{y\triangle l}\left(\frac{2}{\sqrt{3}} ln\left(\frac{y_1}{y_2}\right)\right)^{n+1} \tag{8.9}$$

which is developed in Chapter 5 has been used for calculating the distribution of deformation heat generated in the strip. During its derivation, it is assumed that stress and strain remain independent of volume change in the deforming strip. This assumption may become more realistic when the above mentioned equation (8.9) is developed for small elemental regions. Since, the part of strip at the contact region has been divided into 'j' number of small elemental regions; therefore, for a single element deformation energy rate can be expressed as

$$e_j = \frac{KV_r y_n}{y_j\triangle l_j}\left(\frac{2}{\sqrt{3}} ln\left(\frac{y_j}{y_{j+1}}\right)\right)^{n+1} \tag{8.10}$$

where j indicates the elemental regions that vary from $1, 2, ...M$. e_j is the deformation energy rate for element j, y_j is strip height for any arbitrary elemental region j and Δl_j is the width of elemental region.

Tseng et al. [34] used a uniform (constant) value for deformation energy rate. Figure 8.11 shows the variation of deformation energy in workpiece, that is obtained by using data from Table 8.1. It is important to mention that in a typical study of rolling process Tseng [11] proposed a distribution of deformation energy in the strip by assuming negligible variation of flow stress. The plot obtained from present analysis follows the proposed characteristic distribution of [11], which adds into the reliability of present analysis.

Table 8.2: Data used for checking the accuracy of developed model. [34]

Strip material		1100 *Al Alloy*
Roll material		*Steel Alloy*
Strip Entry Temperature	(T)	21 ^oC
Strip Thermal Conductivity	(k_s)	182 W/m^oC
Strip Thermal Diffusivity	(a_s)	$9.3 \times 10^{-5}\ m^2/s$
Roll Thermal Conductivity	(k_r)	45.6 W/m^oC
Roll Thermal Diffusivity	(a_r)	$1.265 \times 10^{-5}\ m^2/s$
Cooling Heat Transfer Coef.	(h)	9300 $W/m^{2o}C$

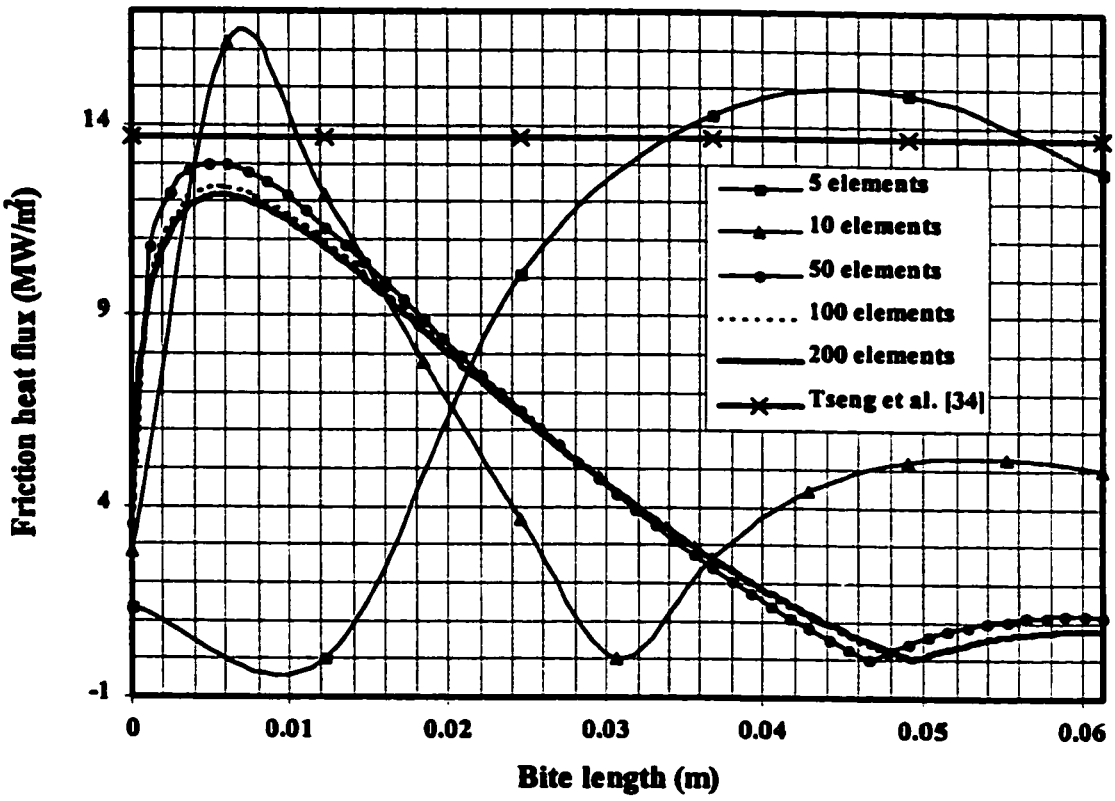

Figure 8.10: Friciton heat flux distribution at the interface between the roll and workpiece.

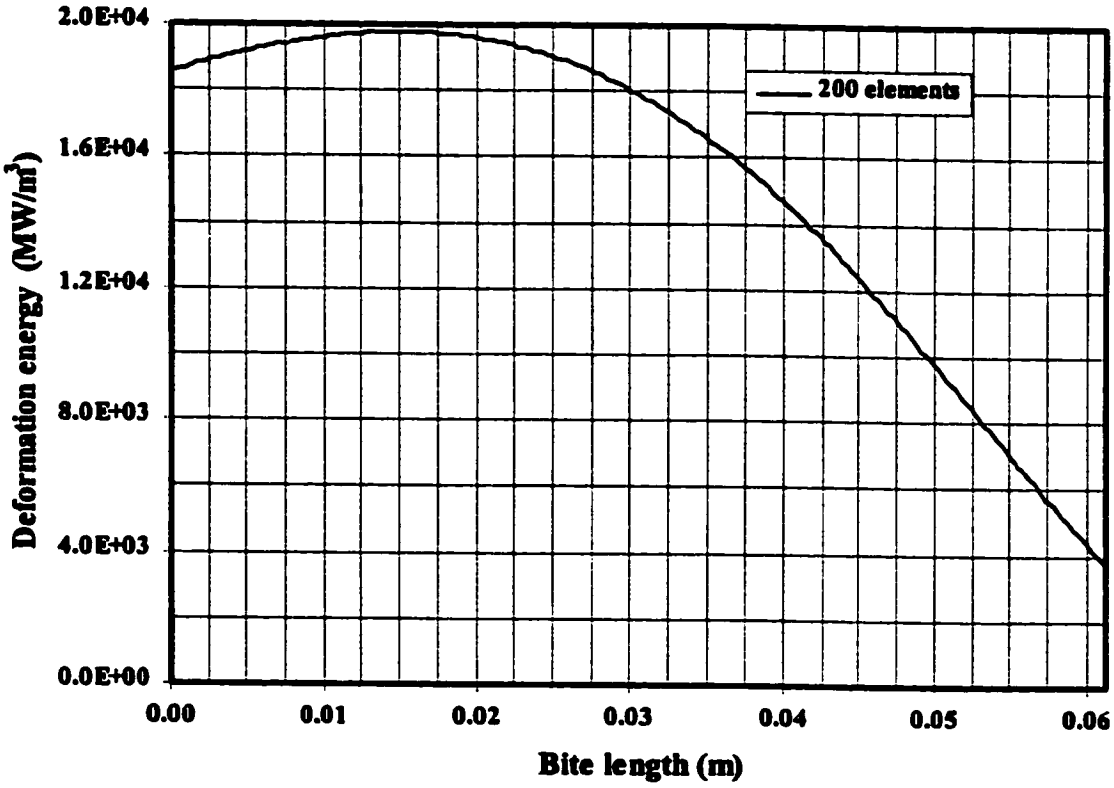

Figure 8.11: Deformation energy rate generated in the workpiece.

8.2.5 Roll temperature

Temperature distribution over the roll has been obtained from the temperature module of the code ROLLTHERM. The differential equation that governs temperature field has been solved by assuming series solution. Furthermore, the developed ascending-modulus algorithm is also incorporated in the temperature module for calculating coefficients of Kelvin functions. After applying boundary and compatibility conditions, the system of linear equations (6.27) has been obtained. To evaluate the set of infinite number of unknown constants $[B_o]_{1\times1}$, $[B_N]_{n\times1}$, $[C_N]_{n\times1}$ and $[\bar{q}_r]_{j\times1}$; the system of equations must be solve simultaneously. An infinite series can not be implemented in simulation, so only a finite number of terms (n) must be retained.

In the present study $n = 40$ terms solution has been employed. Since $[B_o]_{1\times1}$is only a single constant and each $[B_N]_{n\times1}$and $[C_N]_{n\times1}$ will give 40 number of unknown coefficients, therefore, the total number of constants come out by taking $n = 40$ is 81. In addition to this, the bite region has also been divided into j number of elemental regions, so the total number of equations need to be solved is $(j + 81)$. A matrix of $(j + 81) \times (j + 81)$ coefficients has been generated. The system of equations has been solved with the help of Gauss elimination scheme to obtain the set of unknown constants. Temperature over the roll surface has been calculated and the results are shown in Figures 8.12 and 8.13. For coarse elemental division, the predicted temperature distribution was much higher than that of [34], but as the number of divisions increased temperature plots converged towards a common pattern.

A closed examination between calculated temperature at different elemental di-

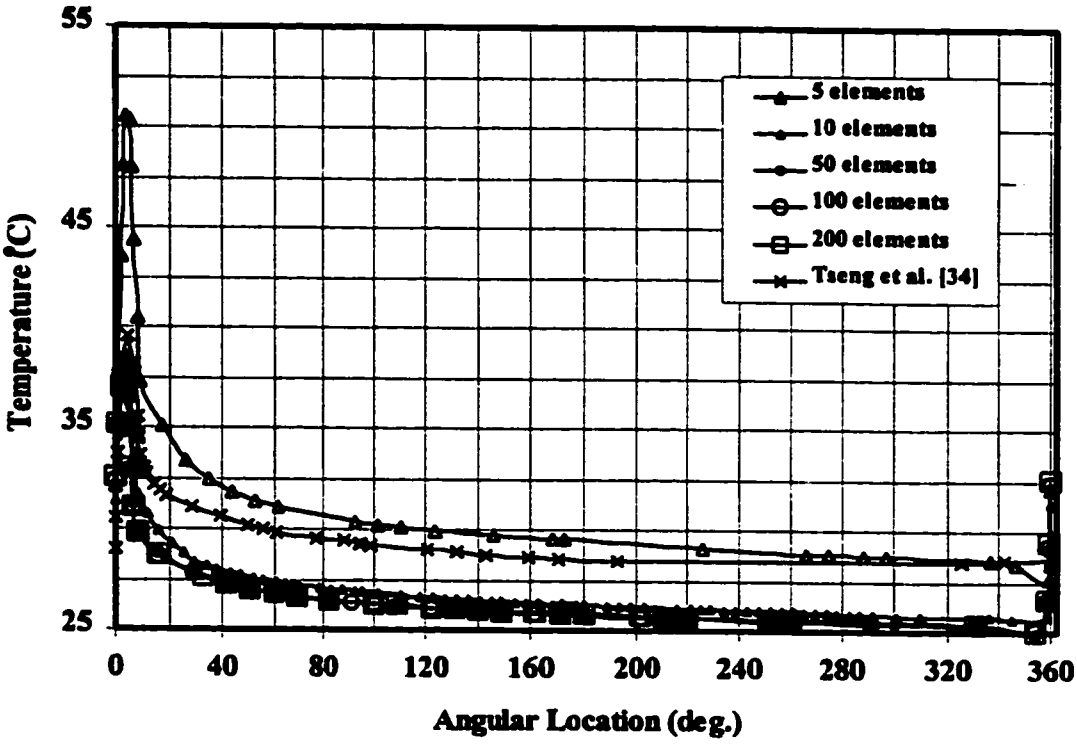

Figure 8.12: Temperature distribution at different elemental divisions over entire roll surface.

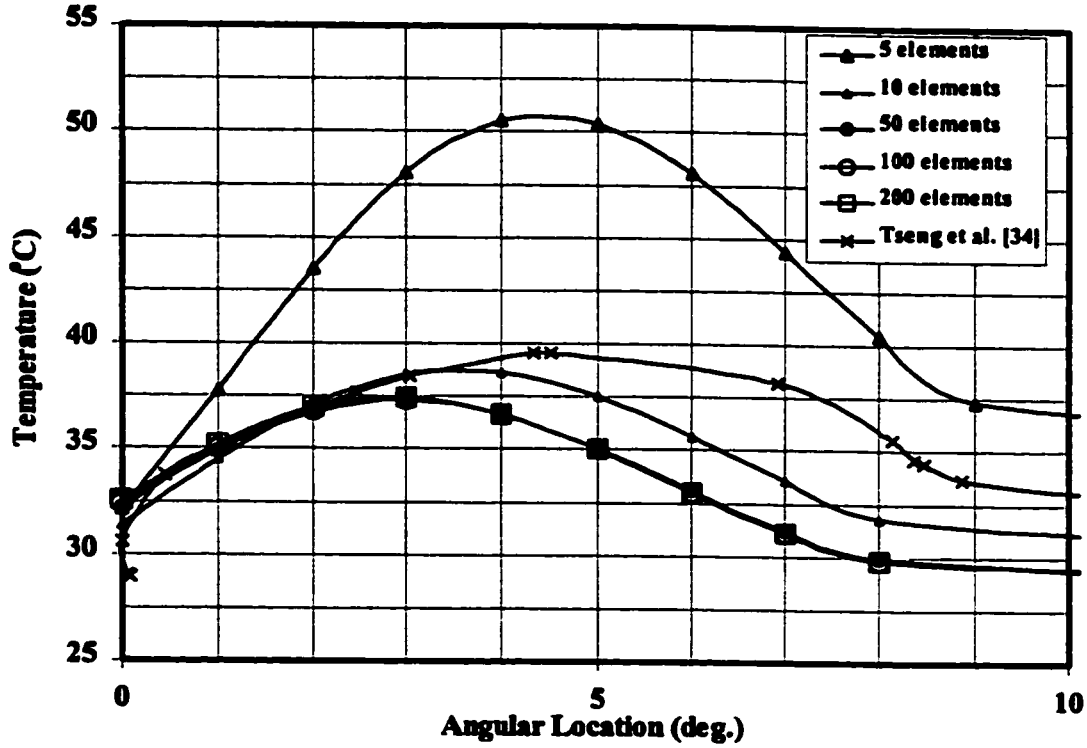

Figure 8.13: Temperature distribution at different elemental divisions zoom view for 10 degrees from entry side.

visions and the temperature distribution given by Tseng et al. [34] shows a drop in overall roll surface temperature is observed. At the bite region, the maximum temperature given by [34] is 39 ^oC whereas temperature distribution for a reasonably fine number of bite division ($j = 200$) is 37 ^oC. Temperature difference over the remaining portion of the roll remained in the range of $3 - 4$ ^oC. The location of maximum temperature is shifted inside the bite region and occurred at 3 degrees from the entry side for 200 elemental regions. (*that is at* $j = 200$).

The expected reasons of discrepancies between present work and that of Tseng et al. [34] are summarized below:

1. Present study employes a non-linear heat flux distribution at the interface that occurs in an actual process, whereas Tseng et al. [34] assumed uniform value throughout the bite region.

2. Friction heat flux and deformation energy generation rate per unit volume have been calculated in the distribution form, instead of using a constant integral value as used by Tseng et al. [34].

3. Tseng et al. [34] neglected heat conduction term in circumferential direction, while present work considers heat transfer in this direction also.

4. Tseng et al. [34] used Fourier integral technique in evaluating temperature distribution over the roll but in the current study modified Bessel's differential equation has been solved.

Contour plots efficiently represent the variation of different parameters at any sec-

tion of a continuum, these plots are capable of presenting two and three dimensional variations. By recognizing this fact, different contour plots has been drawn in this study. Figure 8.14 shows two dimensional temperature plot at the roll cross section; maximum temperature occurred at the bite region. Since cooling is performed over the entire roll except the bite region, a significant drop in temperature is apparent away from the bite region in counter clockwise direction, also almost all inner roll section has uniform temperature distribution. A color plot is shown in Figure 8.15.

Figure 8.16 shows roll heat flux distribution at the bite region. It is interesting to observe that heat flux changes its sign just after entering the roll bite. Actually at the entry side, roll temperature is higher than the strip entry temperature (this would be true when a steady state condition is achieved) that is at $\theta = 0^o$ roll temperature is 31 ^oC whereas strip entry temperature is 21 ^oC; at the initial contact region strip acts as sink and heat starts flowing from roll to the strip. But, when the strip start deforming its temperature will also be increased thus heat will start flowing from strip to the roll causing a sudden change in heat flux direction which indicates an overall flow of heat towards the roll.

During rolling when relatively large reduction is imposed on the strips, heat generation in the strip will be increased, although friction heat at the contact will also be increased, but friction heat is mainly increased by increasing the relative slip velocity. Thus, all these increments will cause an overall heat flow towards the roll. In order to check this subject two studies have been performed at different relative velocity and reductions. Magnitude of relative velocity is controlled by varying the roll speed (V_r) and reduction is controlled by changing the bite angle. Figure 8.17 indicates

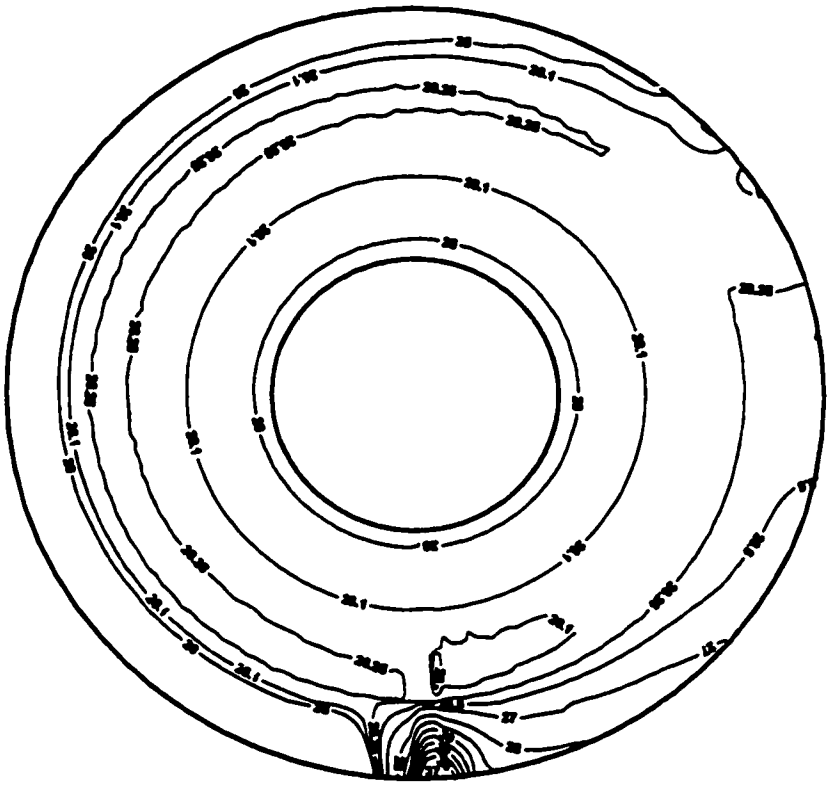

Figure 8.14: Temperature contours (^oC) at different roll radius.

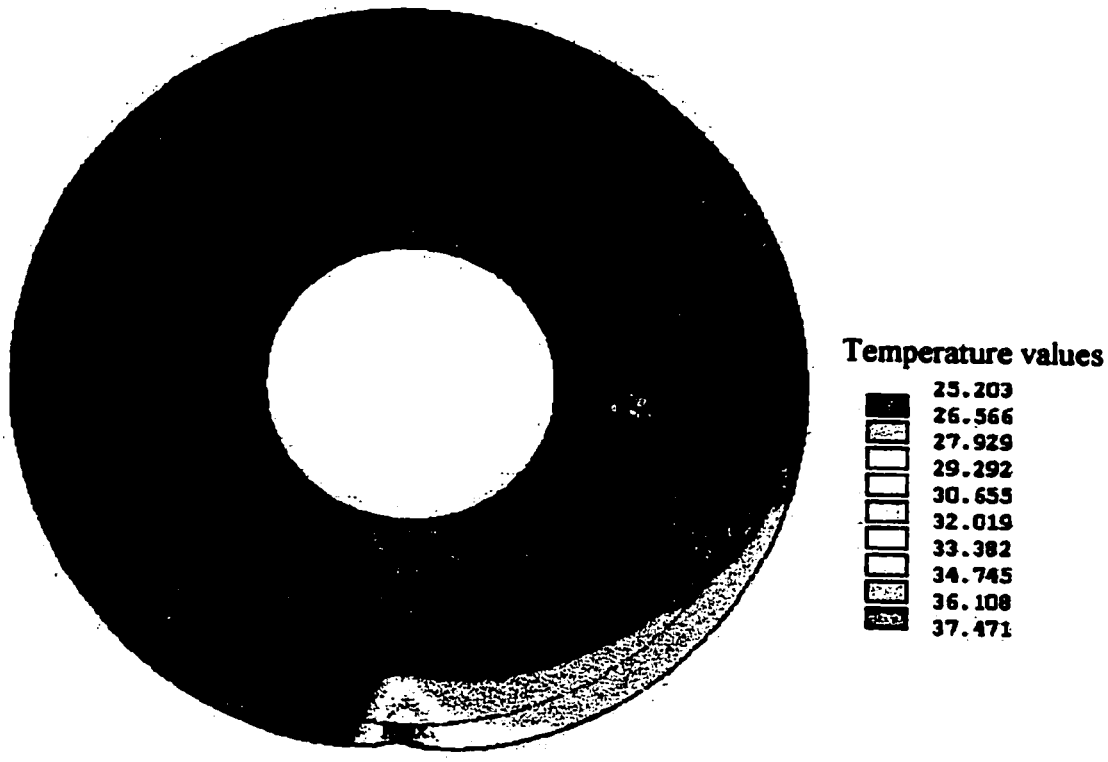

Figure 8.15: Color temperature (^{o}C) contours at different roll radius.

roll heat flux distribution (q_r) obtained by changing relative velocity magnitude. At low relative speed maximum heat flux (q_r) is about 2.5 MW/m^2, but as the speed is increased heat flux (q_r) value is also increased and maximum value is reached in the neighborhood of 12 MW/m^2. Effects of increasing the reduction has been shown in Figure 8.18. For 36.4% reduction (at $\theta_T = 3.51^o$) maximum value of roll heat flux (q_r) is 12 MW/m^2; but as the reduction is increased up to 74.6% (at $\theta_T = 5^o$) roll heat flux is also increased and maximum value is occurred in the neighborhood of 30 MW/m^2 which is very high as compare to the previous cases. It has been cleared from above discussion that increasing reduction greatly affects the roll heat flux variation at the bite region as compare to increasing relative slip velocity. It can be deduce that for a rolling process performed at high relative speed with large reduction non-linear heat flux consideration becomes important. It is thought that errors associated in maximum roll temperature obtained by uniform heat flux distribution could be higher than 10% as compare to the temperature obtained by considering non-linear heat flux distribution.

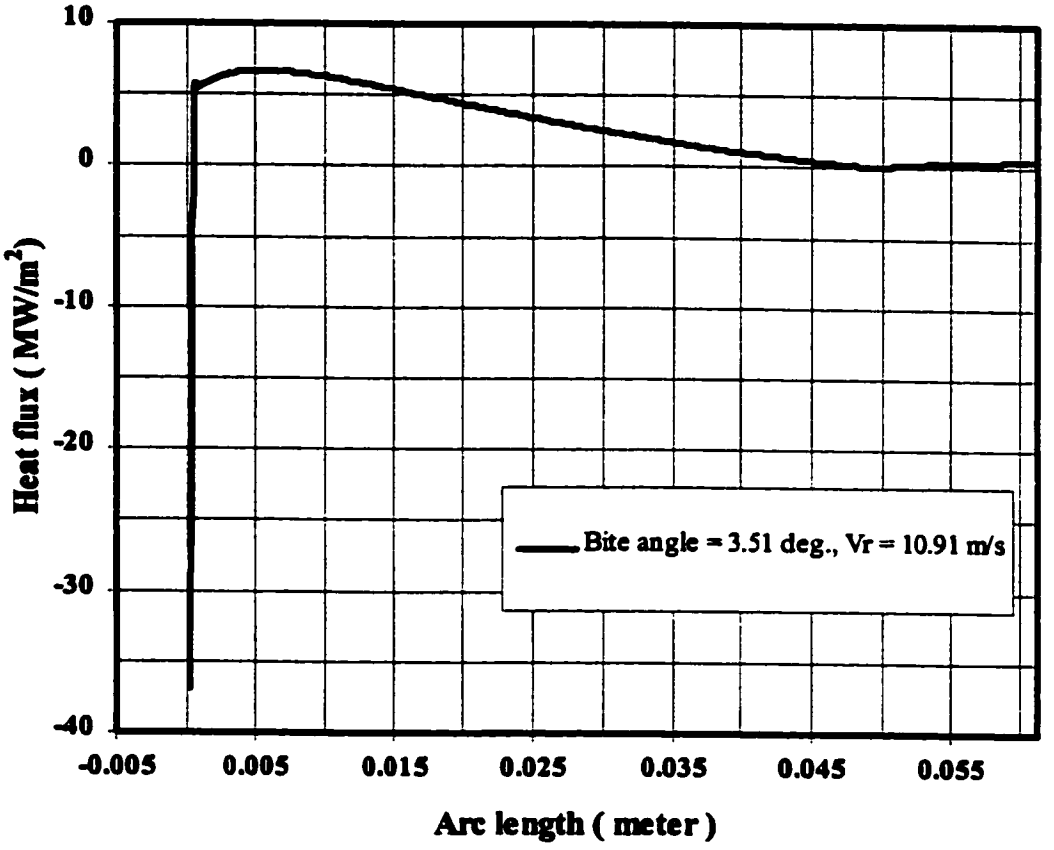

Figure 8.16: Roll heat flux distribution at the bite region.

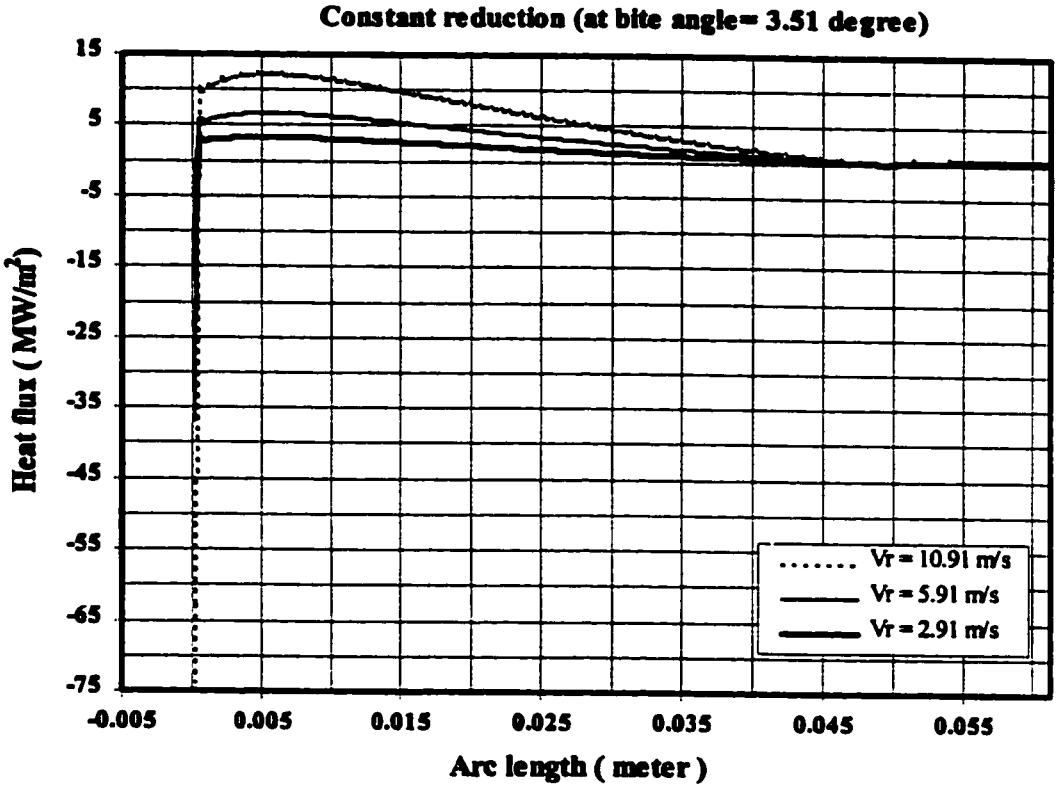

Figure 8.17: Roll heat flux distribution at the bite region for constant reduction.

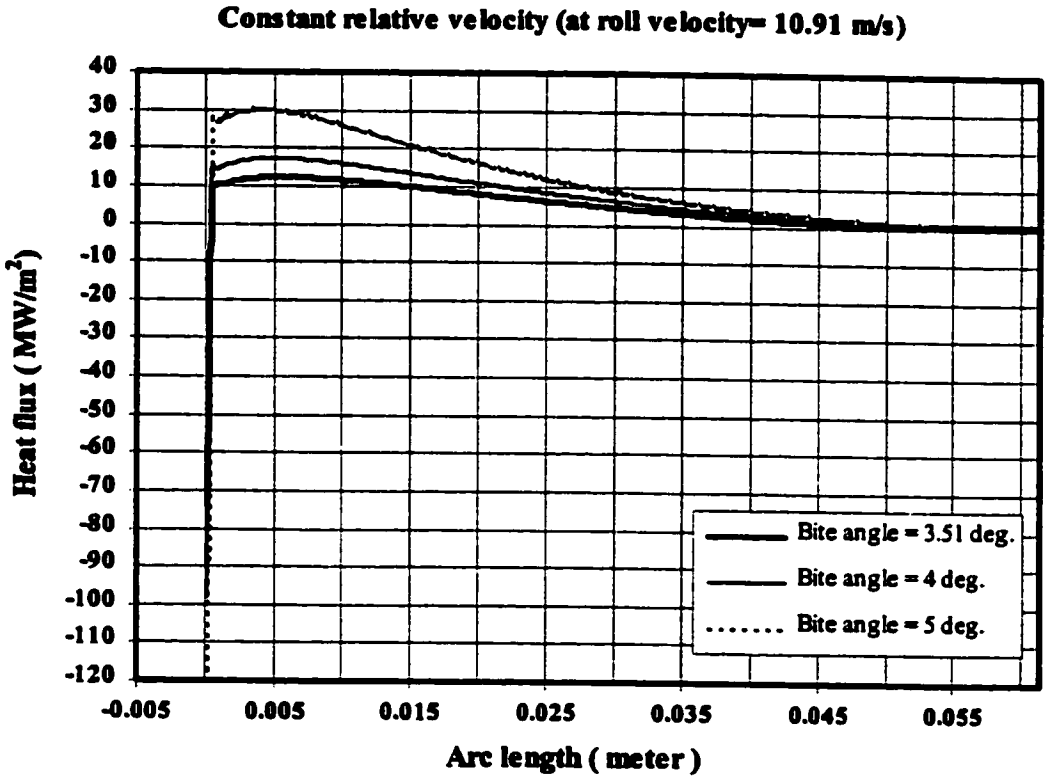

Figure 8.18: Roll heat flux distribution at the bite region for constant relative velocity.

8.2.6 Roll Deformation Analysis

Roll deformation occurs when strip comes in contact with the roll. At one end, high pressure and friction stress cause a compressing deformation at the roll gap; on the other hand temperature causes roll expansion, certainly this complicated load deforms the roll thereby affecting the exit strip gauge and generating stresses in the roll. Thus, roll deformation modeling is the key for controlling the size of rolled strips and the stresses in roll. Following results have been presented by performing roll deformation modeling.

8.2.6.1 Roll deformation behavior

The data has been taken from Tseng et al. [34] and is given in Table 8.1. Three type of analyses have been performed, first finite element analysis is done with mechanical load only; that is without applying temperature distribution over the roll. Secondly, both mechanical and thermal loads have been incorporated in modeling and finally Hitchcock formula [3] has also been utilized in order to compare the results. Roll deformation characteristics can be understood by Figures 8.19 and 8.20. Figure 8.19 indicates roll deformation behavior when only mechanical load is applied which includes pressure and friction stress. Roll deformed inside and slightly twist in counter clockwise direction, inside roll deformation is occurred due to pressure and twist is occurred because of friction shear stress; for this type of load maximum absolute displacement occurred at the bite region. When both thermal and mechanical loads are applied, roll deformation characteristic is shown in Figure 8.20. At the interface of roll and strip displacement is relatively small as compare to the rest of

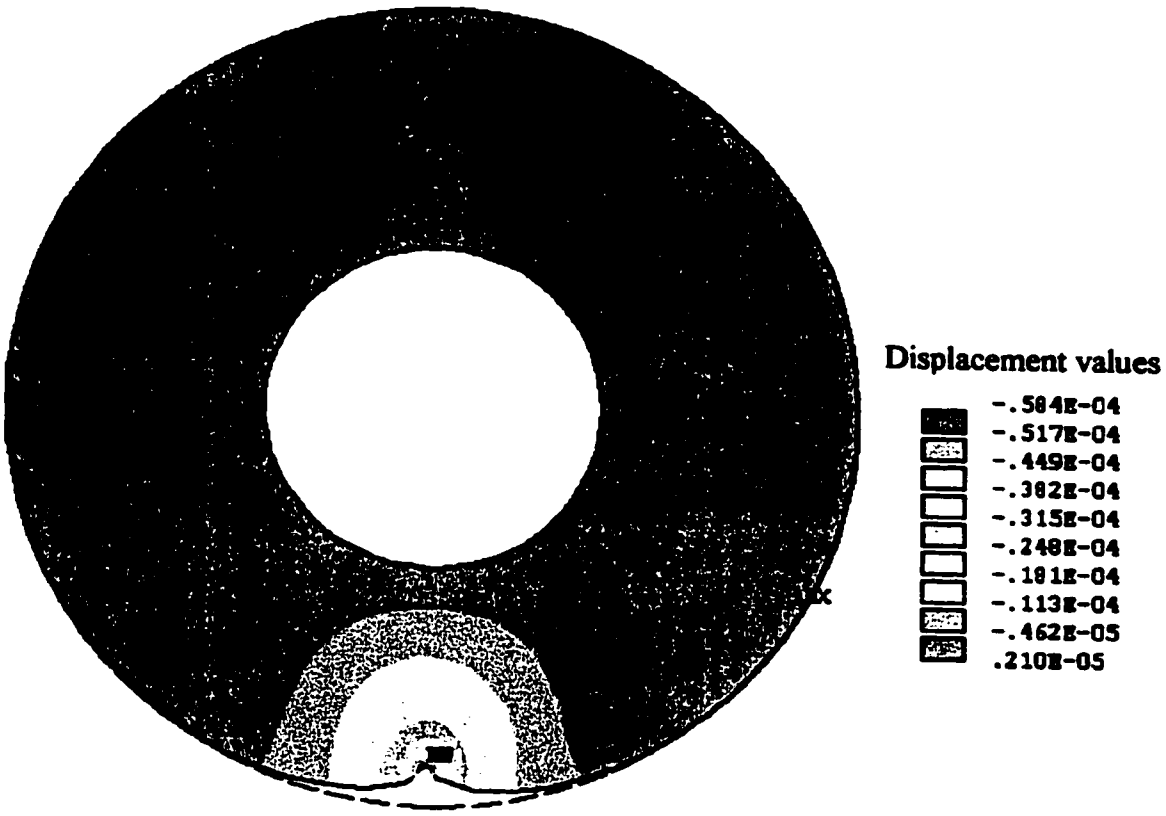

Figure 8.19: Roll deformation behavior with applying mechanical load only.

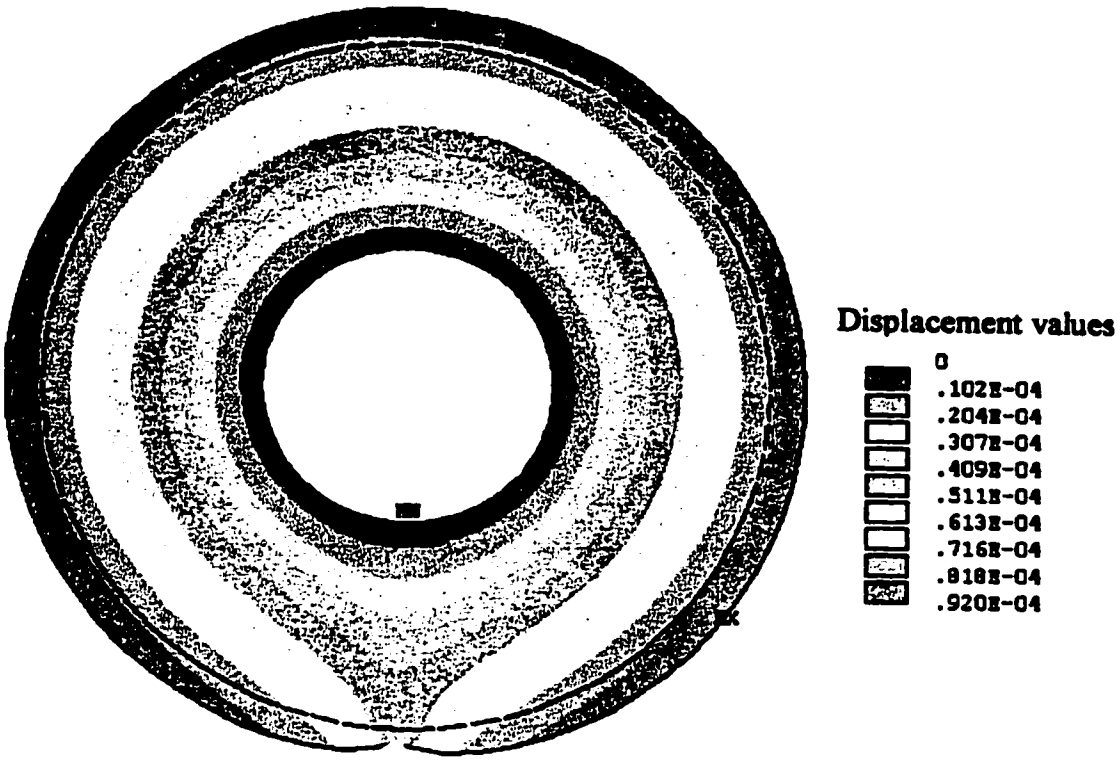

Figure 8.20: Roll deformation behavior with applying thermal and mechanical loads.

the roll surface due to strip action on the roll.

Radial displacement contour plot obtained by applying both mechanical and thermal loads; are shown in Figure 8.21, at the interface of tool and workpiece displacement is relatively small as compare to the rest of the roll surface. This can be explained from the fact that workpiece (strip) contact generates pressure and shear stress at the interface region therefore these forces try to restrict roll expansion in this region whereas other portion of the roll surface remains free so it expands without any restriction, thus causing maximum displacement at the surface which is not in contact with the workpiece. Figure 8.22 shows circumferential displacement contour plot for the roll material under thermo-mechanical loading. Circumferential displacement is relatively small as compare to the radial one. Roll deformation in circumferential direction has two zones one is in compression and other is in tension. Compressive displacement becomes tensile after passing through a point in the bite region and this remain positive up to a certain point at the upper roll portion.

8.2.6.2 Final strip gauge

An average value of radial displacement at the bite region has been calculated and then added to the un-deformed roll radius so that corrected roll radii could be obtained. After calculating corrected roll radius, exit strip thickness (y_f) is obtained by using following relation

$$y_f = y_{f_{theo.}} - 2\delta \tag{8.11}$$

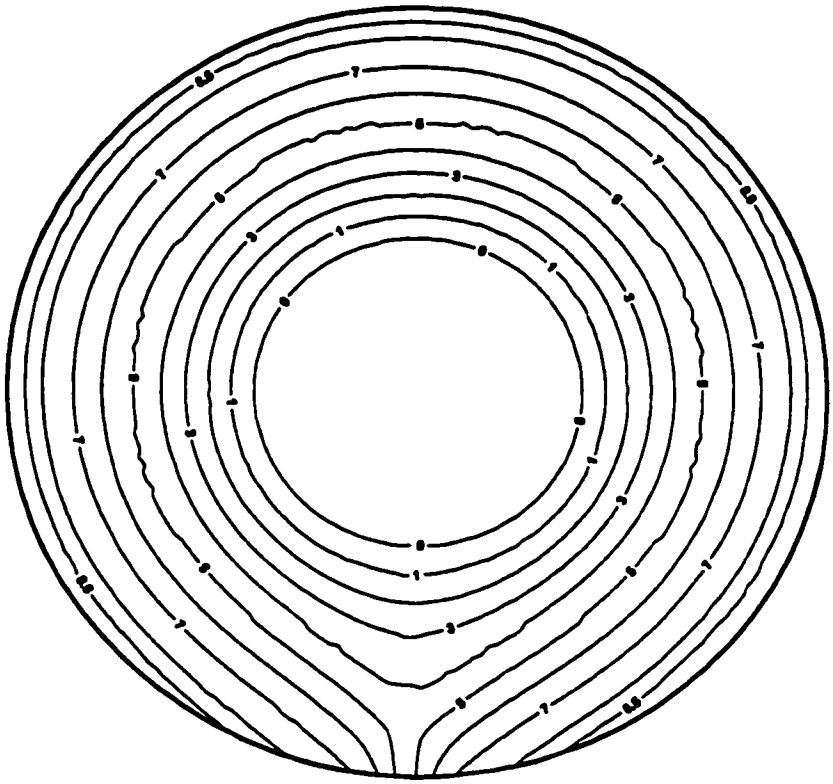

Figure 8.21: Radial displacement inside the roll (in meters, values are multiplied by 10^{-5}).

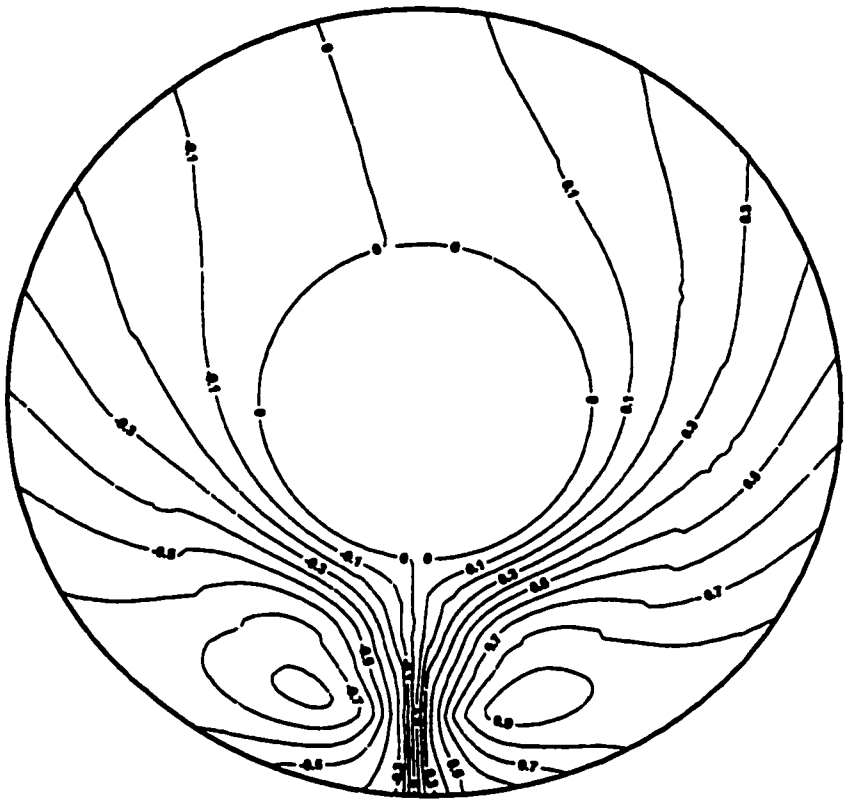

Figure 8.22: Circumferential displacement inside the roll (in meters, values are multiplied by 10^{-5}).

where theoretical final strip thickness ($y_{f_{theo.}}$) is given by

$$y_{f_{theo.}} = y_o + 2R(\cos\theta_T - \cos\theta) \tag{8.12}$$

A comparison is made with experimentally calculated exit gauge value given in the data. Finally, corrected roll radius has been used for second iteration. This will remain in continuation until error in the roll radius is not decreased significantly.

Table 8.3 indicates exit strip thickness obtained by different approaches all dimensions are in centimeter. From economical point of view, consumer satisfaction is the key factor in industries' growth. Controlling the final size of strip not only fulfils consumers requirements but also reduces extra passes needed to get the desired size and shape. The results obtained by the developed model indicate that; Hitchcock formula and finite element analysis without thermal load, give the value for strip exit gauge in the range of $0.1634\ cm - 0.1744\ cm$. Whereas exit gauge got by finite element analysis with temperature distribution over the roll was $0.1564\ cm$, which is much closer to the strip exit thickness $0.159\ cm$ measured by Tseng et al. [34]. Percentage error occurred between experimental gauge and calculated gauge by three approaches is summarized in Table 8.4.

It can be seen that error in the gauge obtained by thermo-mechanical analysis is almost twice as lower than that of Hitchcock formula's. Error in pure mechanical analysis is relatively very high. Thus, by considering Table 8.4, it can be deduced that thermo-mechanical analysis accurately simulates the actual process as well as it is more reliable and suitable for controlling the desired strip thickness.

Table 8.3: Final strip thickness obtained from different analyses.

		Displacement (*centimeter*)	Corrected radius (*centimeter*)	Final strip gauge (*centimeter*)
		δ	$R' = R + \delta$	$y_f = y_{f_{theo.}} - 2\delta$
	First iteration $N = 1$			
I	FEA without temperature	-5.386×10^{-3}	25.394614	0.174478
II	FEA with temperature	3.6398×10^{-3}	25.403639	0.156426
III	Hitchcock formula [3]	1.2981×10^{-4}	25.40012981	0.16345
	Second iteration $N = 2$			
I	FEA without temperature	-5.385×10^{-3}	25.394614	0.17447
II	FEA with temperature	3.64089×10^{-3}	25.403640	0.156424
III	Hitchcock formula [3]	1.2941×10^{-4}	25.40025922	0.16345
	Third iteration $N = 3$			
I	FEA without temperature	-5.385×10^{-3}	25.3946149	0.17447
II	FEA with temperature	3.64089×10^{-3}	25.4036409	0.156424
III	Hitchcock formula [3]	0	25.40025922	0.16345

Table 8.4: Error in final strip gauge calculated for different analyses.

experimental gauge $y_f = 0.159\ cm$	Average values of final gauge (y_f)	Error
FEA with mechanical load only	0.1744 *cm*	9.7%
FEA with thermo-mechanical load	0.1564 *cm*	1.6%
Hitchcock formula [3]	0.1634 *cm*	2.8%

8.2.6.3 Roll stresses

Along with roll deformation and temperature history, a detailed knowledge of stress and strain distributions is necessary for designing rolls, preventing roll plastic deformation and designing cooling system of a rolling mill. This knowledge can only be acquired by observing the variations of these parameters in the roll.

Figures 8.23, 8.24 and 8.25 present two dimensional radial (σ_{rr}), circumferential ($\sigma_{\theta\theta}$) and shear stress ($\sigma_{r\theta}$) contour plots. It is interesting to note that radial stress has negative value near the bite region and a positive value away from that area. Since strip is in contact at the bite region, the resulting pressure and friction stress constraint the thermal expansion and ultimately make a compressive effect over radial stress, but away from bite area roll surface is free so it expands and thus radial stress is positive. Circumferential stress is negative in the entire roll and thus has compressive effects except in a very small region located in the bite angle. Shear stress has relatively small value. Before bite region, it is negative then changes its sign in the small heating zone and becomes positive. Away from the bite region its value decreased rapidly.

Since effective or equivalent stress has the effects of all stresses present in the continuum, its value is used in evaluating whether yielding has occurred or not. Figure 8.26 shows a plot for von Mises effective stress. It has maximum value of 64 MPa at the bite region which is very small as compare to the yield stress 220 MPa of roll's material. Minimum effective stress value occurred near the roll surface. Since inner circle represent a rigid contact with rotating shaft, the stress is relatively high

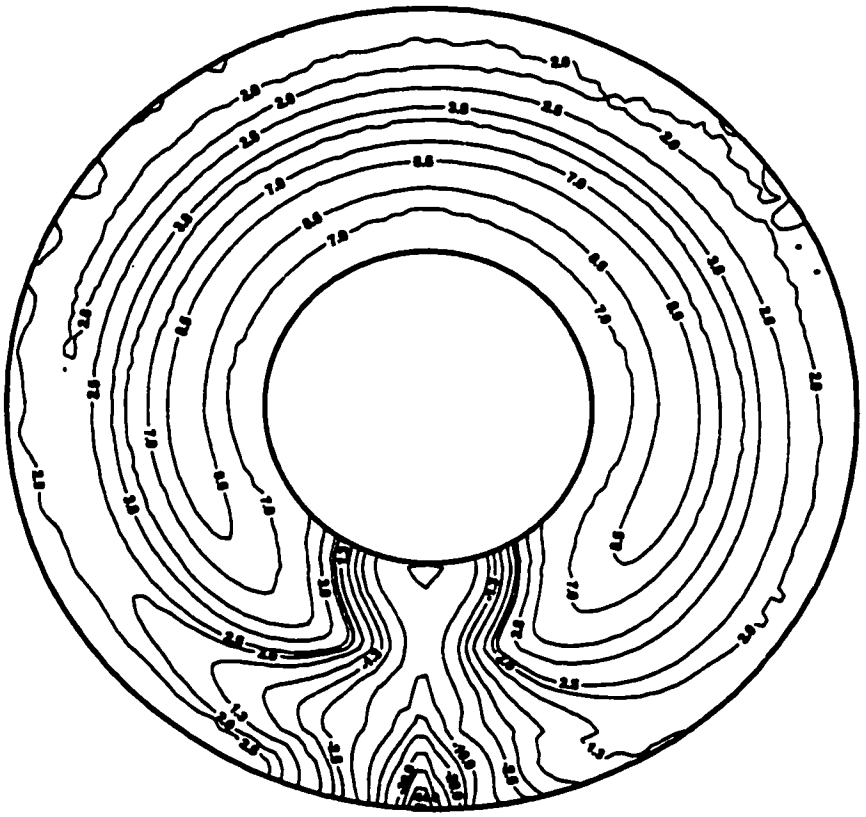

Figure 8.23: Radial stress contours at different roll radius (MPa).

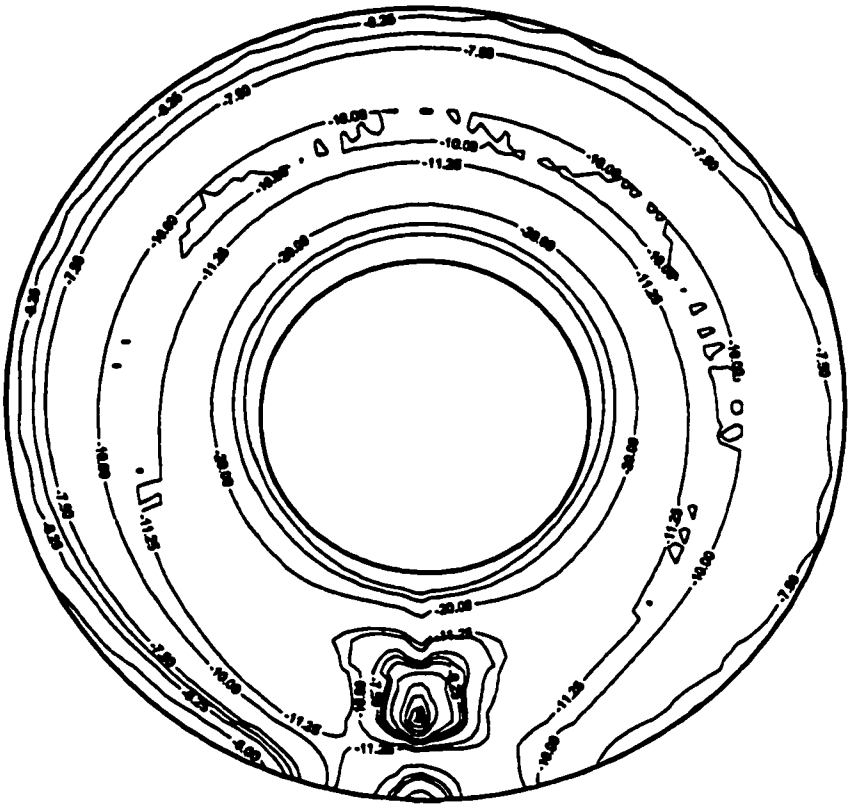

Figure 8.24: Circumferential stress contours at different roll radius (MPa).

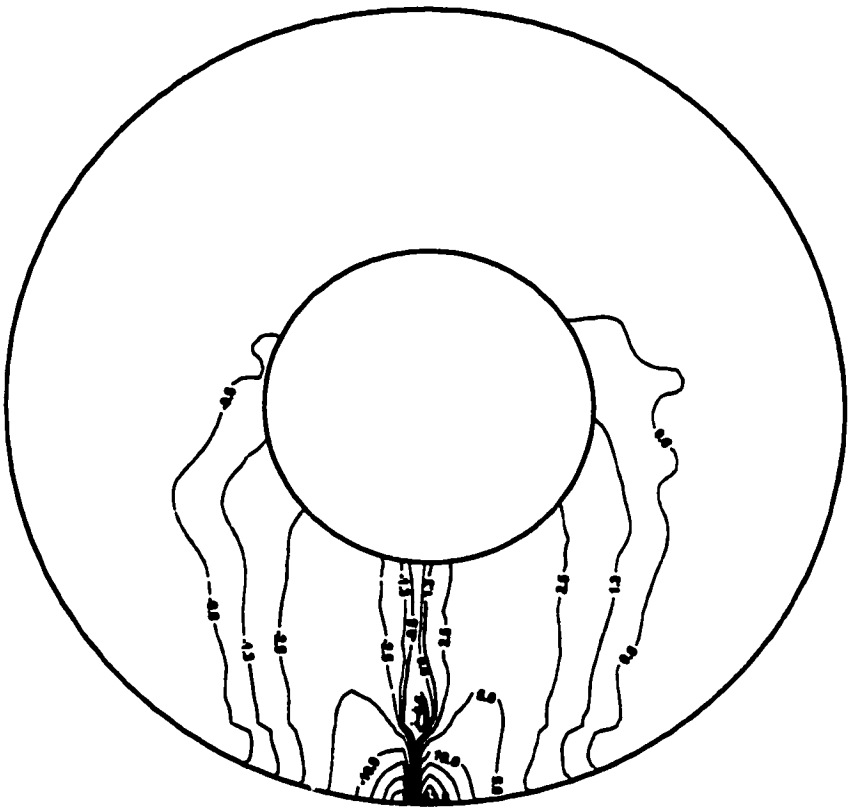

Figure 8.25: Shear stress contours at different roll radius (MPa).

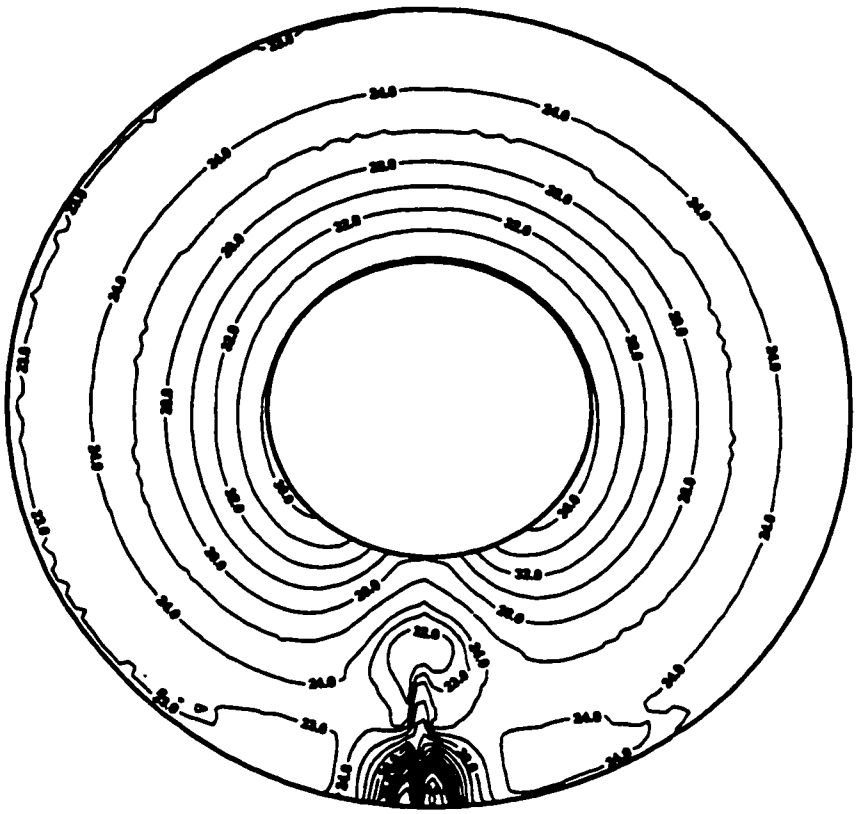

Figure 8.26: von Mises stress contours inside the roll at different radius (MPa).

at that region as compare to the other portion of the roll except the bite region. The maximum value of radial stress and von Mises stress were same and occurred at the bite region.

8.2.6.4 Effects of improper cooling

Sufficient cooling practice over roll is of considerable importance, inadequate cooling gives rise to temperature distribution in the roll which ultimately results in decreasing the roll life. In order to check the effects of reducing cooling over roll, a case involving 90^o degree cooling performed over top right portion of the roll has been studied. For this case, angles have been set at $\alpha = 45^o$, and $\psi = 90^o$. Temperature distribution has been shown in Figure 8.27. Maximum temperature value occurred in the heating zone is 51^oC and roll core temperature value is 40.5^oC whereas for full cooling maximum temperature was 37^oC and inside roll core temperature was 26^oC ; an over all temperature rise of 14^oC has been found. Also a closed examination of cooling region indicates that non-uniformity in temperature distribution increased. A colored plot of temperature distribution has been shown in figure 8.28, it can be seen that counter clockwise motion of roll resists the flow of coolant in clockwise direction and some coolant also flows at the top left portion of the roll with its motion. Effective stress (von Mises) has been shown in Figure 8.29, its maximum value occurred in roll gap and is not much affected, but inside the roll a significant increase has been observed. For full cooling its value inside the roll was 36 MPa whereas for 90^o degree cooling it is 52 MPa.

From above discussion it can be deduced that roll temperature distribution is

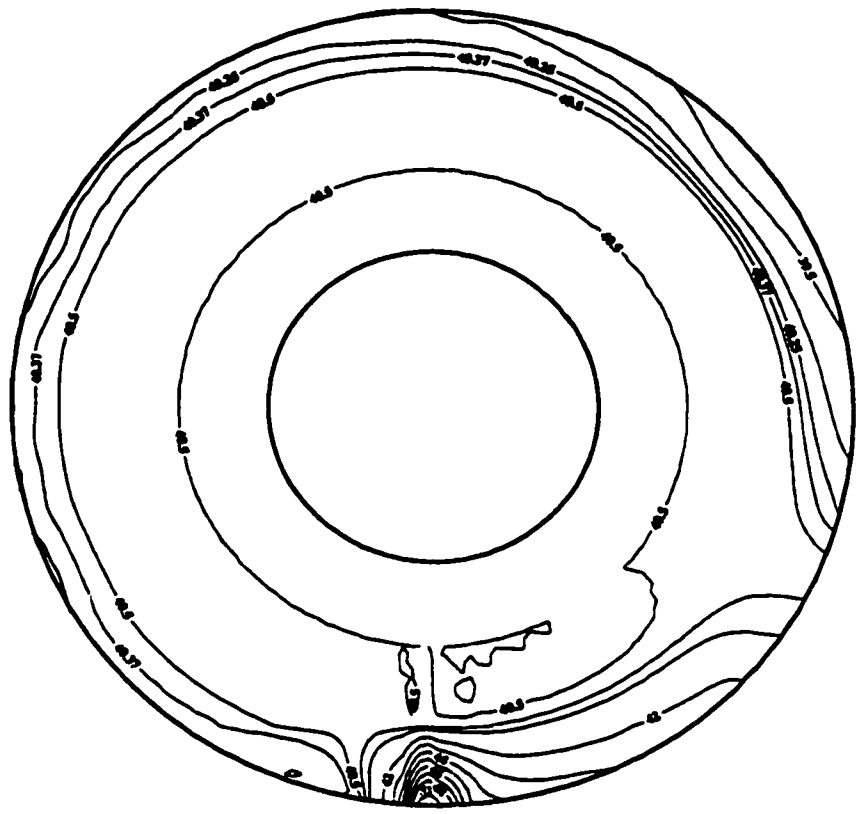

Figure 8.27: Temperature contours ($°C$) for 90 degree cooling over roll.

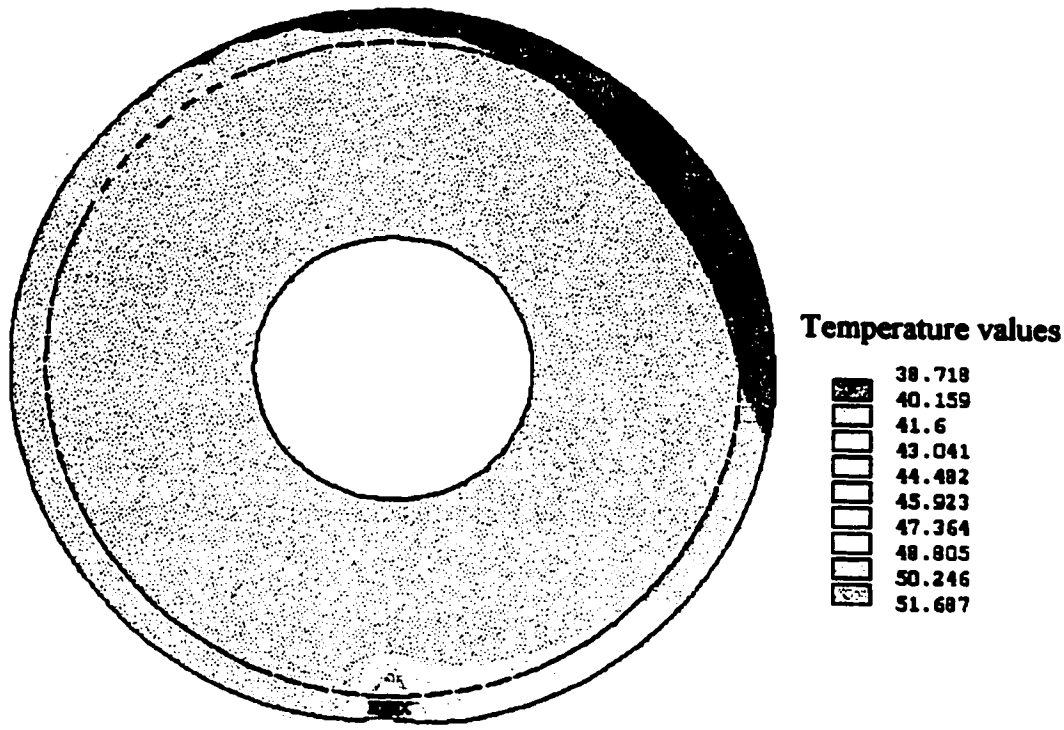

Figure 8.28: Color temperature (^{o}C) contours for 90 degree cooling over roll.

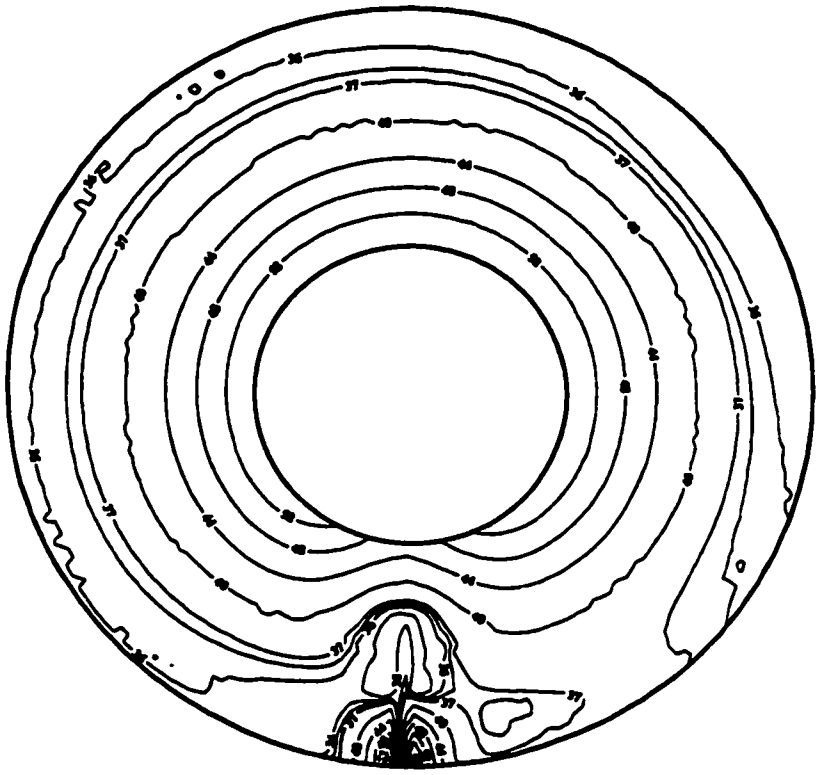

Figure 8.29: von Mises stress contours inside the roll for 90 degree cooling over roll surface (MPa).

directly affected by changing cooling practice over roll. Insufficient cooling has significant effects over roll temperature and stresses. Stresses at the roll core are much more affected, effective von Mises stress inside the roll surface is increased significantly as compare to the value occurred at the bite region.

8.2.6.5 Effects of high reduction

There are many situations exist in which roll operating at a particular reduction used to decrease final strip y_f thickness, that is to increase the reduction. This operation increases deformation heat generation in the strip, which finally increases the value of temperature and stress distributions in the roll. For present study, reduction has been increased up to 74.6% by increasing contact angle of roll and strip from 3.51^o to 5^o. Cooling was performed over the remaining portion of roll as in the original case, temperature plots are shown in Figure 8.30. Maximum roll temperature is increased by 7^oC while inside roll temperature is increased by 3^oC with respect to original case. Figure 8.31 shows von Mises effective stress distribution, for higher reduction its maximum value at the bite region is 95 MPa which is significantly greater than the previously discussed two cases and approximately half of the roll material yield strength. Inside the roll von Mises stress remains same as that of original case.

It can be drawn that by increasing reduction with full cooling, roll temperature at the bite region is increased much more as compare to the remaining roll temperature but if cooling is also reduced temperature changes can be greater. Stresses at the roll bite region would be increased considerably, von Mises stress for high reduction is

very high at the bite region as compare to the remaining roll portion. It is expected that for rolling process involving large reduction of strips and with improper cooling, localized yielding of roll can be occurred.

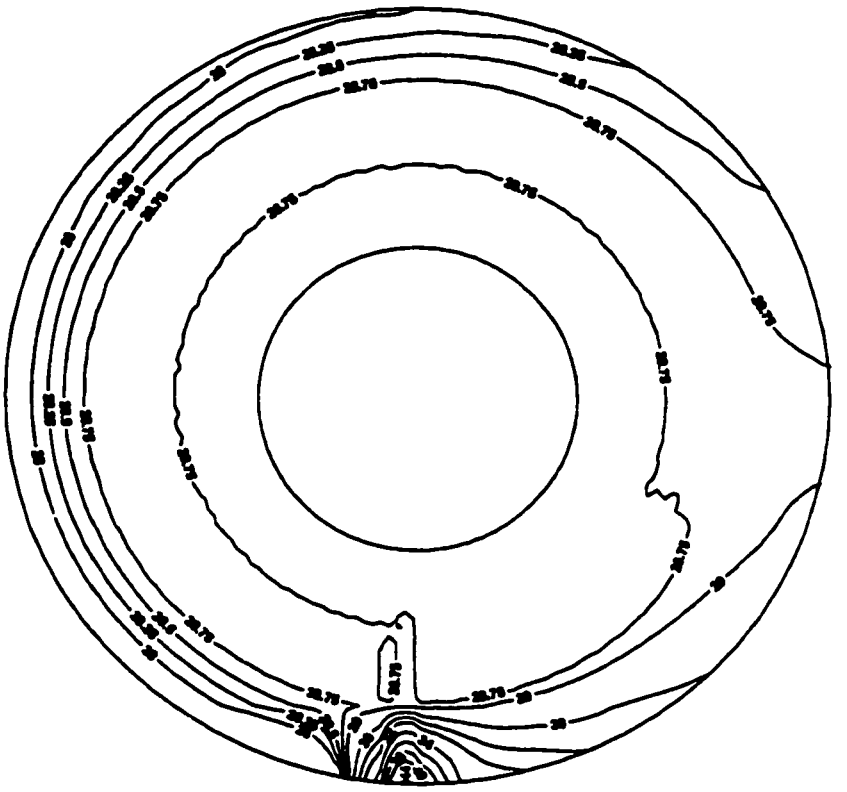

Figure 8.30: Temperature contours (^oC) by increasing reduction upto 74.6% (for bite angle = 5 deg).

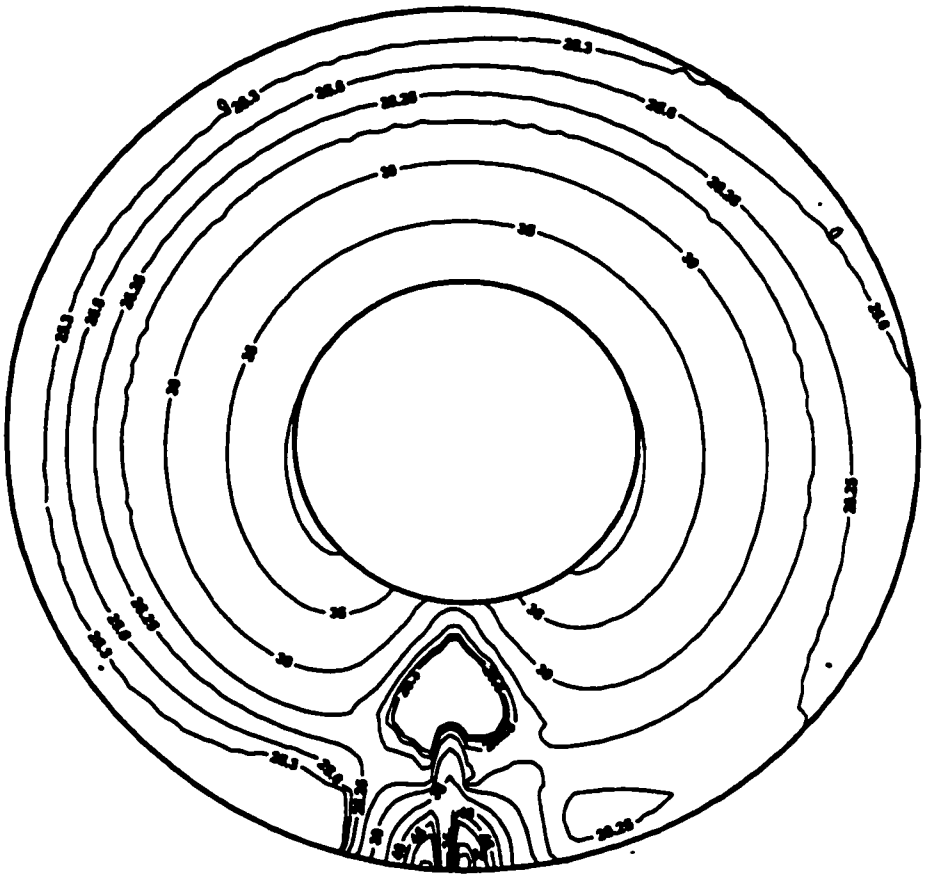

Figure 8.31: von Mises stress (MPa) contours by increasing reduction upto 74.6% (for bite angle = 5 deg).

Chapter 9

Conclusions and Recommendations

A study capable of modeling thermal and mechanical loads acting during metal deformation process has been conducted. A more realistic model for steady-state temperature distribution in the tool and workpiece has been developed. Coupled approach for modeling roll and strip interface has been considered. In particular, attention has been focused over roll and strip interaction, the most critical region in any metal forming process. Pressure and friction stress distributions have been calculated at this region. An analytical model based on deformation work theory is developed for modeling deformation energy distribution in the workpiece. By considering, a variable heat flux distribution at the interface, temperature distribution in the roll has been predicted, which is validated against the classical work of Tseng et al. [34].

First part of this research work involves calculation of roll temperature. For predicting the steady-state temperature distribution in the roll, a combined ascending-modulus algorithm has been developed and successfully applied for evaluating the coefficients of Kelvin functions with variable arguments. This algorithm is then used in the determination of unknown temperature distribution of the roll. Since in actual rolling process heat flux could not necessarily be uniform over the interface, so special emphasize has been paid on this aspect. The temperature model has been developed

by dividing the roll gap into 'j' number of elements, then by assuming a linear variation of heat flux in each element a non-uniform heat flux behavior has been modeled. The compatibility of temperature and heat flux, the necessary condition for coupled approach, has been applied at each element.

As stated earlier, the deformation heat generation in the strip cannot necessarily be uniform; by assuming the conversion of all deformation work into heat energy, a one dimensional analytical model is proposed for modeling strip deformation behavior. Also pressure and friction heat flux models have been developed with the capabilities of modeling a variable heat flux distribution at the interface. The effect of taking different number of elemental division for bite region has been carried out. When bite region was divided into '5' elements, the results were not reliable; however, as the number of divisions increased the refinement in results was also noticed, as evident in results of friction stress, temperature and heat flux distributions.

In the second part, roll deformation occurred during contact with the workpiece has been modeled by using thermo-elastic finite element method. Roll thermal and deformation models have been coupled and an iterative procedure over the whole developed master module has been applied to obtain optimum tool dimension, necessary for controlling the final strip thickness. Finally, exit strip thickness is compared with the experimental value reported in the published literature. First analysis has been performed only with mechanical load that is, by applying pressure and friction stress distributions at the interface. Then both thermal and mechanical loads have been applied over the tool. Hitchcook formula has also been used as a check for predicting actual radius of the deformed roll. It has been found that strip final thickness ob-

tained by applying thermal and mechanical loads (together) to the roll, is very much closer to the experimental data.

On the basis of current study some of the important conclusions and further extension of this work have been suggested. These are summarized below:

- Increasing rolling speed has a little effect on roll heat flux distribution as compare to increasing the reduction.

- A variable heat flux consideration becomes important when a relatively large reduction is required.

- Reducing cooling practice over roll surface markedly increases the roll temperature. In contrast providing full cooling and increasing the reduction will cause relatively less increment in roll temperature distribution.

- Inadequate cooling with same reduction has little effects on maximum value of effective stress occurred at the bite region. But it causes relatively large increase on effective stress inside the roll and at the roll inner surface (where roll is fixed with the rotating shaft). Whereas conducting full cooling and increasing reduction greatly increases von Mises effective stress at the bite region, stress inside the roll is not much affected.

- Since by increasing reduction with optimum cooling effective stress inside the roll is increased significantly, it is thought that for rolling processes involving very large reductions localized yielding over the roll surface can occurr.

- Localized yielding requires plastic analysis of roll material, therefore, in future this work can be extended for elasto-plastic deformation analysis of roll.

- Since roll material which comes in contact with the strip faces a continuous cycle of cooling and heating thus fatigue analysis can also be performed which would help in predicting roll life.

- The developed module can also be investigated for temperature dependent material properties, for example when thermal conductivity (k) and convective heat transfer coefficient (h) become temperature dependent paremeters.

Following some recommendations have been drawn that are:

- Nonuniform heat flux distribution at the roll and strip interface for predicting temperature distribution should be considered.

- Coupled thermo-mechanical analysis is recommended for calculating deformed roll radius and controlling the gauge of exit rolled strip.

- Stresses and strains should be calculated by considering both thermal and mechanical loads.

Bibliography

[1] Schey, J. A., Introduction to Manufacturing Processes, McGraw-Hill Book Co., NY, 1977.

[2] Boulger, F. W., "Metal Forming: Status and Challenges," Towards the Factory of the Fracture, PED-Vol. 1, Winter Annual Meeting, Nov. 16-21, 1980, p. 18, ASME.

[3] Mielnik, E. M.,"Metalworking Sciences and Engineering", Ist edition, McGrawHill, 1991.

[4] Hill, R.,"The Mathematical Theory of Plasticity," Oxford University Press, NY, 1950.

[5] Lenard, J. G., Pietrzyk, M., and Cser, L.,"Mathematical and Physical Simulation of the properties of Hot Rolled Products," Istedition, Elsevier, 1999.

[6] Roberts, W. L., Cold Rolling of Steels, Ist edition, Dekker, NY, 1978.

[7] Schey John A. Metal Deformation Processes, Dekker, NY, 1970.

[8] Tseng, A. A.,"Thermal Modeling of Roll and Strip Interface in Rolling Processes: Part 1-Review," Numer. Heat Transfer, Part A, Vol. 35, pp. 115-133, 1999.

[9] Wilson, W.R.D., Walowit, J.A.,"An Isothermal Hydrodynamic Lubrication The-

ory for Strip Rolling with Front and Back Tension," Tribology Convention 1971, Inst of Mech Eng, London, pp. 164-172.

[10] Tseng, A. A.,"A Numerical Heat Transfer Analysis of Strip Rolling," ASME J. of Heat Transfer, Vol. 106, pp. 512-517, 1984a.

[11] Tseng, A. A., "A Generalized Finite Difference Scheme For Convection-Dominated Metal-Forming Problems," Int. J. Numer. Methods in Eng., Vol. 20, pp. 1885-1900, 1984.

[12] Tseng, A.A.,"Thermal Chracteristics of Roll and Strip Interface in Modeling Rolling Processes," J. Mater. Proc. Manuf Sci., Vol. 6, pp. 3-18, 1997.

[13] Johnson, W., and Kudo, H.,"The Use of Upper-Bound Solutions for the Determination of Temperature Distribution in Fast Hot Rolling and Axi-Symmetric Extrusion Processes," Int. J. Mech. Sci., Vol. 1, pp. 175-191, 1960.

[14] Avitzur, B., and Nowakowski, A.,"Analysis of Strip Rolling as an Adiabatic Process," Proc. 21st Int. Machine Tool Design and Research Conference, ed. by J. M. Alexander, Vol. 1, pp. 29-32, Swansea, UK, 1980.

[15] Dawson, P. R.,"Viscoplastic Finite Element Analysis of Steady State Forming Processes Including Strain History and Stress Flux Dependence," Application of Numerical Methods to Forming Processes, AMD-Vol. 28, pp. 55-66, ASME, 1978.

[16] Haubitzer, W.,"Steady State Temperature Distribution in Rolls," Archufuer das Eisenhuttenwesen, 1974, 46, (10) pp.635-638.

[17] Patula, E. J.,"Steady State Temperature Distribution in a Rotating Roll Subject to Surface Heat Fluxes and Convection Cooling," ASME Journal of Heat Transfer, Vol. 103, pp.36-41 1981.

[18] Troeder, C., Spielvogel, A., and Xu, J.,"Temperature and Thermal Stresses in Work Rolls During the Hot Rolling of Strip," Steel Res., Vol. 56, No. 7, pp. 379-384, 1985.

[19] Guo, R. M.,"Two Dimensional Transient Thermal Behavior of Work Rolls in Rolling Process," Recent Advances in Heat Transfer and Micro-Structure Modelling for Metal Processing, MD-Vol. 67, pp. 79-89, ASME, 1995.

[20] Yuen, W. Y. D.,"On the Steady State Temperature Distribution on a Rotating Cylinder Subject to Heating and Cooling Over Its Surface,"ASME J. Heat Transfer, Vol. 106, pp. 578-585, 1984.

[21] Yuen, W.Y.D.,"Effective Cooling of Work Rolls in Strip Rolling, Mater. Sci. Technol., vol. 4, pp.628-634, 1988.

[22] Gecim, B., Winer, W. O.,"Steady Temperature in a Rotating Cylinder Subject to Surface Heating and Convection Cooling,"ASME J. Tribology, Vol. 106, pp.120-127. 1984.

[23] Tseng, A. A., Tong, S., and Sun, P. F.," Thermal Behavior of Aluminum Rolling,"ASME Proc of 1988 Nat. Heat Transfer Conf., Vol. 3, pp. 485-492, 1988.

[24] Tseng, A. A., Tong, S., and Lin, F. H.,"Thermal Stresses of Rotating Rolls in Rolling Processing," J. of Thermal Stresses, Vol.12 pp.427-450, 1989.

[25] Tseng, A. A.,"Finite-Difference Solutions for Heat Tranesfer in a Roll Rotating at High Speed," Numerical Heat Transfer, Vol. 7, pp. 113-125, 1984.

[26] Cerni, S.,"The Temperature and Thermal Stresses in the Rolling of Metal Strip," Doctorial Dissertation, Dept. of mechanical Engineering, Carnegie-Mellon University, 1961.

[27] Cerni, S., Weinstein, A.S., and Zorowski, C.F.,"Temperature and Thermal Stresses in the Rolling of Metal Strip," Iron and Steel Engineer, Vol. 40, pp. 165-171, 1963.

[28] Hogshead, T. H.,"Temperature Distributions in the Rolling of Metal Strip," Ph.D. Thesis, Carnegie-Mellon University, Pittsburgh, PA, 1967.

[29] Pawleski, O., "Calculating the Temperature Field in the Work Rolls of Hot and Cold Rolling Mills," Archufuer das Eisenhuttenwesen, Vol 42, 1971, pp. 713-720.

[30] Polukhin, P. I., Rudel'son, V. M., Polukhin, V. P., and Nikolaev, V. P., "Thermal processes in the deformation zone during sheet rolling. Communication 1," Steel in The USSR, pp.52-54, January, 1974.

[31] Polukhin, P. I., V. M. Rudel'son, V. P. Polukhin, and V. A. Nikolaev, "Thermal processes in the deformation zone during sheet rolling. Communication 2," Steel in The USSR, pp.52-54, January, 1974.

[32] Yuen, W. Y. D., "On the Heat Transfer of a Moving Composite Strip Compressed by Two Rotating Cylinders," ASME J. Heat Transfer, Vol. 107, pp.541-548, 1985.

[33] Poplawski, J. V., and Seccombe, D. A., Jr., "Bethlehem's Contribution to the Mathematical Modeling of Cold Rolling Tandem Mills," Iron and Steel Engineer, Vol. 57, 1980, pp. 47-58.

[34] Tseng, A. A., Tong, S. X., Maslen, S. H., and Mills, J. J., "Thermal Behavior of Aluminum Rolling," ASME J. Heat Transfer, Vol. 112, pp. 301-308, 1990.

[35] Parke, D. M., and Baker, J. L. L., "Temperature Effect of Cooling Work Rolls," Iron and Steel Engineer, Vol. 49, 1972, pp. 83-88.

[36] Lahoti, G. D., Shah. S. N., and Altan, T., "Computer-Aided Analysis of the Deformations and Temperatures in Strip Rolling," ASME J. of Engineering for Industry, Vol. 100, pp. 159-166, 1978.

[37] Tseng, A. A. and Wang, S. R., "Effects of Interface Resistance on Heat Transfer in Steel Cold Rolling," Steel Res., Vol. 67, No.2, pp. 44-51, 1996.

[38] Tseng, A. A., "Thermal Modeling of Roll and Strip Interface in Rolling Processes: Part 2-Simulation," Numer. Heat Transfer, Part A, Vol. 35, pp. 135-154, 1999.

[39] Wang S. R.,and Tseng, A. A., "Macro- and Micro-Modeling of Hot Rolling of Steel

Coupled by a Micro-Constitutive Relationship," Iron Steel Maker (I & SM), Vol. 23, no. 9, pp. 49-61, 1996.

[40] Tseng, A. A.,"Material Chracterization and Finite Element Simulation for Forming Miniature Metal Parts," Finite Element Anal. and Des., Vol. 6, pp. 251-265, 1990.

[41] Chang, D.,"An Efficient Way of Calculating Temperatures in the Strip Rolling Process," ASME J. of Manuf. Sci. and Engg., Vol. 120 pp. 93-100, 1998.

[42] Yamada, K., Ogawa, S., and Hamauzu, S.,"Two-dimensional Thermo-mechanical Analysis of Flat Rolling Using Rigid-plastic Finite Element Method," ISIJ International, vol. 31, no. 6, pp. 566-570, 1991.

[43] Woodbury, K. A., Beaudoin, Jr. A. J.,"Thermal Consideration in Numerical Simulation of the Strip Rolling Process," ASME PED-Vol. 30, pp. 117-132, 1988.

[44] Dawson, P. R.,"A Model for the Hot or Warm Forming of Metals with Special Use of Deformation Mechanism Maps," Int. J. of Mech. Sci., Vol. 26, no. 4, pp. 227-244, 1984.

[45] Dawson, P. R.,"On Modeling of Mechanical Property Changes During Flat Rolling of Aluminum," Int. J. of Solids and Strucrtures, Vol. 23, no. 7, pp. 947-968, 1987.

[46] Hwang, S. M., Joun, M. S., and Kang, Y. H.,"Finite Element Analysis of Temperatures, Metal Flow, and Roll Pressure in Hot Strip Rolling," ASME J. Engineering for Industry, Vol. 115, pp. 290-298, 1993.

[47] Stevens, P. G., Ivens, K. D., and Harper, P.,"Increasing Work-Roll Life by Improved Roll-Cooling Practice," J. Iron Steel Institute (London), Vol. 209, pp. 1-11, January 1971.

[48] Denisov, Yu. V., Trukhin, B.V., and Kholodov, I. A.,"Determination of temperature at surface of rolling mill work rolls," Steel in The USSR, pp.540-541, October, 1980.

[49] Raudensky, M., Horsky, J., Tseng, A. A., and Weng, C. I.,"Heat Transfer Behavior of Work Rolls in Hot Rolling of Shaped Steels," Steel Res., Vol. 65, no. 10, pp. 375-381, 1994.

[50] Jeswiet, J. and Rice, W. B., "Measurment of Strip Temperature in Roll Gap During Cold Rolling," CIRP Annals, Vol. 24, 1975, pp. 153-156.

[51] Yoshida, H., Yorifuji, A., Koseki, S., and Saeki, M.,"An Integrated Mathematical Simulation of Temperatures, Rolling loads and Metallurgical Properties in Hot Strip Mills," ISIJ International, vol. 31, no. 6, pp. 571-576, 1991.

[52] Orowan, E.,"The Calculation of Rolling Pressure in Hot and Cold Flat Rolling," Proc. Inst. Mech. Engrs., Vol. 106, pp. 512-517, 1943.

[53] Finne, R., Jacob, J. P., and Rissanen, J., "A Mathematical Model of Strip Rolling Mills," IBM Nordiska Laboratorier, Sweden, TP 18.094, 1963.

[54] Maslen, S.H., and Tseng, A. A.,"Program-Rolling Users Manual," Rep. No. MML TR 81-8, Martin Marietta Laboratories, Baltimore, MD, 1981.

[55] Alexander, J. M.,"On the Theory of Rolling," Proc. R. Soc. Lond. A, Vol. 326, pp. 535-563, 1972.

[56] Arpaci, Conduction Heat Transfer, Addison-Wesley, New York, 1966.

[57] Christensen, P., Everfelt, H., and Bay, N.,"Pressure Distribution in Rolling," Annals of the CIRP, Vol. 35(1), pp. 141-146, 1986.

[58] Wanheim, T., Bay, N., Petersen, A. S.,"A theoretically determined model for friction in metal working processes," Wear 28, pp. 251-258, 1974.

[59] Bay, N., Wanheim, T.,"Real area of contact and friction stress at high pressure sliding contact," Wear 38, pp. 201-209, 1976.

[60] Wanheim, T., Bay, N.,"A model for friction in metal forming processes," Annals of the CIRP, Vol. 27, pp. 189-194, 1978.

[61] Gerved, G.,"Analyse af friktions- og trykfordeling ved stukning". MM report No. 85(13), Technical University of Denmark, 1985 (in danish).

[62] Koot, L.W.,"Process Design Criteria for the Cooling of a Cold Strip Mill", Paper presented at ISI Meeting, 'Mathematical Process Models in Iron and Steelmaking', Held at Amsterdem, Holland, 19-21, February, 1973.

[63] Abramowitz, M., and Stegun, I. A., ed., "Handbook of Mathematical Functions, " National Bureau of Standards, US Department of Commerce, pp. 371-382, 1972.

[64] Gratacos, P., Montmitonnet P., Fromholz, C., and Chenot, J. L.,"A Plane-Strain Elastoplastic Finite-Element Model For Cold Rolling Of Thin Strip," Int. Jour. of Mech. Sci., Vol. 34, pp. 195-210, 1992.

[65] Domanti, S. A., McElwain, D. L.,"Cold Rolling Of Flat Metal Products: Contribution Of Mathematical Modeling," Int. Jour. of Mech. Sci., Vol. 212, Part B, pp. 73-86, 1998.

[66] Hitchcock, J. H., "Roll neck bearings," Report of ASME Res. Committee, 1935.

[67] Ford, H., Ellis, F., and Bland, D. R.,"Cold Rolling With Strip Tensions," J. Iron Steel Inst., Vol. 168, pp. 57, 1951.

[68] Bland, D. R. and Ford, H.,"An Approximate Treatment Of The Elastic Compression Of The Strip in Cold Rolling," J. Iron Steel Inst., Vol. 171, pp. 245, 1952.

[69] Jortner, D., Osterle, J. F., Zorowski, C.F.,"An Analysis Of The Mechanics Of Cold Strip Rolling," Int. Jour. of Mech. Sci., Vol. 2, pp. 179, 1960.

[70] Chang, D.,"Thermal Stresses in Work Rolls During The Rolling of Metal Strip," J. of Material Processing Technology, Vol. 94 pp. 45-51, 1999.

[71] ANSYS, release 5.6.2, Swanson Analysis System, Inc., 1994.

[72] Bathe, K. J.,"Finite Element Procedures", Ch. 6, pp. 148-192, Prentice-Hall, Englewood Cliffs, New Jersey, 1991.

[73] Kovach, L. D., "Advanced Engineering Mathematics, "Addison Wesely Publishing Company, Inc. 1982.

VITA

Ovaisullah Khan

- Born: in Karachi, Pakistan.

  Address: 2/7−I, Liaquatabad−2, Karachi−75900, Pakistan.

  Phone: (92-21) 492-5667

  (92-21) 451-3071

- Received Bachelor of Engineering from N.E.D. University of Engineering and Technology (Mechanical engineering) Karachi, Pakistan, 1998.

- Joined Mechanical Engineering Department of King Fahd University of Petroleum and Minerals, Dhahran, as a Research Assistant in 1999.

- Finished Master of Science in Mechanical Engineering from King Fahd University of Petroleum and Minerals, Dhahran, Saudi Arabia, 2002.